Diamine(phosphine)ruthenium(II) Complexes and Their Application in The Catalytic Hydrogenation of α,ß-Unsaturated Ketones in Homogeneous and Heterogeneous Phase

★★★★★★★★★★★★★★★

Diamin(phosphin)ruthenium(II)-Komplexe und ihre Anwendung in der katalytischen Hydrierung von α,ß-ungesättigten Ketonen in homogener und heterogener Phase

DISSERTATION

der Fakultät für Chemie und Pharmazie

der Eberhard-Karls-Universität Tübingen

zur Erlangung des Grades eines Doktors

der Naturwissenschaften

2003

vorgelegt von

Ismail Khalil Warad

Tag der mündlichen Prüfung:	14.07.2003
Dekan:	Prof. Dr. H. Probst
1. Berichterstatter:	Prof. Dr. E. Lindner
2. Berichterstatter:	Prof. Dr. H. A. Mayer

In the Name of Allah, the Most Beneficent, the Most Merciful

To my Parents, Sister and Brothers

To my Wife and my Son (Khalil)

and Daughters (Ikram and Aya)

To my Homeland

Die vorliegende Arbeit wurde am
Institut für Anorganische Chemie der
Eberhard-Karls-Universität Tübingen
unter der Leitung von Prof. Dr. rer. nat. Ekkehard Lindner
angefertigt.

Meinem Doktorvater,
Herrn Prof. Dr. Ekkehard Lindner,
danke ich herzlich für die Themenstellung,
für die Bereitstellung ausgezeichneter Arbeitsbedingungen,
für wertvolle Anregungen und Diskussionen
sowie sein stetes Interesse an dieser Arbeit.

Ich möchte mich herzlich bedanken bei:

dem Graduiertenkolleg der DFG `Chemie in Interphasen`. Ich bedanke mich außerdem für ständige neue Ideen und fachliche Anregungen in bezug auf den Fortgang meiner Arbeit.

Herrn Dr. Klaus Eichele für die Durchführung der Röntgenstrukturanalysen.

Herrn Dr. Taleb Al-Tel für seine Ermutigung zu Beginn meines Bleibens in Deutschland.

Frau Heike Dorn, Frau Angelika Ehmann und den Meßberechtigten am 250 MHz DRX-Gerät für Hochauflösungs-NMR-Spektren.

Herrn Prof. Dr. H. A. Mayer für die Hilfe bei NMR-Problemen.

Herrn Prof. Dr. Helmut Bertagnoli, Herrn Dr. Michael Seiler und Herrn M.Sc. Venkata Krishnan, Universität Stuttgart, Institut für Physikalische Chemie, für die Durchführung und Auswertungen der EXAFS-Messungen.

Herrn Wolfgang Bock für die Durchführung vieler schwieriger Elementaranalysen.

Frau Barbara Saller für viele IR-Spektren.

den ehemaligen 'Labormitinsassen' von 8M14 Herrn Dr. Monther Khanfar, Herrn Dr. Samer Al-Gharabli und Herrn Dr. Mahmoud Sunjuk für das ausgezeichnete Arbeitsklima, wertvolle Diskussionen am Abzug und viele Glasgeräte.

Herrn Prof. Dr. Klaus Albert und seinen Mitarbeiten, Herrn Dr. Zhong-Lin Lu und Herrn Dr. Dayong Wu für zahlreiche fruchtbare Diskussionen.

Herrn Dr. Michael Henes für die Behebung von unlösbaren Computerproblemen.

Herrn Dr. Hani Mohammed, Herrn Dr. Monther Khanfar, Herrn Dr. Samer Al-Gharabli, Herrn M.Sc. Ahmed Al-Sheikh, Herrn M.Sc. Adnan Al-Labadi, Herrn Dipl.-Chem Adeeb Al-Dahaschan, Herrn Dr. Mahmoud Sunjuk, Herrn M.Sc. Ahmed Abu-Rayyan, Herrn M.Sc. Muad Al-Omari, Dr. Yusof Abu-Abed, Herrn M.Sc. Kamal Swiedan für viele entspannende Stunden in der Freizeit.

Frau Roswitha Conrad und Herrn Dr. Ebert für die Hilfe bei bürokratischen Angelegenheiten.

Herrn Prof. Dr. Volker Schurig und seinen Mitarbeiten für die bereitstellung von GCs.

Nicht zuletzt möchte ich mich ganz herzlich bei meiner Familie für ihre Unterstützung und meiner Frau für ihre Geduld und ihren Beistand bedanken.

Introduction

Catalysis is of extraordinary importance to industry and society today. It is evident that the development of new catalysts is a key element for an economically and ecologically improved chemical production of new materials [1]. A typical example is the diastereoselective reduction of ketones to secondary alcohols, which is a major subject of organic synthesis [2]. This important transformation has mainly been accomplished by stoichiometric metal hydride reagents [2,3]. Although a wide range of stereoselective reducing agents are available, each reagent has a limited scope due to the inherent chemical property as well as the difficulty in structural modification. Development of stereoselective hydrogenation catalyzed by transition metal-based molecular complexes is ardently desired because of the higher structural permutability of the catalyst, in addition to a series of practical benefits [2-7].

The hydrogenation of carbonyl compounds to alcohols is among one of the most applied process in organic chemistry [2-14]. Recent developments in this field have been very successful, and a large number of catalytic methods has been elaborated to achieve this purpose [5-14]. Noyori et al. discovered a ruthenium(II) complex system containing diphosphine and 1,2-diamine ligands which, in the presence of a base and 2-propanol, proved to be excellent catalysts for the hydrogenation of ketones under mild conditions [8-10]. Subsequently chiral ruthenium(II) complexes were developed for the asymmetric hydrogenation of functionalized ketones [10-14]. If these complexes are supported no leaching takes place and the activity and enantioselectivity remained constant even after twelve runs [13]. A mechanism of this reaction has been suggested [5, 12, 15-18]. The source of the transferred hydrogen atom was attributed to a metal-centered hydride. Generally, the most widely accepted theory is that at least one NH and a RuH unit is intimately involved in

the hydride transfer process [10, 15, 19-21]. Hartmann and Chen demonstrated that a basic 2-propanol solution obtained by the addition of excess DBU (1,8-diazabicyclo[5.4.0]undec-7-ene) is not sufficient to activate the corresponding ruthenium dichloride precursor *trans*-$RuCl_2$(diamine)(diphosphine), a source of potassium cations is also needed. The authors suggested that the role of the potassium counterion of the alkoxide base in 2-propanol is to coordinate to the amido nitrogen of an intermediate and act as a Lewis acid to assist in the activation of dihydrogen (Scheme1) [21].

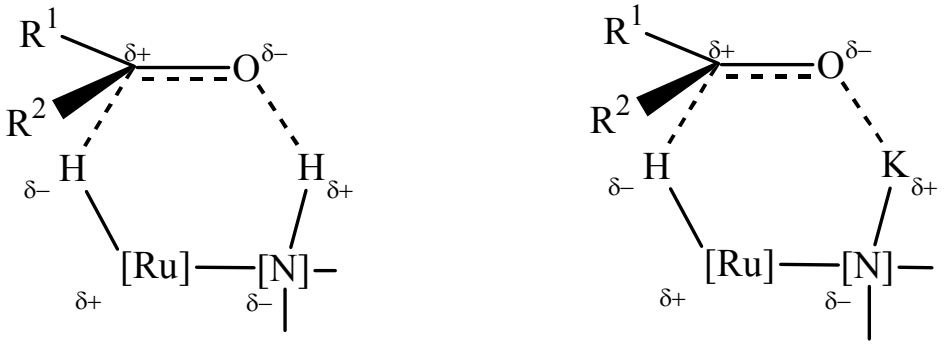

Scheme 1. Transition states of the most accepted carbonyl hydrogenation mechanisms: a) proposed by Noyori; b) proposed by Chen

It has been considered that the catalytic activity is traced back to the electronic properties of the coordination center and that the stereoselectivity is controlled by the chiral ligand [15]. Similar catalyst systems with other chiral diphosphine and diamine ligands were established by Burk, Bergens, and Morris et al. [22-24].

In the first part of this thesis the synthesis of a set of novel neutral diamine–bis(ether–phosphine)ruthenium(II) complexes is reported by treatment of the precursor complex $RuCl_2(\eta^2\text{-}Ph_2PCH_2CH_2OCH_3)_2$ with various chelating diamines. Due to the remarkable effect of the co-ligand on the catalytic activity of such complexes, a series of aliphatic and aromatic diamines was selected to vary the electronic and steric character of the metal center [25-27].

Furthermore by abstraction of a chloride ligand monocationic diamine(ether-phosphine)-ruthenium(II) complexes are in the focus of this investigation [25,29]. Hemilabile ether-phosphines have been extensively investigated in organometallic chemistry as a tool to stabilize empty coordination sites or to create a *pseudo*-vacant coordination site at reactive centers [30-35]. Ligands of this type form a close contact to the metal center via the phosphorus atom so that the ligand can not dissociate completely from the metal center. At the same time the oxygen atom in the ether moiety coordinates to the metal in a labile manner and is involved in an opening and closing mechanism taking over the function of an intramolecular solvent [30]. Also a new and synthetic facile route was established to get an easy access to diamine(diphosphine)ruthenium(II) complexes using 1,3-bis(diphenyl-phosphino)propane as a ligand [28].

A prospective objective is the combination of parallel synthesis and interphase chemistry. In this context several neutral diamine(phosphine)ruthenium(II) complexes were successfully supported onto polysiloxane matrices by the sol-gel route and their use as catalysts in interphases was demonstrated [36-39]. The results in the selective hydrogenation of *trans*-4-phenyl-3-butene-2-one were compared to those of the corresponding homogenous catalysts [26-29]. To enhance the enantioselectivity of the obtained secondary alcohols, the kinetic resolution of enantiomerically enriched *trans*-4-phenyl-3-butene-2-ol was performed in a consecutive approach using lipase-catalyzed enantioselective transesterification of the alcohol in toluene [27].

General Section

1. Synthesis and Structures of the Diamine(ether-phosphine)ruthenium(II) Complexes $3L_1$-$3L_{14}$

1.1 General Considerations

Combinatorial chemistry and parallel syntheses become increasingly important in several areas of chemistry [40,41]. Lately this technique has been transferred to heterogeneous and homogeneous catalysis [42, 43]. In a recent paper [25], we reported on a synthetic route to a set of neutral and cationic diamine–bis(ether–phosphine)ruthenium(II) complexes and their complete structural characterization [25]. Compounds of this type can easily be supported in polysiloxane matrices and are potential candidates for the application of parallel methods. Due to the hemilabile character the oxygen donor is regarded as an intramolecular solvent impeding decomposition of the complex by protection of vacant coordination sites [25,30,44-53]. The weak ruthenium-oxygen bonds in bis(chelate)-ruthenium(II) complexes of the type $Cl_2Ru(P^{\frown}O)_2$ ($P^{\frown}O$ = η^2-*O,P* coordinated ether-phosphine ligand, $Ph_2PCH_2CH_2OCH_3$) are easily cleaved during the reaction with diamines. Complexes with hemilabile ligands are of current interest because of their potential applications in molecular activation, homogenous catalysis, functional materials, and small molecule sensing [5-20, 54].

In this part of the thesis the preparation and characterization of a variety of novel neutral diamine-bis(ether-phosphine)ruthenium(II) complexes using aliphatic diamines with different substituents in the backbone as well as chiral cycloaliphatic and aromatic, and substituted aromatic diamines are reported.

1.2 Synthesis and Spectroscopic Characterization

If the bis(ether-phosphine)ruthenium(II) complex **2** [25-27] is treated with the different diamines $\mathbf{L_1}$-$\mathbf{L_{14}}$ in dichloromethane the yellow, somewhat air-sensitive mixed diamine-bis(ether-phosphine)ruthenium(II) complexes $\mathbf{3L_1}$-$\mathbf{3L_{14}}$ are formed in good to excellent yields (Scheme 2). They are soluble in chlorinated organic solvents and insoluble in ethers and aliphatic hydrocarbons. Their molecular composition was corroborated by FAB-MS. The yield of the complexes $\mathbf{3L_1}$– $\mathbf{3L_{14}}$ strongly depends on electronic and steric factors of the diamine ligands. If one or both hydrogen atoms at the nitrogen donors are replaced by alkyl or aryl groups no reaction takes place. This is clearly a steric effect. On the other hand if in 1,2-phenylenediamine ($\mathbf{L_5}$) a methyl group is introduced in the *para*-position of a NH_2 function the yield increases from 59 [25] to 95 % [26], an observation which is in agreement with an electronic effect. Electron withdrawing substituents like NO_2 groups instead of a methyl function give rise to an inverse effect, the yield drops to about 13 % [55].

In the ^{1}H NMR spectra of the diamine(ether–phosphine)ruthenium(II) complexes $\mathbf{3L_1}$-$\mathbf{3L_{14}}$ characteristic sets of signals are observed, which are attributed to the phosphine as well as to the diamine ligands. Their assignment was supported by two-dimensional H, H-COSY, experiments which establish the connectivity between NH_2 and CH_2 functions in the diamine ligand, and between CH_2O and CH_2P groups in the phosphine fragment. The integration of

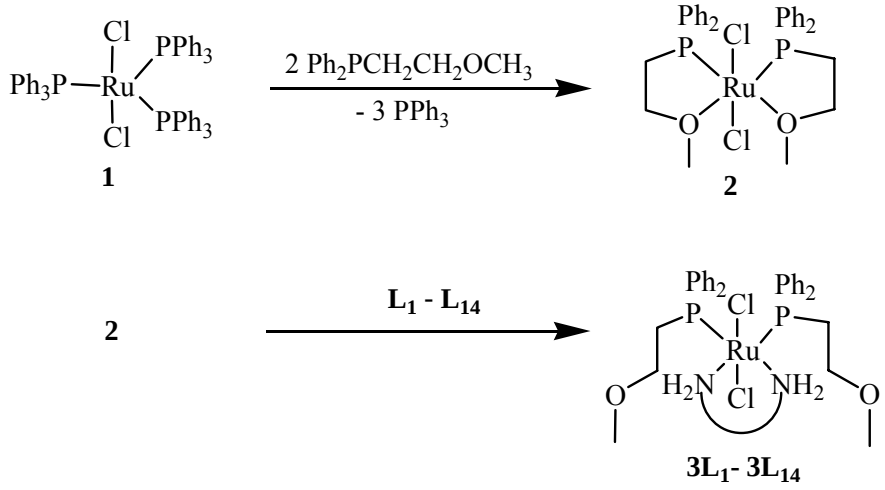

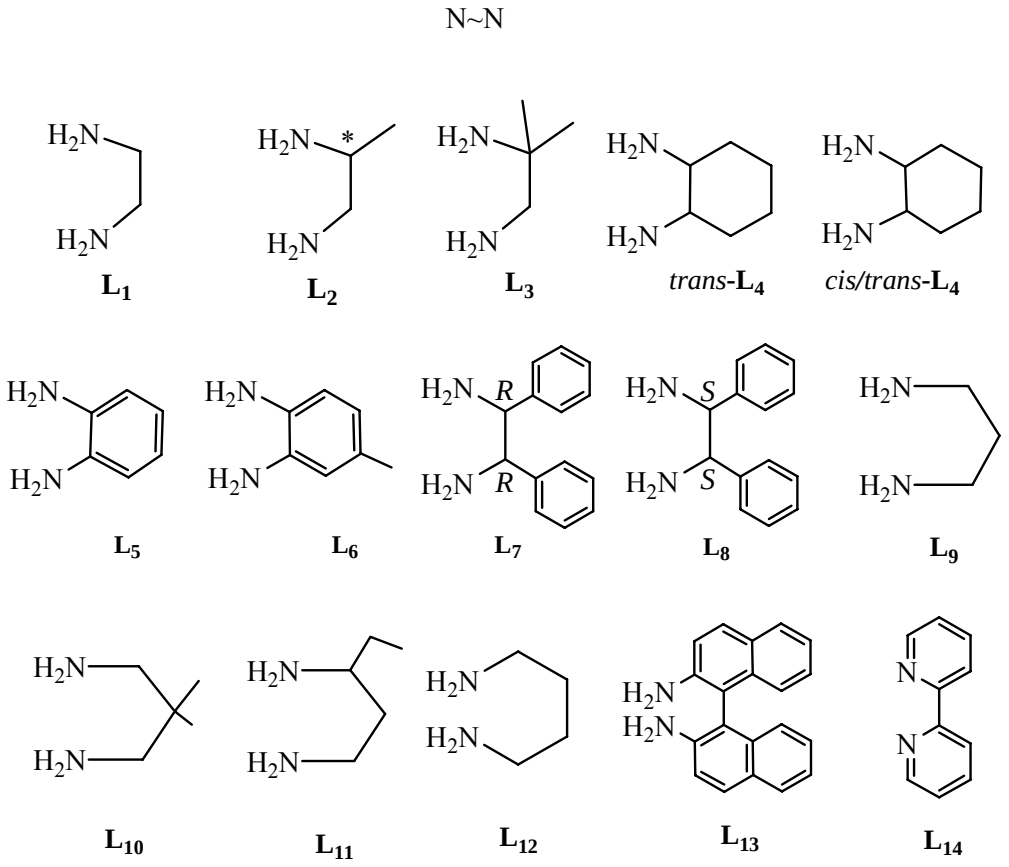

Scheme 2. Synthesis of the neutral diamine-bis(ether-phosphine)ruthenium(II) complexes **3L$_1$-3L$_{14}$**

the ^{1}H resonances confirm that the phosphine to diamine ratios are in agreement with the compositions of **3L$_1$-3L$_{14}$**. Furthermore, the chemical shifts of the singlets due to the protons of the methoxy groups are consistent with an η^1-P~O unit [25,30]. In the $^{31}P\{^{1}H\}$ NMR spectra of **3L$_3$-3L$_5$**, **3L$_7$**, **3L$_8$**, **3L$_{10}$**, and **3L$_{11}$-3L$_{13}$**, the singlets indicate that the phosphine groups are chemically equivalent in solution which is compatible with the C_{2v} symmetry of the $RuCl_2$(ether-phosphine)$_2$diamine complexes. While in the cases of **3L$_2$**, **3L$_3$**, and **3L$_{11}$** the asymmetric diamines cause loss of the C_2 axis resulting in a splitting of the ^{31}P resonances into AB patterns. In **3L$_6$**, the asymmetry is too remote to generate an observable splitting of the $^{31}P\{^{1}H\}$ NMR signal. The phosphorus chemical shifts and the ^{31}P - ^{31}P coupling constants suggest that the ether-phosphines are η^1-P~O coordinated [25-35] which are positioned *cis* to each other. Thus, if a diamine chelate is present, both chlorines have to be in mutual *trans*-arrangements (isomer **II** in Chart 1). Characteristic ^{13}C signals are due to the η^1-P~O binding mode as well as due to the aliphatic and aromatic diamines.

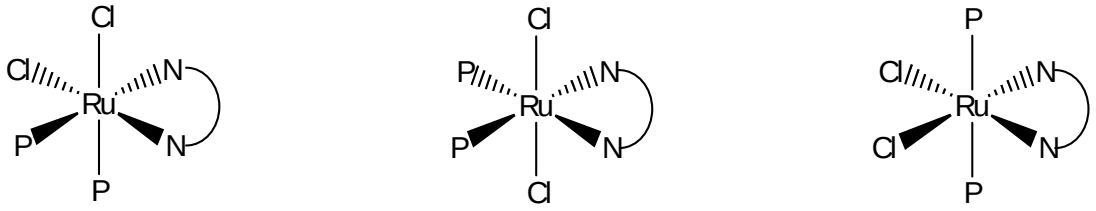

Chart 1. Three possible structural isomers of $RuCl_2(P\sim O)_2(N^{\frown}N)$

The IR spectra of the complexes **3L$_1$-3L$_{13}$** in particular show four sets of characteristic absorptions in the ranges 3386-3300, 3272-3205, 3178-3165, and 280-260 cm^{-1}, which can be assigned to NH_2, amine-CH, phosphine-CH and RuCl stretching vibrations, respectively.

1.3 X-ray Structural Determination of Complexes *trans*-**3L$_4$**, **3L$_{10}$**, and **3L$_7$**

To get a better insight into structural parameters complexes *trans*-**3L$_4$**, **3L$_{10}$**, and **3L$_7$** have been selected for X-ray structural investigations. Crystal structures of *trans*-**3L$_4$**, **3L$_{10}$**, and **3L$_7$** are shown in Figures 1 and 2, relevant bond distances, angles and torsion angles are collected in Tables 1 and 2. Compounds **3L$_4$** and **3L$_{10}$** crystallize as *trans*-chloro-*cis*-phosphine isomers **II** with approximate C_2 symmetry.

Ruthenium is at the center of a mostly regular octahedron, where Ru(1), P(1), P(2), N(1), and N(2) deviate by less than 0.1 Å from the equatorial least-squares plane, while the chlorine ligands are bent away from their axial positions toward the diamine ligand, forming Cl-Ru-Cl angles of 164.89° (**3L$_4$**) and 166.72° (**3L$_{10}$**). The different sizes of the diamine chelate rings result in distinctly different N-Ru-N angles of 77.85° (**3L$_4$**) in the five-membered ring versus 84.54° (**3L$_{10}$**) in the six-membered chelate, but the bite angles of both diamine ligands are obviously sufficiently small to leave the opposing P-Ru-P angles unaffected, 92.39° (**3L$_4$**) and 91.72° (**3L$_{10}$**).

In **3L$_4$**, the *trans*-diaminocyclohexane ligand forms a typical five-membered chelate with twist conformation, similar to the complex with 1,2-diaminoethane [25]. This allows the cyclohexane ring to adopt a chair conformation. In **3L$_{10}$**, the six-membered diamine chelate also has a chair structure, but is flattened about the position of the metal; e.g. the dihedral angle between the planes N(1)-Ru(1)-N(2) and N(1)-C(33)-N(2)-C(35) is 31.09° compared to 56.98° between N(1)-C(33)-N(2)-C(35) and C(33)-C(34)-C(35). This is in contrast to six-membered cobalt(III) diamine rings that tend to form more regular chair conformations [56]. The Ru-N distances of 2.170(4) and 2.209(4) Å in **3L$_{10}$**, where nitrogen is *trans* to phosphorus, are shorter than those in a complex of *trans*-diaminocyclohexane where nitrogen is *trans* to hydrogen atoms, with Ru-N distances of 2.225(5) and 2.284(5) Å [22].

a)

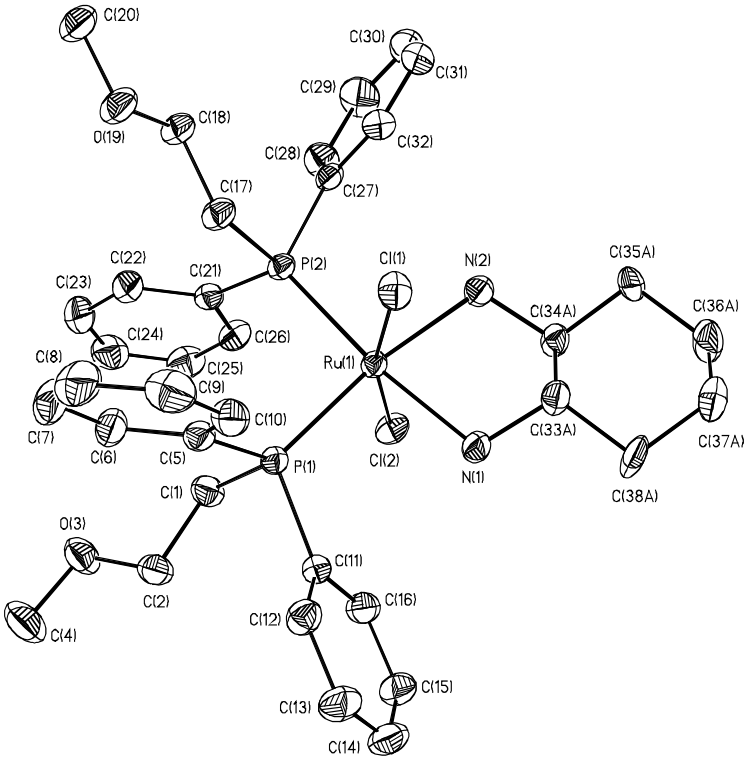

b)

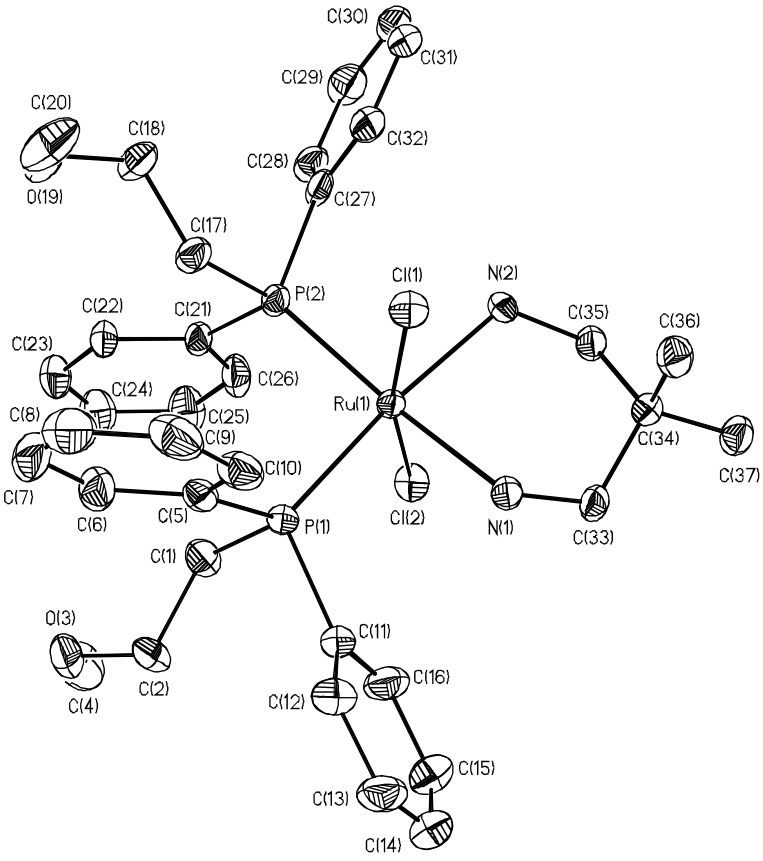

Figure 1. ORTEP plots of $\mathbf{3L_4}$ (a) and $\mathbf{3L_{10}}$ (b) with atom labeling scheme. Thermal ellipsoids are drawn at the 50% probability level, hydrogens are omitted for clarity

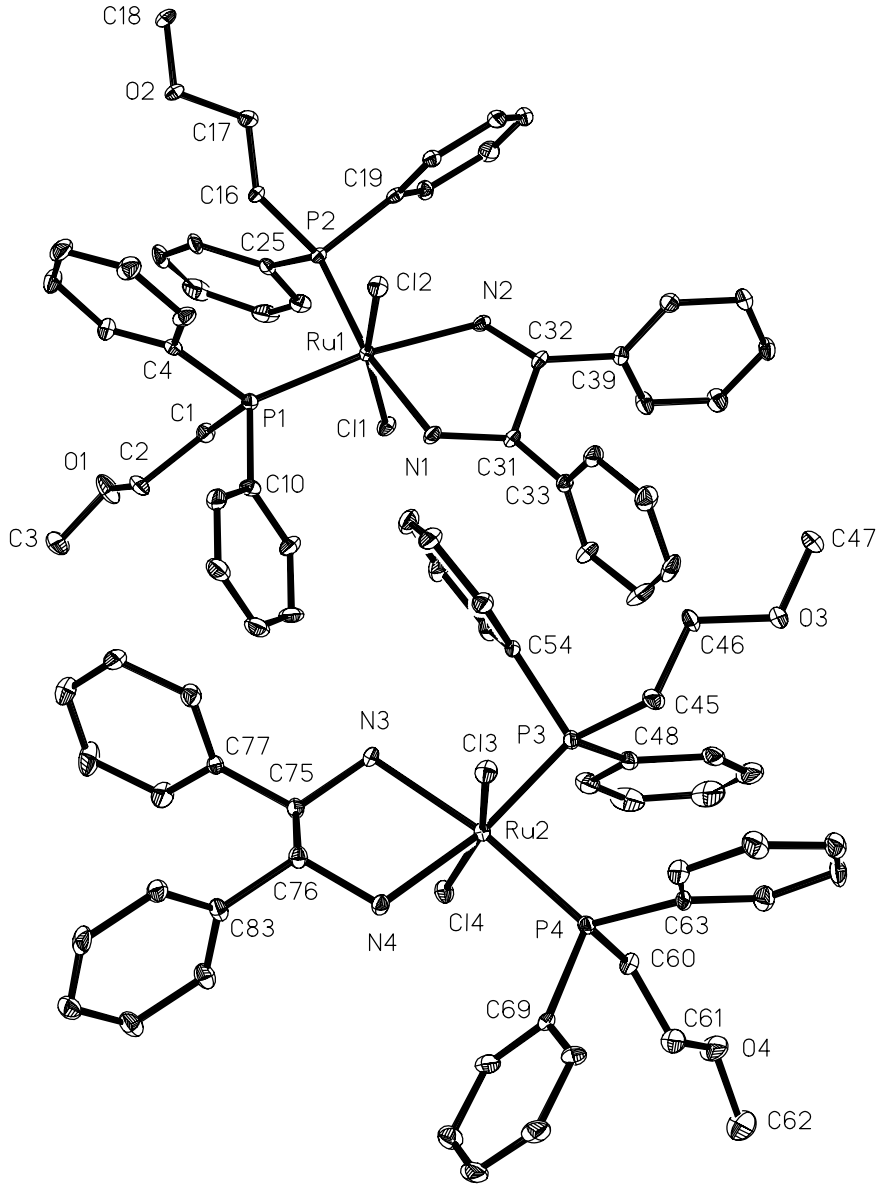

Figure 2. ORTEP plot with atom-numbering scheme showing the two independent molecules in the crystal structure of **3L**$_7$. Thermal ellipsoids are shown at the 20% probability level, hydrogen atoms have been omitted for clarity

Table 1. Selected bond lengths [Å] and bond and torsion angles [°] for *trans*-**3L$_4$** and **3L$_{10}$**

	trans-**3L$_4$**	**3L$_{10}$**
Bond lengths		
Ru(1)-Cl(1)	2.4141(6)	2.4178(13)
Ru(1)-Cl(2)	2.4050(5)	2.4303(14)
Ru(1)-P(1)	2.2737(7)	2.2807(14)
Ru(1)-P(2)	2.2881(5)	2.3037(14)
Ru(1)-N(1)	2.1790(13)	2.170(4)
Ru(1)-N(2)	2.1797(14)	2.209(4)
Bond angles		
Cl(1)-Ru(1)-Cl(2)	164.89(15)	166.72(5)
P(1)-Ru(1)-P(2)	92.38(2)	91.72(5)
N(1)-Ru(1)-N(2)	77.85(5)	84.54(16)
N(1)-Ru(1)-Cl(1)	84.74(4)	83.66(14)
N(2)-Ru(1)-Cl(1)	83.62(4)	82.73(12)
N(1)-Ru(1)-Cl(2)	84.15(4)	88.16(14)
N(2)-Ru(1)-Cl(2)	84.04(4)	86.10(12)
P(1)-Ru(1)-Cl(1)	98.985(15)	99.53(5)
P(2)-Ru(1)-Cl(1)	91.787(15)	89.47(5)
P(1)-Ru(1)-Cl(2)	92.027(16)	90.93(5)
P(2)-Ru(1)-Cl(2)	98.090(15)	98.42(5)
Torsion angles		
N(2)-Ru(1)-N(1)-C(33,33A)	17.5(2)	-38.8(4)
N(1)-Ru(1)-N(2)-C(35)		35.2(4)
N(1)-Ru(1)-N(2)-C(34A)	12.2(2)	
Ru(1)-N(1)-C(33,33A)-C(34,34A)	-43.3(4)	62.6(6)
N(1)-C(33)-C(34)-C(35)		-68.5(6)
N(1)-C(33A)-C(34A)-N(2)	53.1(4)	
Ru(1)-N(2)-C(35)-C(34)		-53.9(6)
Ru(1)-N(2)-C(34A)-C(33A)	-38.6(4)	
C(33)-C(34)-C(35)-N(2)		64.1(6)

Table 2. Selected bond distances [Å], bond angles, and torsion angles [°] for **3L$_7$**

Distances			
Molecule 1		Molecule 2	
Ru(1)-Cl(1)	2.4230(17)	Ru(2)-Cl(3)	2.4121(17)
Ru(1)-Cl(2)	2.4153(17)	Ru(2)-Cl(4)	2.4199(17)
Ru(1)-P(1)	2.277(2)	Ru(2)-P(3)	2.261(2)
Ru(1)-P(2)	2.277(2)	Ru(2)-P(4)	2.272(2)
Ru(1)-N(1)	2.175(6)	Ru(2)-N(3)	2.203(6)
Ru(1)-N(2)	2.154(6)	Ru(2)-N(4)	2.169(6)
Bond Angles			
Cl(1)-Ru(1)-Cl(2)	165.65(7)	Cl(4)-Ru(2)-Cl(3)	166.34(7)
P(1)-Ru(1)-P(2)	92.83(7)	P(3)-Ru(2)-P(4)	93.10(7)
N(1)-Ru(1)-N(2)	77.1(2)	N(3)-Ru(2)-N(4)	77.8(2)
N(1)-Ru(1)-Cl(1)	85.95(16)	N(3)-Ru(2)-Cl(3)	86.66(15)
N(2)-Ru(1)-Cl(1)	81.95(15)	N(4)-Ru(2)-Cl(3)	82.60(15)
N(1)-Ru(1)-Cl(2)	82.01(16)	N(3)-Ru(2)-Cl(4)	83.91(15)
N(2)-Ru(1)-Cl(2)	87.74(16)	N(4)-Ru(2)-Cl(4)	85.76(15)
P(1)-Ru(1)-Cl(1)	91.93(7)	P(3)-Ru(2)-Cl(3)	91.78(7)
P(2)-Ru(1)-Cl(1)	99.09(7)	P(4)-Ru(2)-Cl(3)	97.23(7)
P(1)-Ru(1)-Cl(2)	97.24(7)	P(3)-Ru(2)-Cl(4)	98.66(7)
P(2)-Ru(1)-Cl(2)	91.49(7)	P(4)-Ru(2)-Cl(4)	91.02(6)
Torsion Angles			
N(2)-Ru(1)-N(1)-C(31)	-16.9(4)	N(4)-Ru(2)-N(3)-C(75)	-22.0(4)
N(1)-Ru(1)-N(2)-C(32)	-13.3(4)	N(3)-Ru(2)-N(4)-C(76)	-10.9(3)
Ru(1)-N(1)-C(31)-C(32)	42.7(5)	Ru(2)-N(3)-C(75)-C(76)	50.5(5)
Ru(1)-N(2)-C(32)-C(31)	39.3(5)	Ru(2)-N(4)-C(76)-C(75)	40.7(5)
N(1)-C(31)-C(32)-N(2)	-52.1(5)	N(3)-C(75)-C(76)-N(4)	-59.8(5)
N(1)-Ru(1)-P(1)-C(10)	-0.9(3)	N(3)-Ru(2)-P(3)-C(54)	5.8(2)
N(2)-Ru(1)-P(2)-C(19)	-9.3(3)	N(4)-Ru(2)-P(4)-C(69)	1.1(3)

Complex **3L$_7$** crystallizes with two independent molecules in the unit cell of the chiral, non-centrosymmetric monoclinic space group $P2_1$. Both molecules 1 and 2 are *trans*-chloro-*cis*-phosphine isomers of only approximate C_2 symmetry and differ in the orientation of the substituents at phosphorus relative to the conformation of the diamine ligand. Common to both molecules is the regular octahedral coordination geometry about ruthenium, only perturbed by the phosphine groups pushing the chlorine ligands from their axial positions toward the diamine chelate, as expressed by the deviation of the Cl-Ru-Cl angles from linearity, 165.65(7)° and 166.34(7)° [26]. As expected, the phenyl substituents at the diamine carbon chain favor equatorial positions. Because of the fixed absolute *R,R*-configuration of the diamine, the chelate ring formation with twist conformation results in the predetermined λ configuration. In the case of molecule 2, this twist conformation is actually slightly distorted toward an envelope conformation with C(75) at the tip: C(75) is displaced from the N-Ru-N plane by 0.53 Å, while C(76), C(31), and C(32) show smaller deviations in the range 0.27-0.39 Å.

1.4 Comparative Studies Between EXAFS Investigations and X-ray Diffraction Methods of Complexes 3L$_4$, 3L$_7$, 3L$_9$, and 3L$_{10}$

One of the most powerful methods to obtain the local structure of non-crystalline materials is **EXAFS** (**E**xtended **X**-ray **A**bsorption **F**ine **S**tructure). The analysis of the EXAFS spectrum provides information on the bond distance, the coordination number, the Debye-Waller factor and the nature of the scattering atoms surrounding an excited atom [36, 57-60].

In the analysis of the experimental k^3 weighed $\chi(k)$ function, a three shell model can be fitted for the complexes **3L$_4$**, **3L$_7$**, **3L$_9$**, and **3L$_{10}$.** The first shell has two nitrogen backscatterers, the second shell contains two phosphorus backscatterers, and the third shell has two chlorine backscatterers. As an example, the experimental data and the fitted functions of complex **3L$_{10}$** are shown in k space as well as by Fourier transformations in real space (Figure 3).

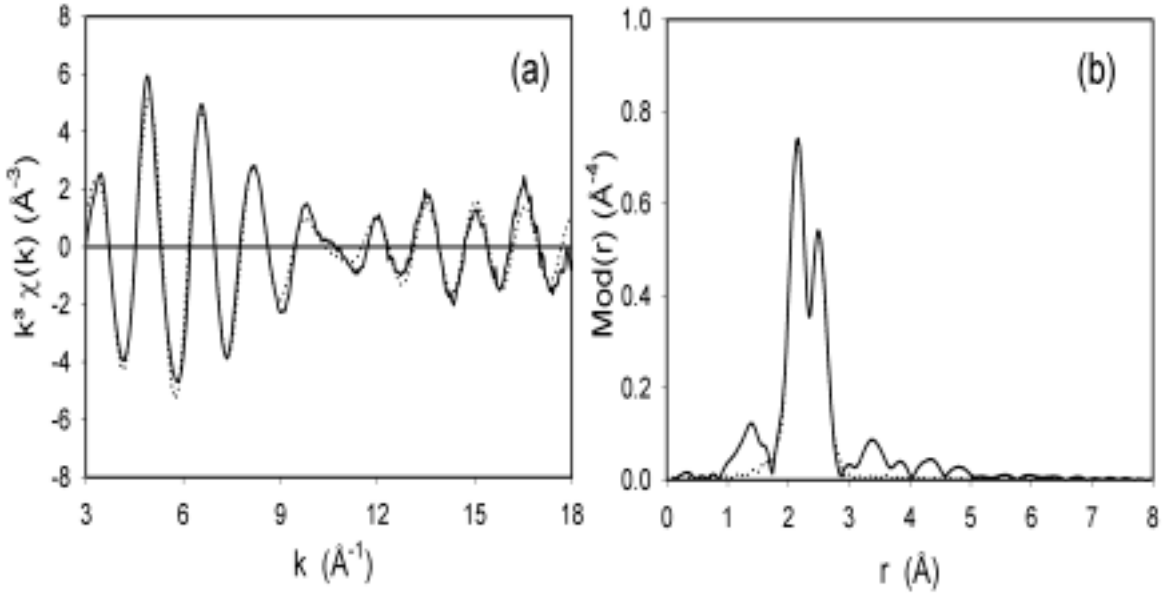

Figure 3. Experimental (solid line) and calculated (dotted line) k^3 χ (k) functions (a) and their Fourier transforms (b) for **3L$_{10}$** in the *k*–range 3.00-18.00 $Å^{-1}$

The structural parameters of the complexes obtained from EXAFS and X-ray diffraction are compared in Table 3.

Table 3. Structural parameters for the complexes **3L$_4$**, **3L$_7$**, **3L$_9$**, and **3L$_{10}$** obtained from X-ray diffraction and EXAFS

Complex	Bond type	r[Å], X-ray data	r[Å], EXAFS data	Debye-Waller factor σ [Å]	R factor and E_0 value
trans-**3L$_4$**	Ru–N	2.18 ± 0.02	2.18 ± 0.02	0.050 ± 0.005	25.03
	Ru–P	2.28± 0.02	2.28± 0.02	0.062 ± 0.006	22.07
	Ru–Cl	2.41± 0.02	2.41± 0.02	0.058 ± 0.006	
3L$_7$	Ru–N	2.17 ± 0.02	2.17 ± 0.02	0.050 ± 0.005	22.06
	Ru–P	2.27± 0.02	2.27± 0.02	0.067 ± 0.007	22.26
	Ru–Cl	2.41± 0.02	2.42± 0.02	0.054 ± 0.005	
3L$_9$	Ru–N	2.19 ± 0.02	2.18 ± 0.02	0.050 ± 0.005	23.28
	Ru–P	2.29± 0.02	2.29± 0.02	0.068 ± 0.007	21.71
	Ru–Cl	2.42± 0.02	2.41± 0.02	0.063 ± 0.006	
3L$_{10}$	Ru–N	2.19 ± 0.02	2.18 ± 0.02	0.050 ± 0.005	21.88
	Ru–P	2.29± 0.02	2.29± 0.02	0.069 ± 0.007	21.57
	Ru–Cl	2.42± 0.02	2.42± 0.02	0.061 ± 0.006	

The bond distances obtained from X-ray diffraction and EXAFS are in very good agreement with each other.

2. Synthesis and Structures of the Cationic Diamine(ether-phosphine)ruthenium(II) Complexes $4L_3$-$4L_5$, $4L_7$, $4L_8$, $4L_{10}$, and $4L_{14}$

2.1 General Considerations

In continuation of our investigations in this part of the thesis the synthesis and characterization of novel monocationic diamine(ether-phosphine)ruthenium(II) complexes are reported and their catalytic behavior is compared with their neutral precursors [25-27,61]. The intention was to improve the activity as hydrogenation catalysts. The abstraction of a chloride from the corresponding neutral ruthenium(II) complexes leaves a vacant coordination site which subsequently is occupied by an ether-oxygen donor. By incoming substrates this very weak bond is easily ruptured [26,30,36], a process which may enhance the formation of a mono- or dihydride intermediate in the mechanism of the hydrogenation of α,ß-unsaturated ketones [5,24,25].

2.2 Synthesis and Spectroscopic Characterization

If the *trans*-dichloro(diamine)(ether-phosphine)ruthenium(II) complexes **3** [25] are treated with one equivalent of $AgBF_4$, (**$3L_3$**, **$3L_5$**, **$3L_{10}$**, **$3L_{14}$)** or AgOTf (*trans*-**$3L_4$**, **$3L_7$**, **$3L_8$)** in dichloromethane only one chloride is abstracted. The vacant coordination site in each complex is occupied by an ether-oxygen atom resulting in the formation of the cationic complexes **$4L_3$-$4L_5$**, **$4L_7$**, **$4L_8$**, **$4L_{10}$**, and **$4L_{14}$** (see Scheme 3).

In contrast to the reaction with $AgBF_4$ which needs several hours that one with AgOTf proceeds within a few seconds [25-27]. The brown cationic complexes are sensitive to aerial oxygen, dissolve readily in chlorinated organic solvents, and are insoluble in ethers and aliphatic hydrocarbons. Their molecular composition was corroborated by FAB mass spectra.

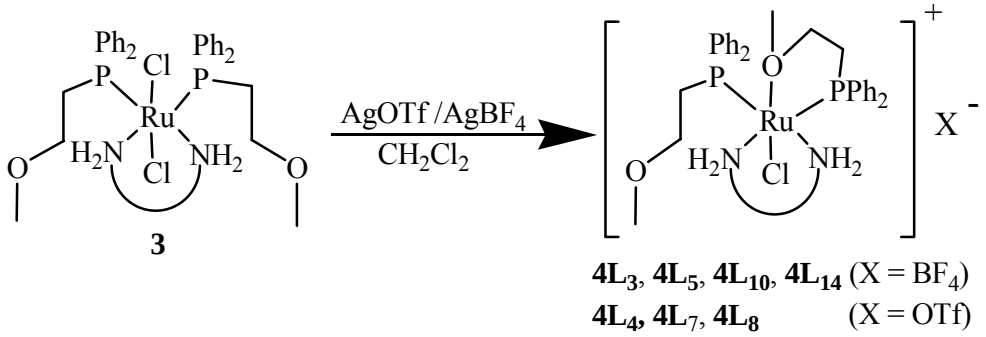

3

$4L_3$, **$4L_5$**, **$4L_{10}$**, **$4L_{14}$** (X = BF_4)
$4L_4$, **$4L_7$**, **$4L_8$** (X = OTf)

N~N

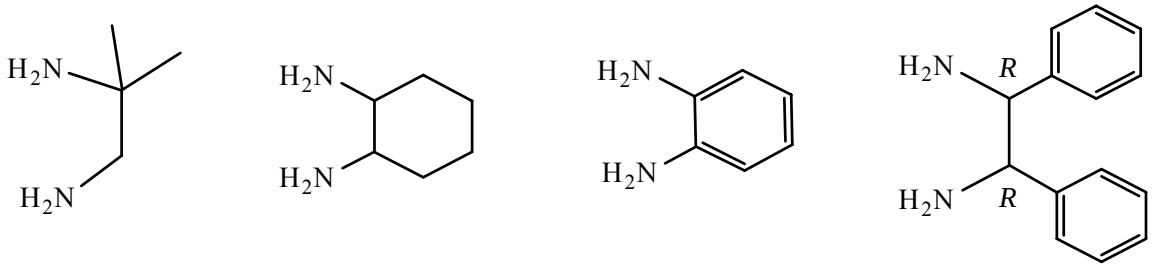

L_3 *trans*-**L_4** **L_5** **L_7**

L_8 **L_{10}** **L_{14}**

Scheme 3. Synthesis of the cationic diamine-bis(ether-phosphine)ruthenium(II) complexes **$4L_3$**-**$4L_5$**, **$4L_7$**, **$4L_8$**, **$4L_{10}$**, and **$4L_{14}$**

The formation of only one η^2-P⌒O chelate ring by abstracting of one chloride ion from complexes **4L$_3$-4L$_5$**, **4L$_7$**, **4L$_8$**, **4L$_{10}$**, and **4L$_{14}$** can be investigated by the ^{1}H, ^{13}C{^{1}H}, and ^{31}P{^{1}H} NMR spectra.

In the ^{1}H and ^{13}C{^{1}H} NMR spectra of **4L$_3$-4L$_5$**, **4L$_7$**, **4L$_8$**, **4L$_{10}$**, and **4L$_{14}$** characteristic sets of ^{1}H and ^{13}C signals are observed which arise from the phosphine and diamine ligands, respectively. The integration of the proton resonances indicates that the phosphine to diamine ratio is in agreement with the expected composition of **4L$_3$-4L$_5$**, **4L$_7$**, **4L$_8$**, **4L$_{10}$**, and **4L$_{14}$**. Furthermore, the chemical shifts and the number of resonances indicate the formation of only one η^2-P⌒O chelate ring, when one chloride has been abstracted.

In the ^{31}P{^{1}H} NMR spectra, the doublet of doublets which are observed for **4L$_3$-4L$_5$**, **4L$_7$**, **4L$_8$**, **4L$_{10}$**, and **4L$_{14}$** with typical coupling constants between 36.2 and 38.7 Hz agree with the *cis* arrangement of the phosphine ligands. The number of signals due to the methoxy protons in the ^{1}H NMR spectra, is consistent with the isomers which are detected by ^{31}P{^{1}H} NMR spectroscopy. Characteristic features in the ^{13}C{^{1}H}NMR spectra are the singlets of the methoxy carbon atoms of the η^2-P⌒O function, which are shifted downfield (2-5 ppm) compared to those of the η^1-P~O ligands. For those diamine ligands with reduced symmetry, chiral centers are generated in the complexes which lead to diasteroisomers, and thus to additional resonances in the NMR spectra (see experimental part). Four *cis*-oriented coordination isomers with C_1 symmetry can be formed (Chart 2). As in neutral diamine(ether-phosphine)ruthenium(II) complexes, isomers with phosphine ligands located *trans* to the diamines are favored in solution [25] (see Chart 2**)**.

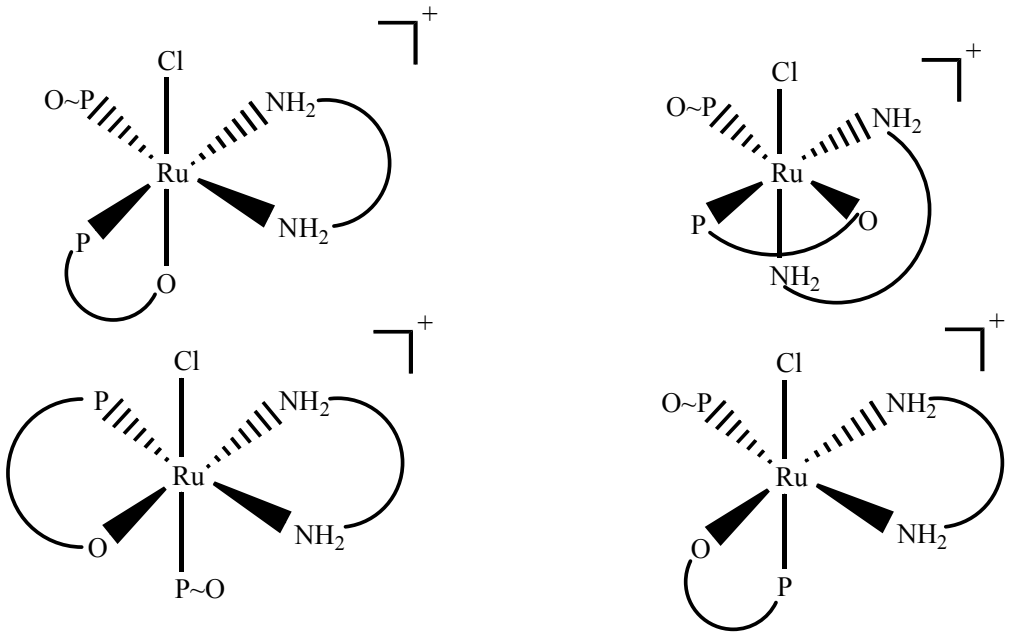

Chart 2. Possible *cis*-isomers of **4L$_4$**, **4L$_5$**, **4L$_{10}$**, and **4L$_{14}$** (with C_2 symmetric *N*-ligands)

The IR spectra of the complexes **2L$_1$-2L$_6$** in particular show four sets of characteristic absorptions in the ranges 3352-3314, 3265-3200, 3168-3155, and 280-260 cm^{-1}, which can be assigned to NH_2, amine-CH, phosphine-CH and RuCl stretching vibrations, respectively.

2.3 X-ray Structural Determination of Complex 4L$_3$

Crystals suitable for an X-ray structural analysis have been obtained for **4L$_3$** · H_2O. The molecular structure is shown in Figure 4, selected bond distances and angles are summarized in Table 4.

There are two ether-phosphine ligands in this cationic complex that differ in their hapticity. The ether chain of the η^1-*P*-coordinated phosphine ligand adopts an all-*trans*

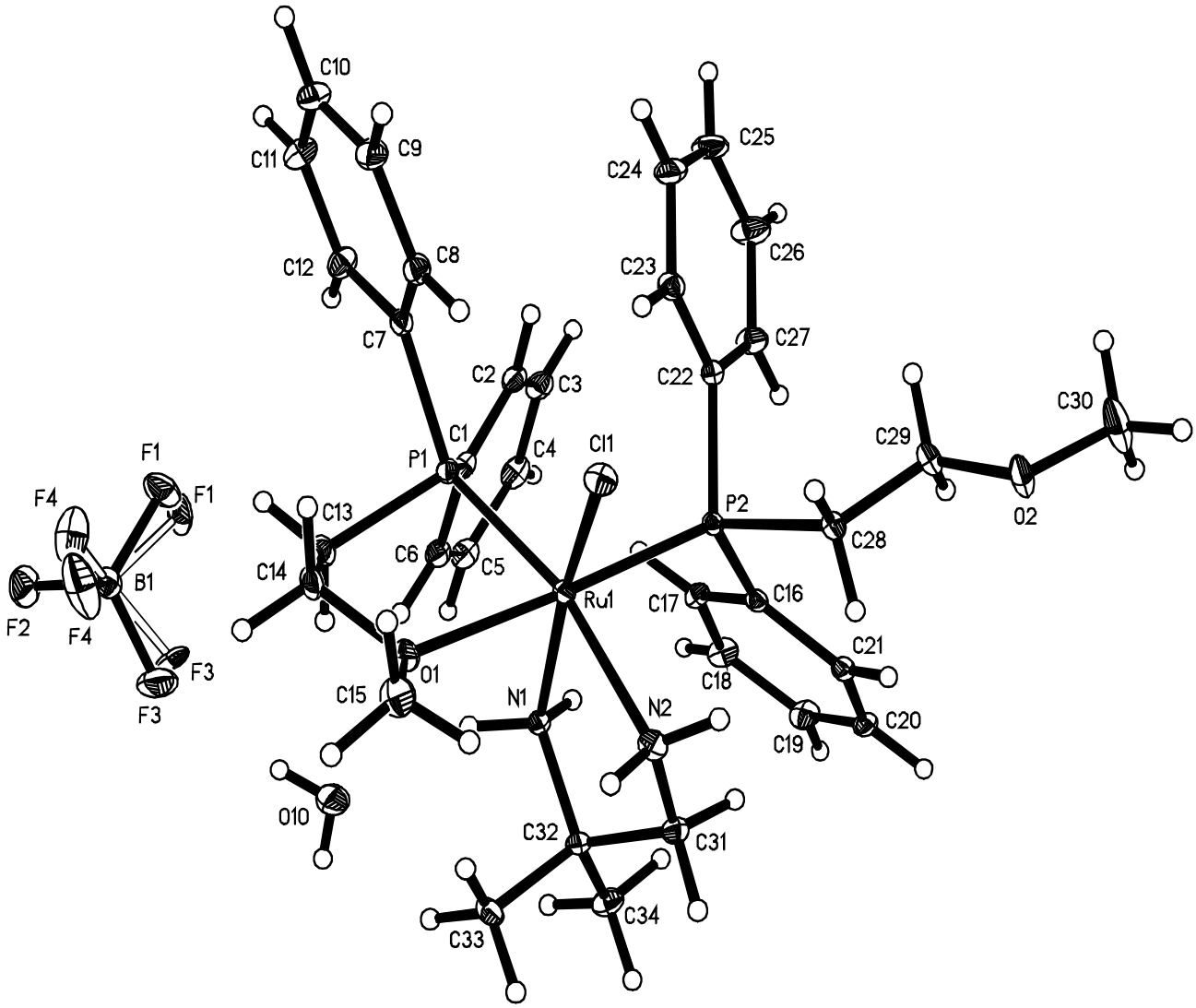

Figure 4. Molecular structure of **4L$_3$** · H_2O. Thermal ellipsoids are drawn at the 20% probability level

Table 4. Selected bond lengths [Å] and bond and torsion angles [°] for **4L$_3$** · H_2O

	4L$_3$ · H_2O
Bond lengths	
Ru(1)-Cl(1)	2.416(8)
Ru(1)-O(1)	2.244(2)
Ru(1)-P(1)	2.304(9)
Ru(1)-P(2)	2.226(15)
Ru(1)-N(1)	2.135(2)
Ru(1)-N(2)	2.184(3)
Bond angles	
P(1)-Ru(1)-O(1)	80.98(6)
P(1)-Ru(1)-P(2)	98.17(3)
N(1)-Ru(1)-N(2)	79.20(9)

conformation, with torsional angles in the range of 168.4 to 175.1°, while the ether chain of the η^2-*O*,*P*-coordinated phosphine forms part of a chelate ring in the twist conformation, with C(13) and C(14) displaced by 0.61 and -0.18 Å above and below the P(1)-Ru(1)-O(1) plane. A similar conformation is found for the chelate ring formed by the diamine ligand, with C(31) and C(32) displaced by -0.48 and 0.17 Å from the N(1)-Ru(1)-N(2) plane. The solvent water forms hydrogen bonds with two neighboring tetrafluoroborate anions, O(19)-H(10A)···F(2) 2.11 Å, O(10)-H(10B)···F(3) 1.94-2.13 Å, resulting in a helical arrangement of alternating water and BF_4^- groups. The cation of **4L$_3$** is „docked“ to this helix via weaker hydrogen bonds involving the protons of the amines: N(1)-H(1A)···O(10) 2.34 Å, N(2)–H(2A)···F(1) 2.22 Å.

3. Synthesis and Structures of Diamine(diphosphine)ruthenium(II) Complexes $6L_1$-$6L_{12}$

3.1 General Considerations

In the preceding chapters novel neutral and cationic diamineruthenium(II) complexes were introduced which were provided with hemilabile ether-phosphine ligands [25-27]. By introduction of T-silyl functions into the ether-phosphine ligands, these complexes can be supported onto a polysiloxane matrix after a sol-gel process [36,39]. Now a facile and fast synthesis of a series of diamine(diphos)ruthenium(II) complexes is presented. As a diphos ligand 1,3-bis(diphenylphosphino)propane was selected, because in principle it can easily be attached to a spacer unit at the symmetric carbon atom 2 of the ligand backbone [36-38].

3.2 Synthesis and Spectroscopic Characterization

The precursor compound *trans*-$Cl_2Ru(dppp)_2$ (**5**) was obtained by a substitution reaction starting from $Cl_2Ru(PPh_3)_3$ (**1**) and dppp in dichloromethane [62]. If **5** is treated with the diamines $\mathbf{L_1}$-$\mathbf{L_{12}}$ in dichloromethane, the yellow, somewhat air-insensitive mixed diamine[bis(diphenylphosphino)propane]ruthenium(II) complexes $\mathbf{6L_1}$-$\mathbf{6L_{12}}$ were formed in good to excellent yields. Even in the presence of excess diamine only one dppp ligand was exchanged (Scheme 4). The yields of the complexes $\mathbf{6L_1}$-$\mathbf{6L_{12}}$ depend on steric factors of the diamine ligands. If one or both hydrogen atoms at the nitrogen donors are replaced by alkyl or aryl groups no reaction takes place. Bipyridine and other aromatic *N*-derivatives do not react

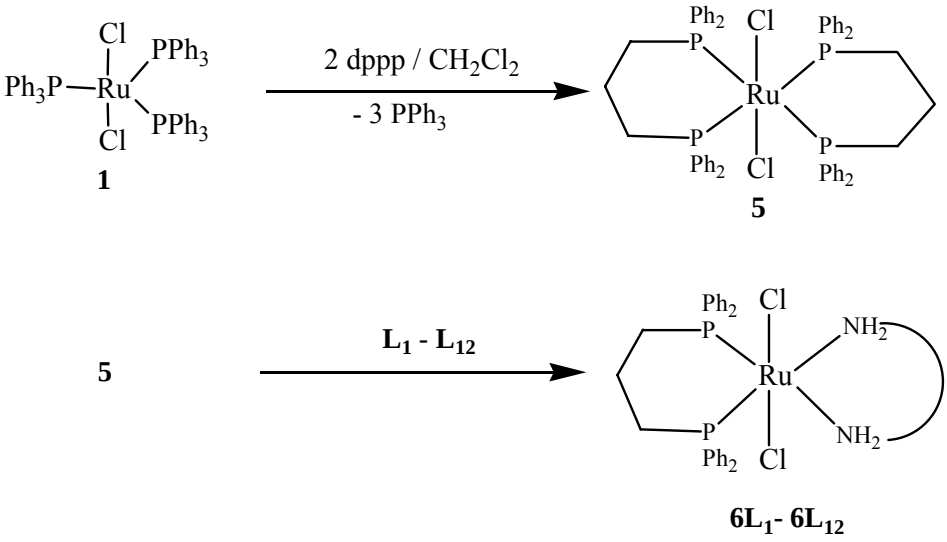

N~N

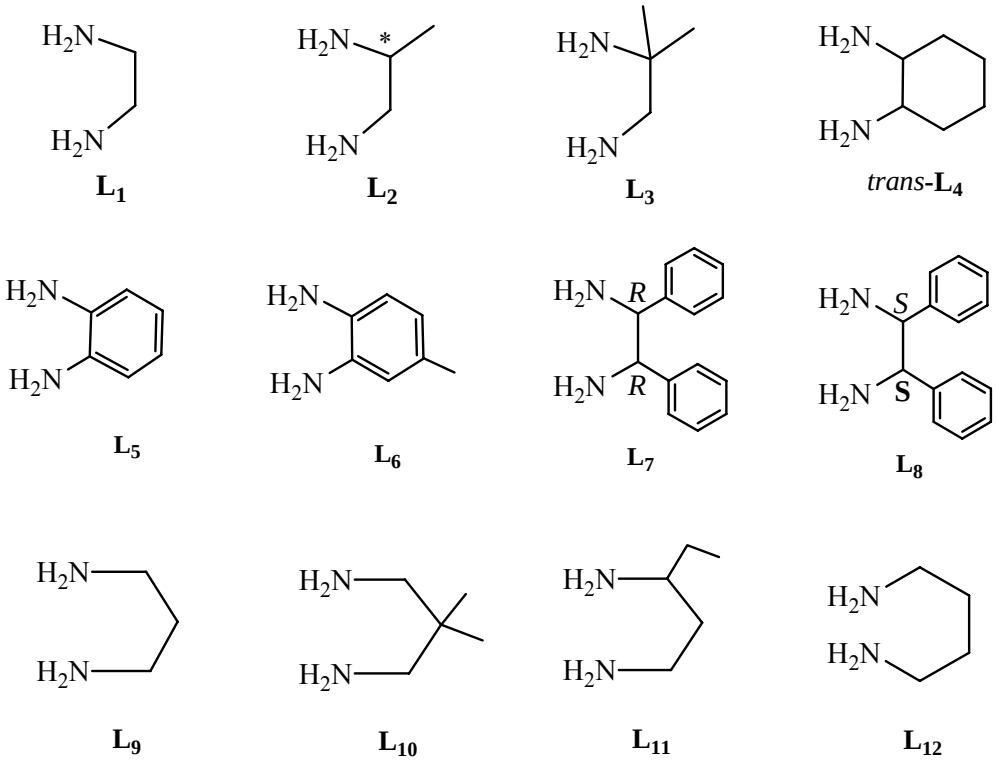

Scheme 4. Synthesis of the diamine(diphosphine)ruthenium(II) complexes **6L$_1$-6L$_{12}$**

with complex **5**, even under elevated conditions. Complexes **6L$_1$-6L$_{12}$** are soluble in chlorinated organic solvents and insoluble in ethers and aliphatic hydrocarbons. Their molecular composition was corroborated by FAB mass spectra.

In the ^{1}H NMR spectra of the diamine(dppp)ruthenium(II) complexes **6L$_1$-6L$_{12}$** characteristic sets of signals were observed, which are attributed to the phosphine and diamine ligands. Their assignment was supported by two-dimensional H,H-COSY experiments, which establish the connectivity between NH_2 and CH_2 functions in the diamine ligands, as well as between CH_2 and CH_2P groups in the phosphine fragments. The integration of the ^{1}H resonances confirm that the phosphine to diamine ratios are in agreement with the compositions of **6L$_1$-6L$_{12}$**. Because singlets are observed in the $^{31}P\{^1H\}$ NMR spectra of the $RuCl_2$(dppp)diamine complexes **6L$_1$**, **6L$_4$**, **6L$_5$**, **6L$_7$-6L$_{10}$**, and **6L$_{12}$** the C_1 symmetric structure **V** in Chart 3 is ruled out. In the cases of **6L$_2$**, **6L$_3$**, and **6L$_{11}$** the asymmetric diamines cause a loss of the C_2 axis which results in a splitting of the ^{31}P resonances into AB patterns. However, in **6L$_6$** this asymmetry is too remote from the phosphorus atoms to generate an observable splitting of the $^{31}P\{^1H\}$ NMR signal. The ^{31}P chemical shifts and the ^{31}P-^{31}P coupling constants are consistent with a *cis* arrangement of the P groups according to structure **IV** (Chart 3).

IV **V**

Chart 3. Tow possible structural isomers of $RuCl_2(P^{\frown}P)(N^{\frown}N)$

Characteristic sets of resonances between 15-30 and 35-49 ppm are found in the $^{13}C\{^{1}H\}$ NMR spectra of **$6L_1$–$6L_{12}$**, which are attributed to the aliphatic part of the phosphine and diamine ligands, respectively. AXX´ splitting patterns were observed for the aliphatic and aromatic carbon atoms directly attached to phosphorus. They are caused by the interaction of the magnetically inequivalent phosphorus atoms with the ^{13}C nuclei. This pattern is also consistent with structure **IV** (Chart 3).

The IR spectra of the complexes **$6L_1$-$6L_{12}$** in particular show four sets of characteristic absorptions in the ranges 3336-3319, 3268-3215, 3178-3165, and 275-254 cm^{-1}, which can be assigned to NH_2, amine-CH, phosphine-CH and RuCl stretching vibrations, respectively.

3.3 X-ray Structural Determination of Complexes $6L_1$, $6L_2$, and $6L_8$

Crystals suitable for X-ray structural analysis have been obtained for complexes **$6L_1$**, **$6L_2$**, and **$6L_8$**. Their molecular structures are shown in Figure 5 and selected bond distances, bond angles, and torsion angles are listed in Table 5. All three compounds feature two different chelate systems: a six-membered bis(phosphine) ring that is common to all three and adopts a similar chair conformations in each case, and a five-membered diamine ring that differs from complex to complex only in the number and kind of substituents at the carbon backbone. While the bis(phosphine) ring allows for P-Ru-P angles very close to the ideal value of 90°, the smaller diamine enforces N-Ru-N angles that are 9-13° less than the ideal value. The most striking difference between the three complexes is the finding that **$6L_1$** and **$6L_2$** form the *cis*-chloro isomer **V** (Chart 3), while **$6L_8$** crystallizes as the more usual *trans*-chloro isomer **IV**, although all three compounds were shown by spectroscopic methods to be the *trans*-chloro isomer in solution (*vide supra*).

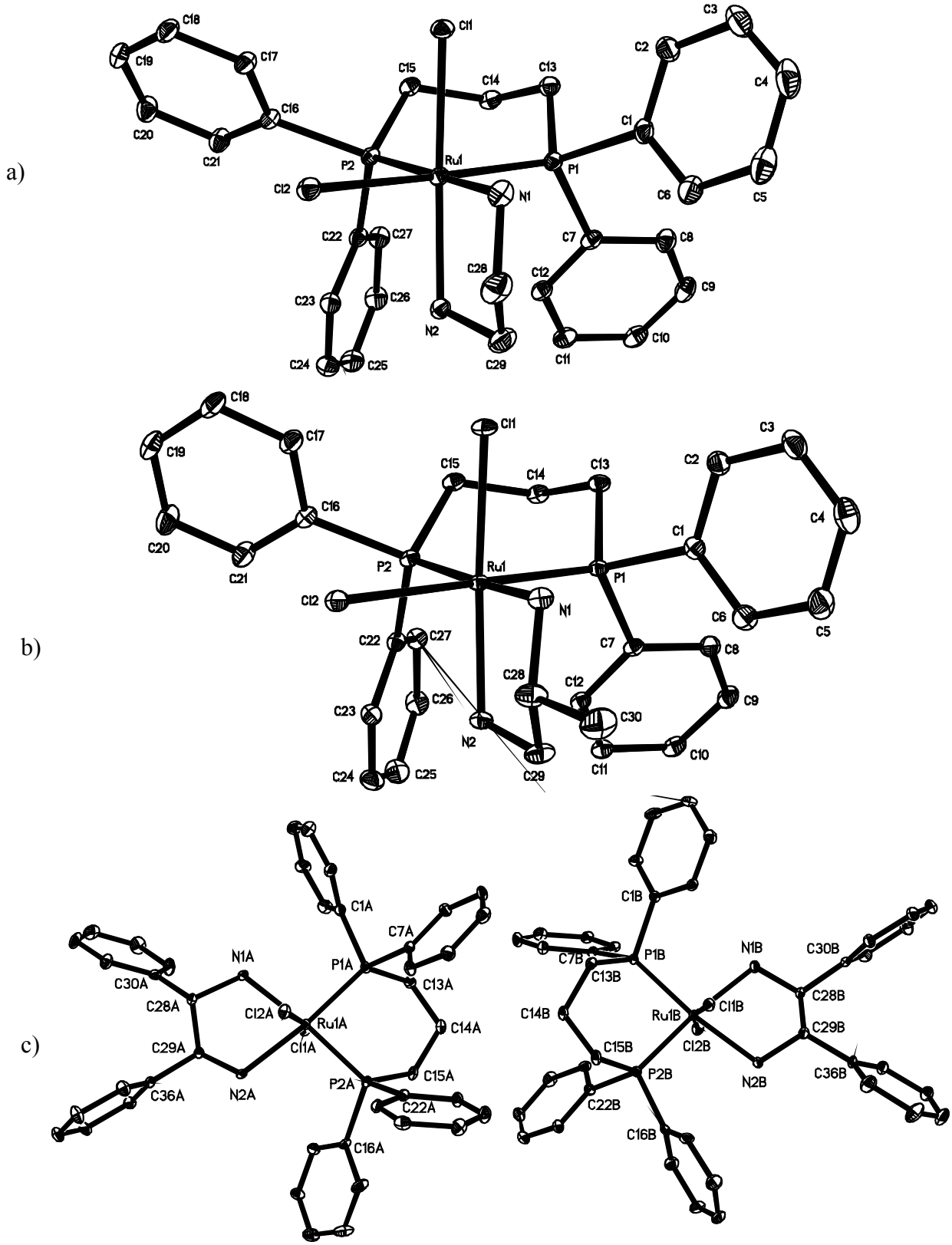

Figure 5. ORTEP plots of $\mathbf{6L_1}$ (a), $\mathbf{6L_2}$ (b) and the two crystallographically nonequivalent molecules of $\mathbf{6L_8}$ (c) with atom labeling scheme. Thermal ellipsoids are drawn at the 20% probability level, hydrogens and solvent molecules are omitted for clarity

The structure of **6L$_1$** is similar to that of the bis(ether-phosphine)ruthenium complex, $RuCl_2(H_3COCH_2CH_2PPh_2)_2$(en), described earlier [25-27]: the Ru-P and Ru-N distances *trans* to chlorine are slightly shorter than those *trans* to nitrogen or phosphorus, respectively. Similarly, the Ru-Cl distances *trans* to nitrogen are slightly shorter than those *trans* to phosphorus. The diamine chelate prefers the twist conformation, with C(28)-0.24 Å below and C(29) 0.42 Å above the N(1)-Ru(1)-N(2) plane. Figure 5 and the data in Table 5 indicate that the structure of **6L$_2$** is quite similar to that of **6L$_1$**, albeit the former cocrystallizes with one molecule of dichloromethane. It appears that, otherwise, the methyl substituent at C(28) exerts little effect on the structural, parameters, although the twist conformation of the diamine is more regular, with C(28) and C(29) displaced by -0.32 and 0.33 Å below and above the N(1)-Ru(1)-N(2) plane. In contrast, the phenyl substituents of the diamine in **6L$_8$** cause a change in the symmetry of the complex: **6L$_8$** crystallizes as the *trans*-chloro isomer with two independent molecules in the asymmetric unit. Both molecules are arranged about a pseudo-inversion center that approximately maps the greater part of molecule A to molecule B, except for the *S,S*-configuration of the diamine ligand that does not allow for a centrosymmetric space group. In addition, the diamine chelates adopt slightly different conformations: in molecule B it is the normal twist conformation, with C(28B) and C(29B) by 0.31 and -0.50 Å above and below the N-Ru-N plane, but in A it is close to an envelope with C(29A) at the top: C(28A) and C(29A) are displaced by -0.07 and 0.59 Å from the N-Ru-N plane.

Table 5. Selected bond lengths [Å] and bond and torsion angles [°] for **6L$_1$**, **6L$_2$**, and molecules A and B of **6L$_8$**

	6L$_1$	**6L$_2$**	**6L$_8$**, A	**6L$_8$**, B
Bond lengths				
Ru(1)-Cl(1)	2.404(2)	2.4208(8)	2.4293(10)	2.4227(11)
Ru(1)-Cl(2)	2.466(2)	2.5103(10)	2.4164(11)	2.4122(11)
Ru(1)-P(1)	2.2321(18)	2.2440(10)	2.2563(12)	2.2640(12)
Ru(1)-P(2)	2.2820(14)	2.2769(8)	2.2652(12)	2.2518(12)
Ru(1)-N(1)	2.172(2)	2.1629(19)	2.171(4)	2.183(4)
Ru(1)-N(2)	2.147(3)	2.1333(18)	2.172(4)	2.193(4)
Bond angles				
Cl(1)-Ru(1)-Cl(2)	89.13(9)	91.98(3)	165.80(4)	167.15(4)
P(1)-Ru(1)-P(2)	91.67(6)	90.88(3)	89.21(4)	89.35(4)
N(1)-Ru(1)-N(2)	80.80(10)	79.87(7)	78.07(14)	77.28(14)
N(1)-Ru(1)-Cl(1)	86.11(8)	84.71(6)	83.75(11)	87.97(11)
N(2)-Ru(1)-Cl(1)	166.24(6)	164.14(5)	89.23(10)	83.99(11)
P(1)-Ru(1)-Cl(1)	87.89(9)	87.94(3)	88.53(4)	89.78(4)
P(2)-Ru(1)-Cl(1)	91.48(5)	90.95(3)	90.70(4)	89.07(4)
N(1)-Ru(1)-Cl(2)	80.85(8)	83.24(6)	83.07(11)	84.19(11)
N(2)-Ru(1)-Cl(2)	84.66(10)	82.62(6)	82.89(10)	84.37(11)
P(1)-Ru(1)-Cl(2)	174.25(2)	177.88(2)	98.04(4)	101.25(4)
P(2)-Ru(1)-Cl(2)	93.32(6)	91.24(3)	101.91(4)	97.54(4)
Torsion angles				
P(2)-Ru(1)-P(1)-C(13)	40.48(10)	44.08(9)	49.65(16)	46.73(16)
Ru(1)-P(1)-C(13)-C(14)	-61.45(18)	-63.64(16)	-65.1(3)	-50.41(17)
P(1)-C(13)-C(14)-C(15)	72.2(2)	71.1(2)	68.6(4)	65.1(5)
C(13)-C(14)-C(15)-P(2)	-69.4(3)	-68.3(2)	-67.0(5)	-68.3(5)
C(14)-C(15)-P(2)-Ru(1)	55.51(19)	55.55(18)	59.9(3)	66.3(4)
C(15)-P(2)-Ru(1)-P(1)	-38.22(10)	-39.71(8)	-46.34(17)	-50.41(17)
N(2)-Ru(1)-N(1)-C(28)	-10.06(18)	-13.47(16)	2.8(2)	13.1(2)
Ru(1)-N(1)-C(28)-C(29)	35.2(3)	37.6(3)	-28.7(3)	-43.9(3)
N(1)-C(28)-C(29)-N(2)	-52.1(3)	-50.8(3)	49.0(3)	61.5(3)
C(28)-C(29)-N(2)-Ru(1)	41.9(3)	38.9(2)	-47.3(3)	-50.3(3)
C(29)-N(2)-Ru(1)-N(1)	-17.43(17)	-13.88(16)	24.9(2)	20.7(2)

3.4 Comparative Studies Between EXAFS Investigations and X-ray Diffraction Methods of Complexes $6L_2$, *trans*-$6L_4$, and $6L_8$

In the analysis of the experimental k^3 weighed $\chi(k)$ function, a three shell model can be fitted for the complexes **$6L_2$**, **$6L_4$**, and **$6L_8$**. The first shell has two nitrogen backscatterers, the second shell contains two phosphorus backscatterers, and the third shell has two chlorine backscatterers. As an example, the experimental data and the fitted functions of complex **$6L_8$** is shown in k space as well as by Fourier transformations in real space (Figure 6).

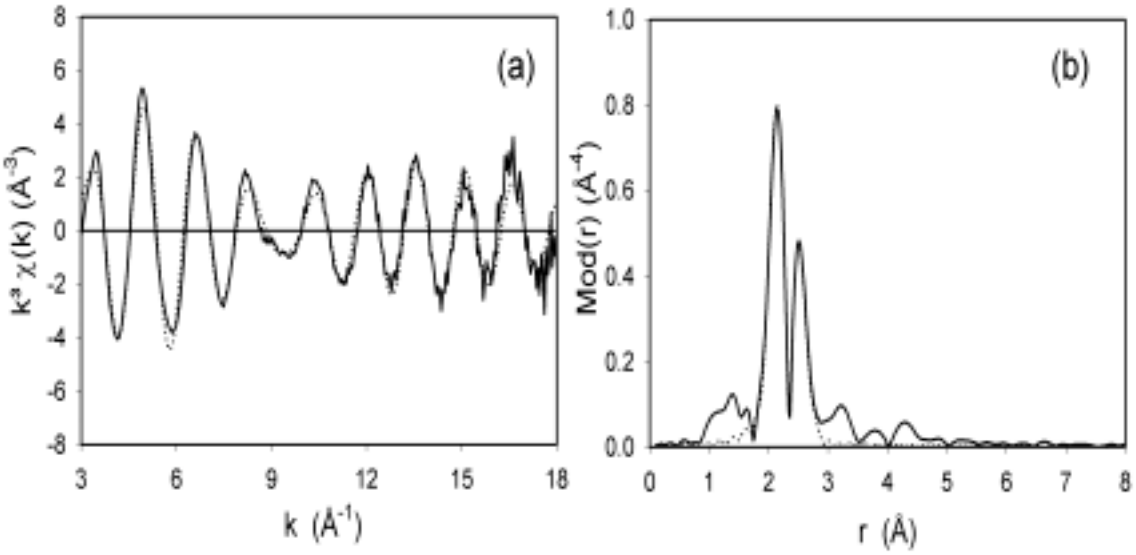

Figure 6. Experimental (solid line) and calculated (dotted line) $k^3 \chi$ (k) functions (a) and their Fourier transforms (b) for **$6L_8$** in the *k*-range 3.00 - 18.00 $Å^{-1}$

The structural parameters of the complexes obtained from EXAFS and X-ray diffraction are compared in Table 6.

Table 6. Structural parameters for the complexes **6L$_2$**, *trans*-**6L$_4$**, and **6L$_8$** obtained from X-ray diffraction and EXAFS

Complex	Bond type	r[Å], X–ray data	r[Å], EXAFS data	Debye-Waller factor σ [Å]	R factor and E_0 value
6L$_2$	Ru–N	2.16 ± 0.02	2.19 ± 0.02	0.050 ± 0.005	22.47
	Ru–P	2.26± 0.02	2.26± 0.02	0.056 ± 0.006	21.99
	Ru–Cl	2.45± 0.02	2.41± 0.02	0.065 ± 0.007	
trans-**6L$_4$**	Ru–N	2.17 ± 0.02	2.19 ± 0.02	0.064 ± 0.006	23.07
	Ru–P	2.26± 0.02	2.26± 0.02	0.048 ± 0.005	22.66
	Ru–Cl	2.45± 0.02	2.41± 0.02	0.065 ± 0.0067	
6L$_8$	Ru–N	2.18 ± 0.02	2.17 ± 0.02	0.050 ± 0.005	25.05
	Ru–P	2.26± 0.02	2.26± 0.02	0.060 ± 0.006	21.78
	Ru–Cl	2.41± 0.02	2.42± 0.02	0.063 ± 0.006	

The bond distances obtained from X–ray diffraction and EXAFS are in very good agreement with each other.

4. Synthesis and Characterization of the Sol-Gel-Processed T-Silyl Functionalized Diamine(ether-phosphine)ruthenium(II) Complexes $8L_1(T^3)(Me\text{-}T^3)$, $8L_2(T^3)(Me\text{-}T^3)$, and $8L_9(T^3)(Me\text{-}T^3)$

4.1 General Considerations

Interphase catalysts [62,37,39] have attained a remarkable importance since they are able to combine the advantages of homogeneous and heterogeneous catalysis with a considerable reduction of notorious drawbacks like leaching and limited catalytic activity of the reactive centers [63-67]. Interphases are systems in which a stationary phase (e.g. a reaction center linked to a matrix via a spacer) and a mobile component (e.g. a gaseous, liquid, or dissolved reactant) penetrate each other on a molecular scale without forming a homogeneous phase [63-66]. If such interphases are provided with a swellable polymer, they are able to imitate homogeneous conditions, because the active centers become highly mobile simulating the properties of a solution and hence they are accessible for substrates (Figure 7)[65-68,39].

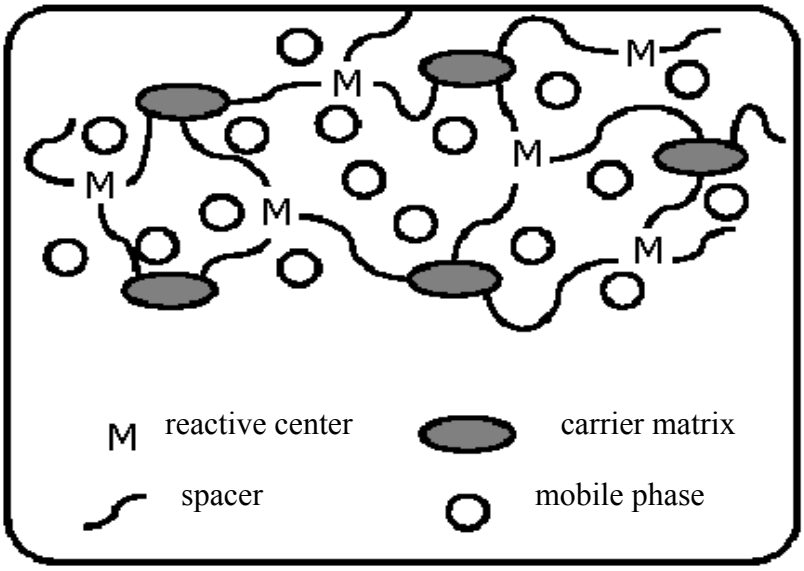

Figure 7. Schematic description of an interphase

In an earlier investigation the above-mentioned diamine-bis(ether-phosphine)-ruthenium(II) complexes [25-27] were provided with spacer functions at the periphery of the phosphine ligands with hydrolyzable T-silyl groups at their ends [39]. In continuation of the mentioned work now it is reported on the poly-co-condensation of a set of T-silyl functionalized diamine-bis(ether-phosphine)ruthenium(II) complexes with 10 equivelant amounts of $MeSi(OMe)_3$ (**Me-T°**). An indispensable technique to characterize these polymeric materials is solid-state NMR spectroscopy. Some of the hybrid catalysts were also exemplarily probed by EXAFS, EDX, SEM, and BET measurements [36,38-39].

4.2 Sol-Gel Processing

For the access of reproducible polymeric materials uniform reaction conditions have to be maintained. The properties of the sol-gel processed products strongly depend on reaction conditions like type of solvent, kind of catalyst, concentration of the monomers, reaction time, and temperature [69,70]. All polycondensations were performed in a mixture of THF/MeOH with an excess of water and $(n\text{-Bu})_2Sn(OAc)_2$ as catalyst. The alcohol is necessary to homogenize the reaction mixture. Sol-gel processes were carried out at ambient temperature in the presence of the co-condensation agent **Me-T°**. The stationary phases $\mathbf{8L_1(T^3)(Me\text{-}T^3)_{10}}$, $\mathbf{8L_2(T^3)(Me\text{-}T^3)_{10}}$, and $\mathbf{8L_9(T^3)(Me\text{-}T^3)_{10}}$ were synthesized by co-condensation of $\mathbf{7L_1(T^0)}$, $\mathbf{7L_2(T^0)}$, and $\mathbf{7L_9(T^0)}$ with **Me-T°** in a ratio of 1 : 10 (Scheme 6).

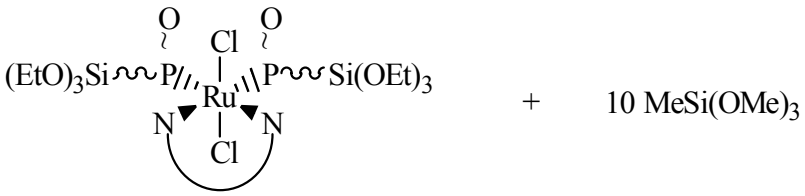

$7L_1(T^o)$, **$7L_2(T^o)$**, and **$7L_9(T^o)$**

\+ 10 $MeSi(OMe)_3$

Me-T°

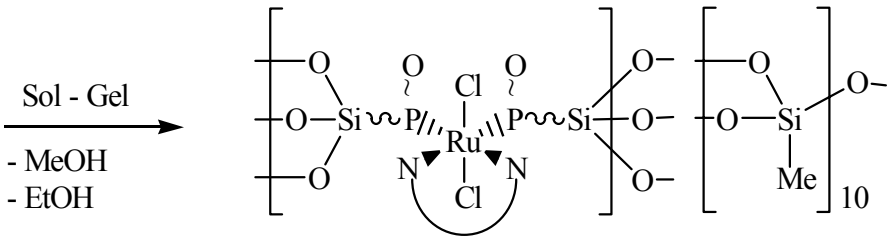

$8L_1(T^3)(Me\text{-}T^3)_{10}$, **$8L_2(T^3)(Me\text{-}T^3)_{10}$**, and **$8L_9(T^3)(Me\text{-}T^3)_{10}$**

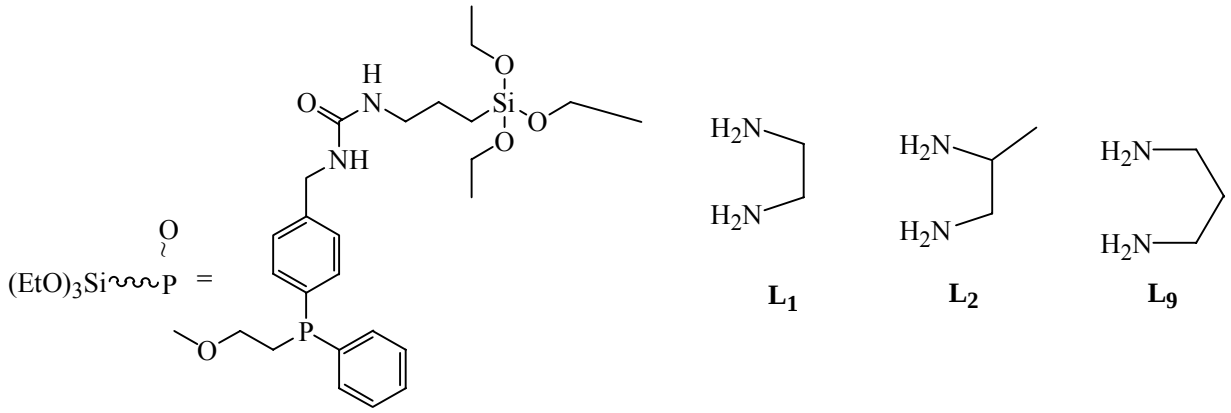

L_1 **L_2** **L_9**

Scheme 6. Structures and idealized compositions of **$8L_1(T^3)(Me\text{-}T^3)_{10}$**, **$8L_2(T^3)(Me\text{-}T^3)_{10}$**, and **$8L_9(T^3)(Me\text{-}T^3)_{10}$**

4.3 Solid-State ^{29}Si, ^{13}C, and ^{31}P CP/MAS Spectroscopic Investigations

Due to cross-linking effects the solubility of the polymeric materials **8L$_1$(T^3)(Me-T^3)$_{10}$**, **8L$_2$(T^3)(Me-T^3)$_{10}$**, and **8L$_9$(T^3)(Me-T^3)$_{10}$** is rather limited. Therefore solid-state NMR spectroscopy was used as a powerful technique for their characterization.

The ^{29}Si CP/MAS NMR spectra of the different materials show signals for substructures corresponding to T^n functions. The average chemical shifts for T^2 (δ = –58.0), and T^3 (δ = –65.3) are in agreement with values reported in the literature for comparable systems [70]. Since all silicon atoms are in direct proximity of protons the *Hartmann-Hahn* [71] match could efficiently be achieved. This allows the cross polarization method to be adapted for ^{29}Si solid-state NMR spectroscopic investigations.

In the ^{13}C CP/MAS NMR spectra of the supported complexes **8L$_1$(T^3)(Me-T^3)$_{10}$**, **8L$_2$(T^3)(Me-T^3)$_{10}$**, and **8L$_9$(T^3)(Me-T^3)$_{10}$** characteristic peaks at approximately δ = –0.3 and –3.8 are assigned to the carbon atoms of the silicon adjacent methyl groups in the Si–O–Si substructure of the poly-co-condensates. As a consequence of the sol-gel process, resulting in the formation of hybrid polymers, the carbon nuclei of the silicon neighboring methylene functions are shifted to lower field of about 5 ppm compared to the monomeric starting compounds. In some of the spectra only weak ^{13}C signals were assigned to residual Si–OR functionalities which point to a high degree of hydrolysis [71].

All ^{31}P resonances in the ^{31}P CP/MAS NMR spectra of **8L$_1$(T^3)(Me-T^3)$_{10}$**, **8L$_2$(T^3)(Me-T^3)$_{10}$**, and **8L$_9$(T^3)(Me-T^3)$_{10}$** are found in the expected ranges and are broadened due to the chemical shift dispersion [71].

4.4 EDX and BET Measurements

The complexes **8L$_1$(T^3)(Me-T^3)$_{10}$**, **8L$_2$(T^3)(Me-T^3)$_{10}$**, and **8L$_9$(T^3)(Me-T^3)$_{10}$** have been subjected to EDX (***E**nergy **D**ispersive **X**-ray analysis*) studies. The employment of the co-condensation agent **Me-T^o** leads to an uneven surface in the case of **8L$_1$(T^3)(Me-T^3)$_{10}$**. From **BET** (***B**runauer-**E**mmett-**T**eller-**M**ethod*) [36-39] measurements low surface areas between 2.3 and 5.94 m^2/g for **8L$_1$(T^3)(Me-T^3)$_{10}$**, **8L$_2$(T^3)(Me-T^3)$_{10}$**, and **8L$_9$(T^3)(Me-T^3)$_{10}$** are derived [36].

From the typical EDX measurements, the K_α lines of carbon, oxygen, silicon, phosphorus, and chlorine and the L line series of ruthenium and tin are visible. An overlap occurs between the L lines of ruthenium and the K lines of chlorine. This phenomenon is corrected by peak deconvolution. Due to its high fluorescence yield, the Au-M_α line also appears under the K_β emission of phosphorus. Despite the numerous sources of error EDX is the only method to provide a simultaneous quantification of all present elements, including oxygen in the presence of silicon, which is usually not possible with chemical methods due to the formation of silicon carbide during the combustion process. The elemental analyses of stationary phases **8L$_1$(T^3)(Me-T^3)$_{10}$**, **8L$_2$(T^3)(Me-T^3)$_{10}$**, and **8L$_9$(T^3)(Me-T^3)$_{10}$** by EDX are summarized in Table 7 and compared to data obtained from the stoichiometry of the educts. These have been renormalized excluding nitrogen and hydrogen, which is a single-electron atom and thus does not emit characteristic X-rays. Finally it has to be noted that an average amount of 4 mass % tin is observed in the materials.

Table 7. Elemental analysis of compounds **8L$_1$(T^3)(Me-T^3)$_{10}$**, **8L$_2$(T^3)(Me-T^3)$_{10}$**, and **8L$_9$(T^3)(Me-T^3)$_{10}$** by EDX [36]

	Reference data [a]						EDX [b]					
	Composition [%]											
Complexes	C	O	P	Si	Cl	Ru	C	O	P	Si	Cl	Ru
8L$_1$(T^3)(Me-T^3)$_{10}$	40.4	22.8	4.0	21.7	4.6	6.5	40.7	21.2	4.8	23.2	3.0	7.1
8L$_2$(T^3)(Me-T^3)$_{10}$	40.8	22.6	4.0	21.6	4.5	6.5	34.8	16.7	6.3	28.7	4.4	9.1
8L$_9$(T^3)(Me-T^3)$_{10}$	40.8	22.6	4.0	21.6	4.5	6.5	39.4	19.0	5.6	24.3	3.5	8.2

[a] Derived from the stoichiometry of the educts, excluding hydrogen and nitrogen. [b] Quantified by the ZAF correction procedure.

5. Application of the Diamine(phosphine)ruthenium(II) Complexes 2-6 and 8 as Hydrogenation Catalysts

5.1 General Considerations

To study the catalytic activity of the homogeneous and heterogeneous diamine(diphosphine)ruthenium(II) complexes**,** α,ß-unsaturated ketones are generally of interest as model substrates for different reasons: i) the hydrogenation of such substrates is not easy, because of their conformational flexibility [2]; ii) the ketone reveals UV activity, which disappears upon hydrogenation of the ketone due to interruption of the conjugation. This effect can be used to carry out kinetic investigations [55]; iii) the chosen ketones allow to study the selectivity of the catalysts. Three different possibilities of the hydrogenation process are to be expected (Scheme 7). The selective hydrogenation of the carbonyl function affords the corresponding unsaturated alcohol **A**, which is the most desired product. Unwanted and hence of minor interest is the hydrogenation of the C=C double bond, leading to the saturated ketone **B**. Also not in the focus of our interest is the hydrogenation of both the C=O and C=C bonds, resulting in the formation of the saturated alcohol **C** [28].

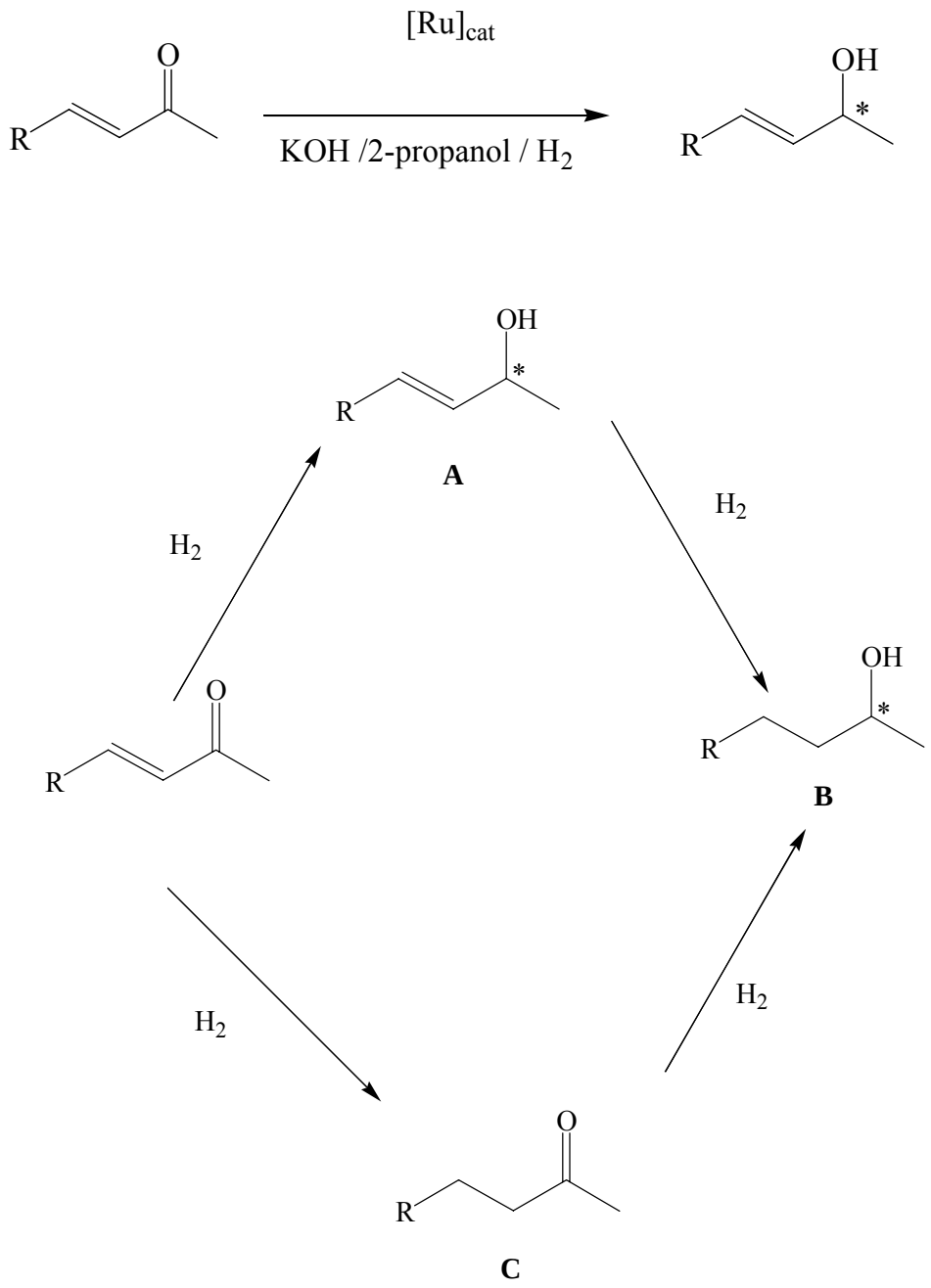

Scheme 7. Possible reaction products in the catalytic hydrogenation of α,ß-unsaturated ketones

5.2 Hydrogenation Conditions

All hydrogenations were carried out under mild conditions (1-4 bar hydrogen pressure and T = 35 C^o using several co-catalysts like KOH, *t*BuOK, and AgOTf) in a special low-pressure Schlenk tube (Figure 8).

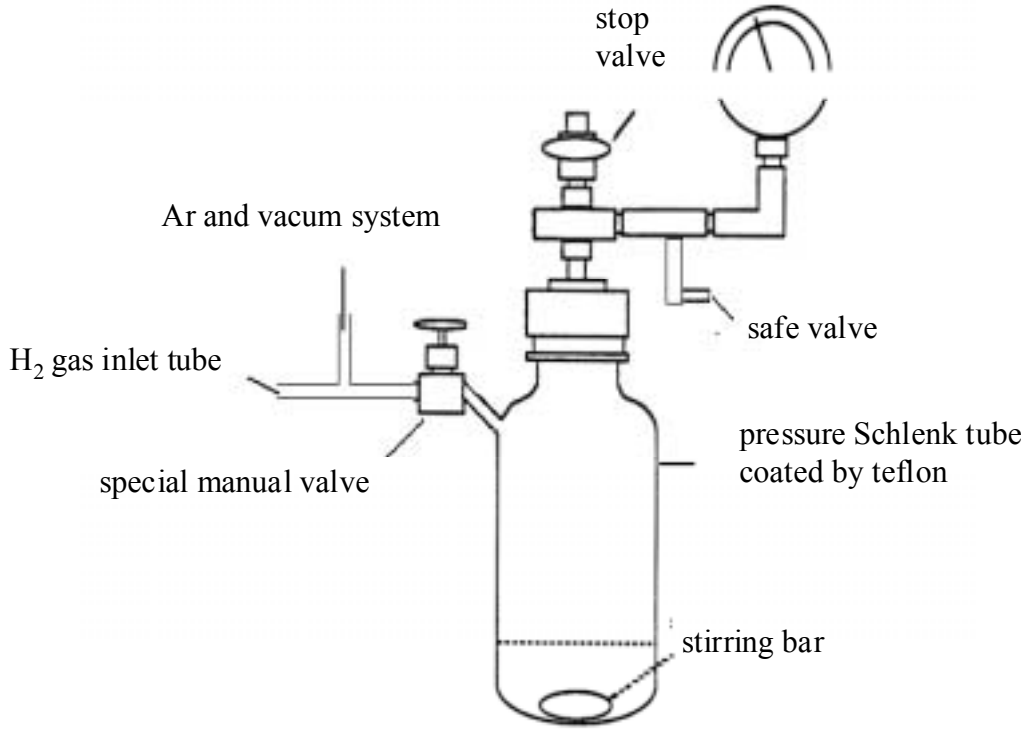

Figure 8. Schematic representation of a low-pressure Schlenk-tube for hydrogenations

2-Propanol served as a solvent, but the catalysts were only active in the presence of excess hydrogen and a co-catalyst (KOH or *t*BuOK) [9-27]. Aprotic and chlorinated solvents resulted only in moderate to low yields.

5.3 Different Examples for Hydrogenations

5.3.1 Neutral and Cationic Diamine(ether-phosphine)ruthenium(II) Complexes 2-4

In the present investigations *trans*-4-phenyl-3-butene-2-one (R = Ph in Scheme 7) has been selected as a substrate to be hydrogenated. As expected, the starting complex **2** was inactive (Table 8, run 1). This behavior is traced back to the absence of diamines. However, in the case of **3** and **4** excellent activities and selectivities in the hydrogenation of the carbonyl group were observed (Table 8), the latter is reminiscent of a stoichiometric reduction with $NaBH_4$. Turnover frequencies and conversions decreased when methyl groups were introduced at one carbon atom of the diamine in the complexes $\mathbf{3L_1}$-$\mathbf{3L_3}$. This is clearly due to steric effects (Table 8, runs 2-4). The hydrogen pressure has not affected the regioselectivity, but strongly influences the turnover frequencies (Table 8, runs 9-14). When the reaction was carried out in 2-propanol using catalyst $\mathbf{3L_8}$ at 35 ^{o}C with a molar substrate : catalyst (S/C) ratio of 1000 : 1, the turnover frequency was 200 h^{-1} at 0.4 bar of hydrogen pressure. By increasing the H_2 pressure to 1, 2, and 4 bar the turnover frequencies were enhanced from 1204 via 1688 to 2439 h^{-1} (Table 8, runs 11-14). However, only complexes were successful which were provided with 1,2-diamines. If 1,3-diamines were employed as co-ligands the selectivity decreases in favor of the hydrogenation of the C=C bond (Table 8, runs 15-20 and 33, and Scheme 7, **C**). If 1,4-diamines were employed as co-ligands no selectivity was achieved and all three hydrogenated compounds **A**, **B**, **C** were detected (Table 8, run 20). No catalytic activity was established when the aprotic diamine ruthenium complexes $\mathbf{3L_{14}}$ and $\mathbf{4L_{14}}$ were used (Table 8, runs 21 and 38). Only in the case of catalysts $\mathbf{3L_5}$, $\mathbf{3L_6}$, and $\mathbf{4L_5}$

Table 8. Hydrogenation of *trans*-4-phenyl-3-butene-2-one[a] using catalysts **2**, **3**, and **4**

Run	Catalyst	Conversion (%)[b]	H_2 (bar)	TOF[c]	Selectivity (%)[c] (**A B C**)
1	**2**	32	3	130	100 **C**
2	**3L$_1$**	90	3	1120	100 **A**
3	**3L$_2$**	80	3	960	100 **A**
4	**3L$_3$**	67	3	670	100 **A**
5	**3L$_4$**	100	3	1590	100 **A**
6	**3L$_4$**	100	2	1350	100 **A**
7	**3L$_5$**[d]	10	3	9	100 **C**
8	**3L$_6$**[d]	17	2	15	100 **C**
9	**3L$_7$**	100	4	1240	100 **A**
10	**3L$_7$**	100	2	1010	100 **A**
11	**3L$_8$**	40	0.4	200	100 **A**
12	**3L$_8$**	100	1	1200	100 **A**
13	**3L$_8$**	100	2	1690	100 **A**
14	**3L$_8$**	100	4	2440	100 **A**
15	**3L$_9$**	100	1	1500	79 **A** 21 **C**
16	**3L$_{10}$**	61	1	610	76 **A** 24 **C**
17	**3L$_{10}$**	97	4	1429	82 **A** 18 **C**
18	**3L$_{10}$**	93	2	930	82 **A** 18 **C**
19	**3L$_{11}$**	100	4	1000	72 **A** 28 **C**
20	**3L$_{12}$**[d]	27	3	18	18 **A** 43 **B** 57 **C**
21	**3L$_{14}$**[d]	0	2	0	0
22	**3L$_8$**[e]	100	2	1460	100 **A**

23	**3L$_7$**[e]	100	2	1030	100 **A**
24	**3L$_8$**[f]	100	2.5	520	100 **A**
25	**3L$_7$**[f]	100	2.5	480	100 **A**
26	**3L$_8$**[g]	100	2.5	1990	89 **A** 11 **B**
27	**3L$_7$**[g]	100	2.5	1880	87 **A** 13 **B**
28	**3L$_8$**[h]	100	2.5	1500	100 **A**
29	**3L$_7$**[h]	100	2.5	1090	100 **A**
30	**4L$_3$**	100	3	350	100 **A**
31	**4L$_4$**	100	3	570	100 **A**
32	**4L$_5$**[d]	3	3	2	100 **C**
33	**4L$_7$**	100	3	480	100 **A**
34	**4L$_8$**	100	3	610	100 **A**
35	**4L$_{10}$**	100	3	500	73 **A** 27 **C**
36	**4L$_7$**[e]	100	3	590	100 **A**
37	**4L$_8$**[e]	100	3	490	100 **A**
38	**4L$_{14}$**[d]	0	3	0	0

[a]Reaction was conducted at 35 C[o] using 3-10 g of substrate (S/C=1000) in 50 ml of 2-propanol. [Ru : KOH: Sub.][1:10:1000]. [b]Yields and selectivities were determined by GC. [c]TOF: turnover frequency (mol_{sub} mol^{-1}_{cat} h^{-1}). [d]15 h reaction. [e][Ru : *t*BuOK : Sub.][1:10:1000]. [f][Ru : KOH : AgOTf: Sub.][1:10: 5: 1000]. [g][Ru : KOH : Sub.][1:40:1000]. [h][Ru : KOH : Sub.][1:10:4000].

a complete hydrogenation to give **C** was observed with a low turnover frequency (Table 8, runs 7, 8, and 32). In runs 22, 23, 36, and 37 *t*BuOK as co-catalyst was applied. Similar conversions and turnover frequencies as in case of KOH were observed at the same conditions. The turnover frequencies decreased when AgOTf was applied as a co-catalyst, but the selectivity is still 100% toward the formation of **A** (Table 8, runs 24, 25). The saturated alcohol **B** was detected only in small amounts, when the concentration of the co-catalyst (KOH) was increased (≥ 40 mol) (Table 8, runs 26, 27). It is of high interest to note that both neutral and monocationic complexes with aromatic (**3L$_5$**, **3L$_6$**, and **4L$_5$**, Table 8, runs 7, 8, 32) and aprotic (**3L$_{14}$** and **4L$_{14}$**, Table 8, runs 21 and 38) diamines are catalytically inactive under mild conditions which is in agreement with the literature [2]. The monocationic complexes **4L$_3$**, **4L$_4$**, **4L$_7$**, **4L$_8$**, and **4L$_{10}$** (Table 8, runs 30-37) are highly active under mild conditions and except **4L$_{10}$** they give rise to a 100% selective hydrogenation toward the C=O group in the presence of a C=C function (Table 8, run 35). The same is true for the neutral diamine-bis(ether-phosphine)ruthenium(II) complexes **3L$_3$**, **3L$_4$**, **3L$_7$**, **3L$_8$**, and **3L$_{10}$** (Table 8, runs 3-7, 9-20) however, their activity is twice as high as that one of their monocationic counterparts (Figure 9).

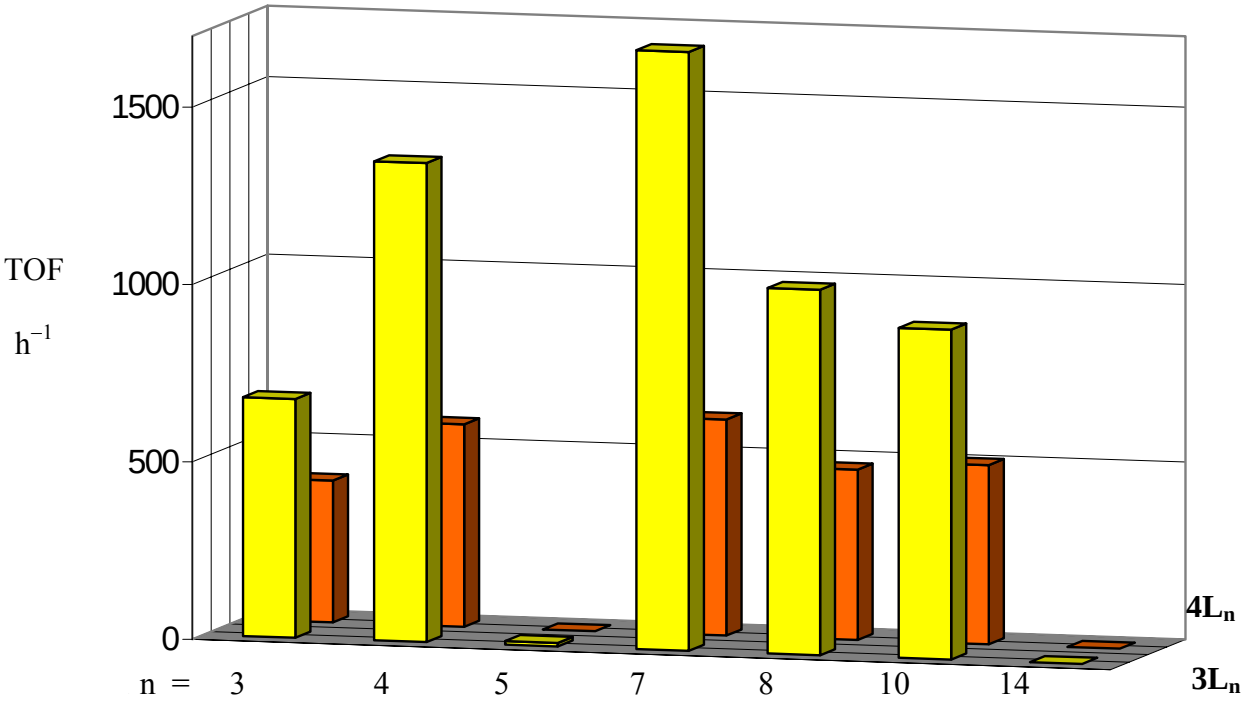

Figure 9. Hydrogenation of *trans*-4-phenyl-3-butene-2-one by the neutral and monocationic ruthenium(II) complexes **3L$_n$** and **4L$_n$**, respectively. Reaction conditions: 2-propanol as solvent, KOH as co-catalyst, T = 35 ^{o}C, P_{H_2} = 3 bar

5.3.2 Diamine(diphosphine)ruthenium(II) Complexes 6

Again *trans*–4-phenyl-3-butene-2-one served as a model substrate for the hydrogenation experiments. All hydrogenations were carried out under mild conditions at 3 bar H_2 pressure and T = 35 ^{o}C. 2-Propanol served as a solvent, but the catalysts were only active in the presence of excess hydrogen and a co-catalyst (e.g. KOH). Results are listed in Table 9.

Similar to the corresponding (ether-phosphine)ruthenium(II) complex **2** (chapter 5.3.1), $RuCl_2(dppp)_2$ (**5**) was completely inactive in the hydrogenation of unsaturated ketones. The starting complex $RuCl_2(PPh_3)_2$ (**1**) was only slightly active under the applied mild reaction conditions. However, the selectivity was low, because both the C=O and C=C functions were hydrogenated to give **C** with a conversion of only 28% (Table 9). With the exception of **$6L_5$, $6L_6$,** and **$6L_{12}$** all ruthenium(II) complexes (**$6L_1$-$6L_4$**, **$6L_7$-$6L_{11}$)** revealed high activity and excellent selectivity. In the case of **$6L_1$**, **$6L_4$**, **$6L_7$-$6L_9$**, and **$6L_{11}$**, a conversion of 100% has been achieved in less than one hour, and the only product was **A** (Table 9). If one or two methyl groups are introduced into the backbone of 1,2-diamines, a constant decrease of the turnover frequencies (TOFs) and the conversions was observed, which is probably due to steric effects (Table 9 and Figure10).

Table 9. Hydrogenation of *trans*-4-phenyl-3-butene-2-one [a] using catalysts **1**, **5**, and **6**

Run	Catalyst	Conversion (%) [b]	TOF [c]	Selectivity (%)[b]
				A B C
1	**1**	28 [d]	12	100 **C**
2	**5**	0 [d]	0	0
3	**6L$_1$**	100	1080	100 **A**
4	**6L$_2$**	90	776	100 **A**
5	**6L$_3$**	54	540	100 **A**
6	**6L$_4$**	100	1210	100 **A**
7	**6L$_5$**	28 [e]	18	100 **C**
8	**6L$_6$**	0 [d]	0	0
9	**6L$_7$**	100	1490	100 **A**
10	**6L$_8$**	100	1724	100 **A**
11	**6L$_9$**	100	926	100 **A**
12	**6L$_{10}$**	92	920	100 **A**
13	**6L$_{11}$**	100	2000	100 **A**
14	**6L$_{12}$**	25 [e]	17	45 **A** 55 **C**

[a] Reaction was conducted at 35 C^o using 3-10 g of substrate (S/C = 1000) in 50 ml of 2-propanol, P_{H_2} = 3 bar, [Ru : KOH : Substrate][1:10:1000]. [b]Yields and selectivities were determined by GC. [c]TOF: turnover frequency (mol_{sub} mol^{-1}_{cat} h^{-1}). [d] Overnight reaction. [e]15 h reaction.

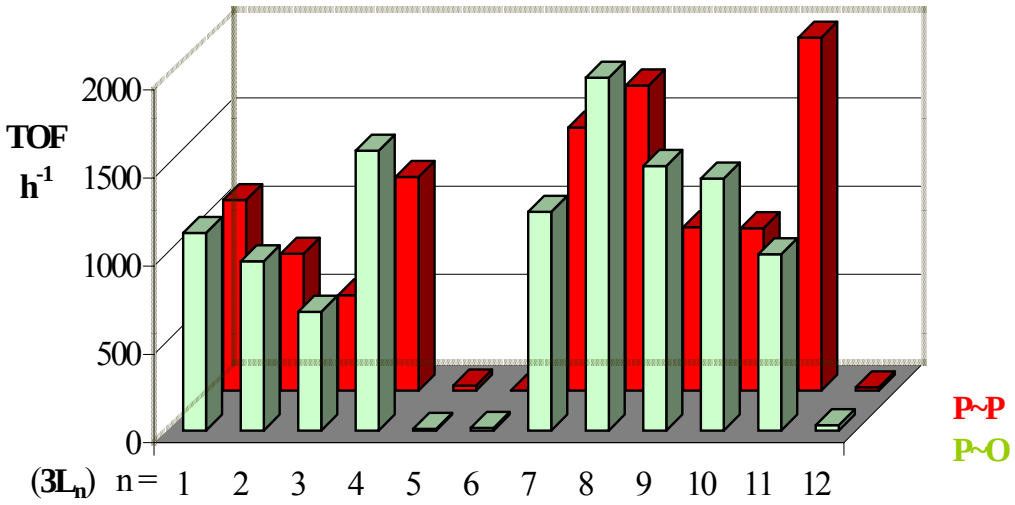

Figure 10. Ruthenium-catalyzed hydrogenation of *trans*-4-phenyl-3-butene-2-one. P~P ≅ is $RuCl_2$(diphos)diamine, P~O ≅ $RuCl_2$(ether-phosphine)$_2$diamine [26]. Reaction conditions: 2-propanol, KOH as co-catalyst, T = 35°C and P_{H_2} = 3 bar

5.3.3 Polysiloxane-Supported Diamine(ether-phosphine)ruthenium(II) Complexes $8L_1(T^3)(Me\text{-}T^3)_{10}$, $8L_2(T^3)(Me\text{-}T^3)_{10}$, and $8L_9(T^3)(Me\text{-}T^3)_{10}$

For reasons of comparison the substrate *trans*-4-phenyl-3-butene-2-one was again selected for the hydrogenation experiments with the interphase catalysts **$8L_1(T^3)(Me\text{-}T^3)_{10}$**, **$8L_2(T^3)(Me\text{-}T^3)_{10}$**, and **$8L_9(T^3)(Me\text{-}T^3)_{10}$**. All reactions proceeded under mild conditions (2 bar H_2 pressure, ratio Ru(II) : KOH : Sub. = 1 : 10 : 1000, T = 35 °C, 2-propanol as solvent).

Table 10. Hydrogenation of *trans*-4-phenyl-3-butene-2-one[a] using interphase catalysts **8** (comparison between interphase and the corresponding homogenous catalysts)

Run	Catalyst	Time (h)	Conversion (%) [b]	Selectivity (%) [b]
				A B C
1	**$3L_1$**	2	100	100 **A**
2	**$8L_1(T^3)(Me\text{-}T^3)_{10}$**	2	8	99 **A**
3	**$8L_1(T^3)(Me\text{-}T^3)_{10}$**	24	75	94 **A**
4	**$8L_1(T^3)(Me\text{-}T^3)_{10}$**	48	100	94 **A**
5	**$3L_2$**	2	100	100 **A**
6	**$8L_2(T^3)(Me\text{-}T^3)_{10}$**	48	100	99 **A**
7	**$3L_9$**	2	100	80 **A**
8	**$8L_9(T^3)(Me\text{-}T^3)_{10}$**	48	98	55 **A**

[a] Reaction was conducted at T = 35 C^o using 3-10 g of substrate (S/C = 1000) in 50 ml of 2-propanol, P_{H_2} = 3 bar, [Ru : KOH : Substrate][1:10:1000]. [b]Yields and selectivities were determined by GC.

From Table 10 it is derived that the tested interphase ruthenium(II) complexes show conversions between 98 and 100 %. Catalysts **8L$_1$(T^3)(Me-T^3)$_{10}$**, **8L$_2$(T^3)(Me-T^3)$_{10}$**, and **8L$_9$(T^3)(Me-T^3)$_{10}$** with 1,2-diamines as co-ligands revealed the highest selectivities toward the formation of **A**. The remaining 1-6 % selectivity is equally divided between **B** and **C**. However, the selectivity of **8L$_9$(T^3)(Me-T^3)$_{10}$** with an 1,3-diamine as a co-ligand is much lower and was found to be 55% toward **A** (Table 10 and Scheme 7). These results are in agreement with the corresponding homogeneous catalysts [25].

5.4 Experiments on the Role of the Co-catalysts

It is well known that the addition of a basic co-catalyst like NaOH, KOH, or *t*BuOK is an important issue in the described hydrogenation process [9-12]. Weak basic co-catalysts as K_2CO_3 show much lower catalytic rates [10, 55]. Several authors recently have evidenced that the bifunctional *cis*-oriented Ru–H/N–H motif plays a key role in the hydrogenation of unsaturated ketones [5,14,19-24]. In case of KOH the nucleophile OH^- attacks the ruthenium(II) center and replaces one chloride ligand to form a Ru–OH intermediate, which is an important precondition for the uptake of hydrogen [72]. Because of the hemilabile character of ether-phosphine ligands [35] the cationic ruthenium(II) complexes **4L$_3$-4L$_5$**, **4L$_7$**, **4L$_8$**, **4L$_{10}$**, and **4L$_{14}$** should be suitable to reconstruct such a process. As an example served complex **4L$_7$** which was dissolved in 1 ml of 2-propanol in an NMR tube. When this solution was treated with *t*BuOK at room temperature, the main ^{31}P signals at δ 58.5/58.1, 54.6/54.3, and 48.2/47.9 gradually disappear in favor of a new resonance at δ = 38.6 (see Figure 11).

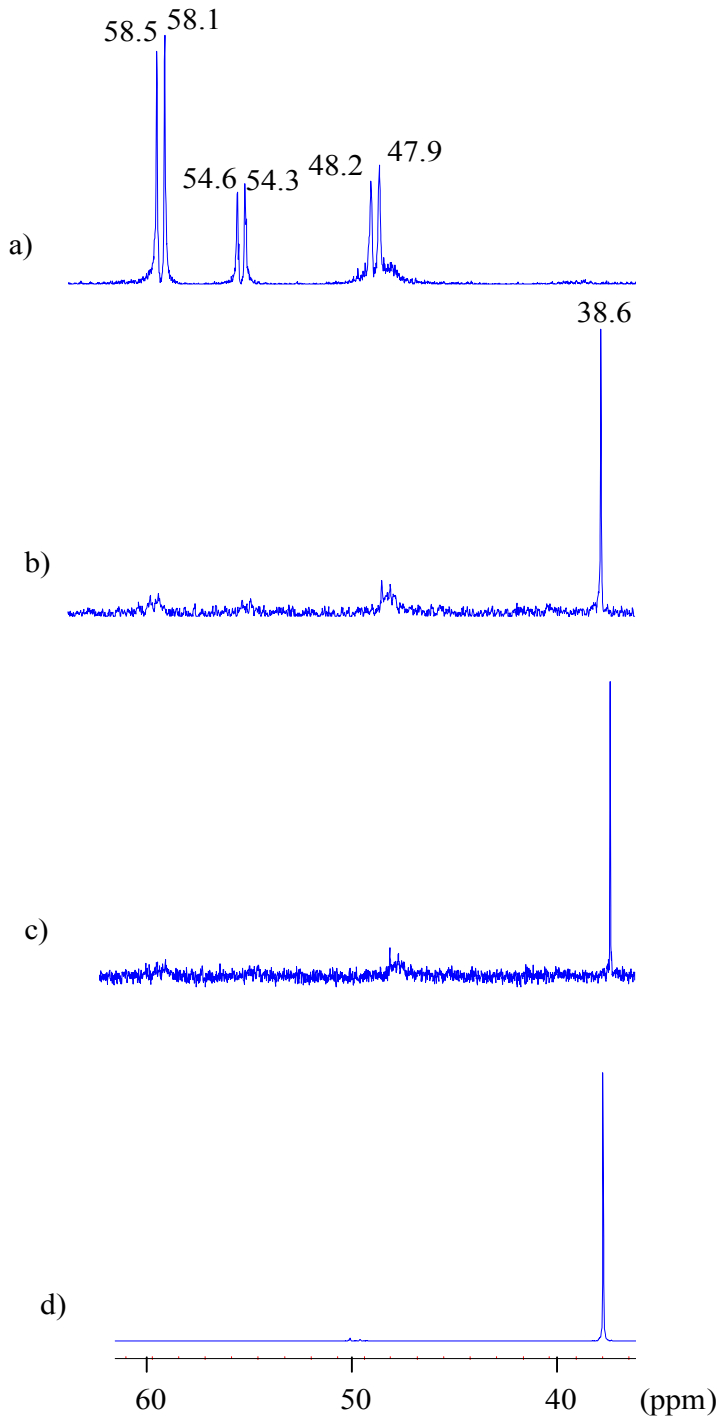

Figure 11. Time-dependent $^{31}P\{^{1}H\}$ NMR spectroscopic control the reaction between the monocationic complex **4L$_7$** and *t*BuOK in 2-propanol [a) before addition of *t*BuOK; b) 5 min after addition of *t*BuOK; b) 15 min after addition of *t*BuOK; c) 30 min after addition of *t*BuOK]

Together with a FAB mass spectrum (m/z = 909.2, M^+) this result is in agreement with the formation of the neutral complex **3L$_4$**. Although it is still an active hydrogenation catalyst, its reaction with dihydrogen did not lead to reliable results, probably due to the instability of RuCl(OBu)(P~O)$_2$N^N (**9L$_7$**). A similar result was obtained, if **4L$_{10}$** was reacted with KOH (see Scheme 8).

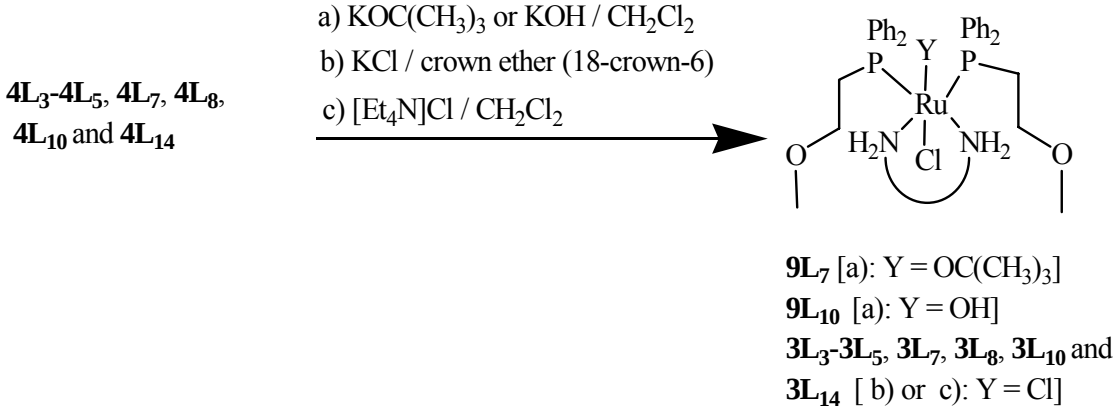

9L$_7$ [a): Y = OC(CH$_3$)$_3$]
9L$_{10}$ [a): Y = OH]
3L$_3$-3L$_5$, **3L$_7$**, **3L$_8$**, **3L$_{10}$** and
3L$_{14}$ [b) or c): Y = Cl]

Scheme 8. Effect of the co-catalysts KOH and *t*BuOK, or KCl and [Et$_4$N]Cl, respectively

If **4L$_3$-4L$_5$**, **4L$_7$**, **4L$_8$**, **4L$_{10}$** and **4L$_{14}$** were refluxed in 2-propanol in the presence of NH$_4$Cl or KCl and 18-crown-6, expectedly the starting materials **3L$_3$-3L$_5$**, **3L$_7$**, **3L$_8$**, **3L$_{10}$**, and **3L$_{14}$** were re-obtained [25], which is a nice corroboration of the hemilabile character of the ether-phosphine ligands in these complexes [25-27,35].

For reasons of comparison the same reaction has been carried out with the neutral complex **3L$_7$**. Treatment of **3L$_7$** with *t*BuOK in 2-propanol (1 ml) in the presence or absence of dihydrogen showed, that the ^{31}P signal of **3L$_7$** at δ = 38.4 slowly disappears and a new resonance occurs at δ = 32.8 (Figure 12). Unfortunately it was not possible to unequivocally identify this product [29].

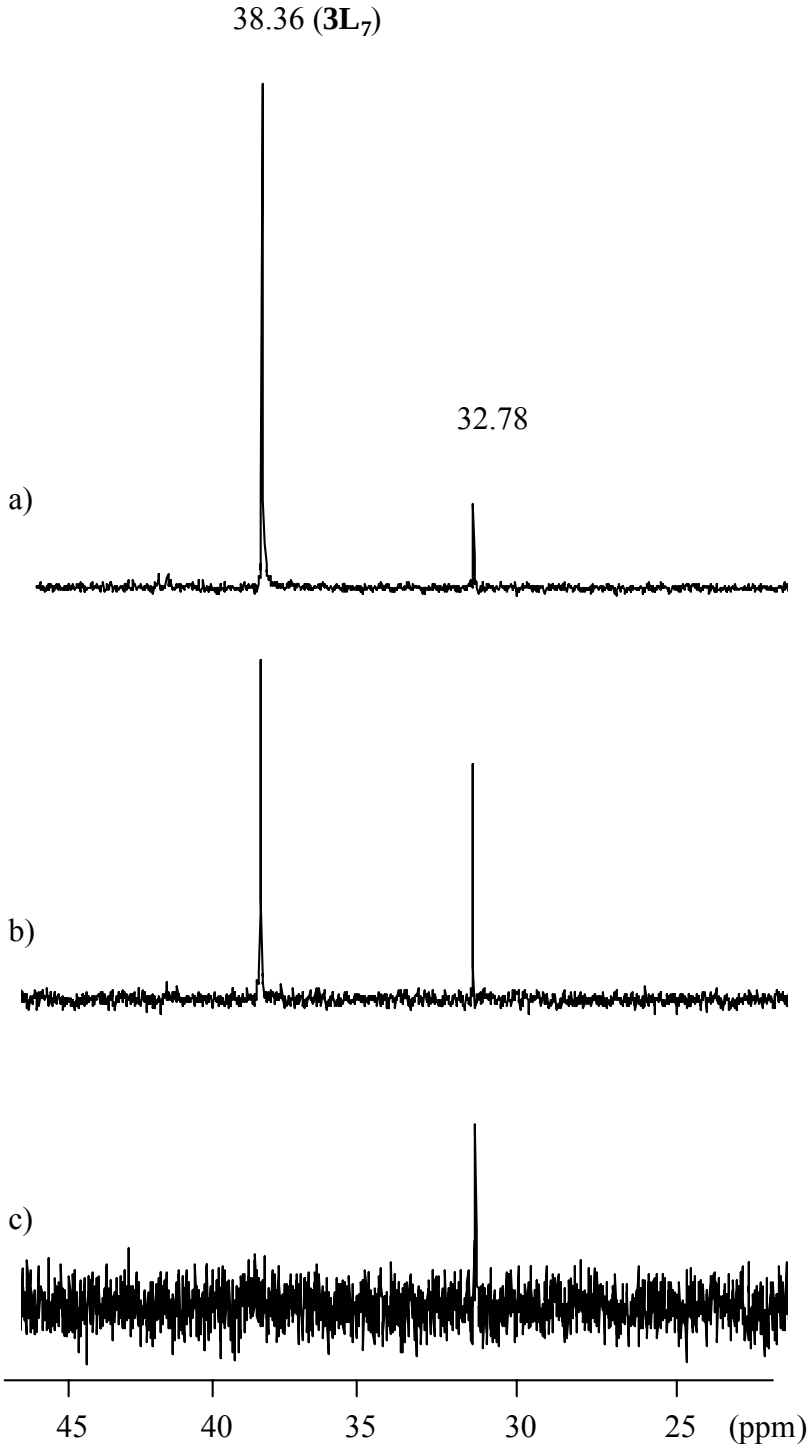

Figure 12. Time-dependent $^{31}P\{^{1}H\}$ NMR spectroscopic control of the reaction between the neutral complex **3L$_7$** and *t*BuOK in 2-propanol [a) 30 min after addition of *t*BuOK; b) 3 h after addition of *t*BuOK; c) 7 h after addition of *t*BuOK]

5.5 Conclusion

In this study a series of neutral and cationic diamine(ether-phosphine)ruthenium(II) and neutral diamine(diphosphine)ruthenium(II) complexes were made available and structurally characterized, which are provided with different aliphatic, cycloaliphatic, and aromatic diamines. While in solution all these complexes prefer a *trans*-$RuCl_2$ configuration, in the solid state *cis*- and *trans*-isomers were formed. With exception of complexes with aprotic, aromatic, and 1,4-aliphatic diamines all other species proved to be highly active catalysts in the hydrogenation α,ß-unsaturated ketones. Most of them show excellent conversions and turnover frequencies, even under mild conditions. Also they reveled a 100% selectivity toward the hydrogenation of only the carbonyl group. As a suitable model substrate for these hydrogenations served *trans*-4-phenyl-3-butene-2-one.

Because of the hemilabile character of ether-phosphine ligands in the cationic ruthenium(II) complexes, a *pseudo*-vacant coordination site is available, which could enhance the formation of a mono- or dihydride intermediate in the mechanism of the hydrogenation of α,ß-unsaturated ketones. However, the cationic species showed only half of the catalytic activity compared to their neutral counterparts. Further experiments were devoted to the role of the co-catalysts. It was evidenced that co-catalysts like OH^- or tBuO$^-$ are able to occupy the *pseudo*-vacant coordination site in the case of complex **4L$_7$** to give the neutral species **9L$_7$**. Although it was still active as a catalyst, reactions with dihydrogen failed, because of the instability of **9L$_7$**.

Also the interphase catalysts **8L$_1$(T^3)(Me-T^3)$_{10}$**, **8L$_2$(T^3)(Me-T^3)$_{10}$**, and **8L$_9$(T^3)(Me-T^3)$_{10}$** displayed catalytic activity in the selective hydrogenation of *trans*-4-phenyl-3-butene-2-one. As a precondition, the reactive centers have to be accessible for the substrates, which is

mainly achieved by swelling the processed polymeric materials in appropriate solvents to form interphase systems. Essentially the accessibility depends on the mobility of the entire polymeric matrix and hence on the type and amount of a co-condensation agent. Therefore in this investigation $CH_3Si(OCH_3)_3$ (**Me-T°**) was used. As could be demonstrated T-silyl functionalized materials are provided with somewhat higher BET values by which the accessibility is enhanced compared to those having D-silyl groups [36].

The monomeric ruthenium(II) precursor complexes were provided with T-silyl functions to increase the cross linkage of the poly-co-condensates. Such an anchoring to the polymeric carrier matrix suppresses the leaching problem that could arise and increase both the surface area and the stability of the polymeric materials. As their homogeneous congeners the mentioned interphase catalysts show a high degree of activity and selectivity in the hydrogenation of *trans*-4-phenyl-3-butene-2-one under mild conditions.

6. Asymmetric Hydrogenation of α,ß-Unsaturated Ketones by the Diamine(ether-phosphine)ruthenium(II) Complexes $3L_1$-$3L_3$, $3L_7$, and $3L_8$ and Lipase-Catalyzed Transesterification: A Consecutive Approach

6.1 General Considerations

During the last two decades, the synthesis of enantiomerically pure, or enriched, compounds has emerged into one of the most important fields of organic synthesis [2,73]. Enantiomerically pure and enriched secondary alcohols are useful chiral building blocks for many natural products. In particular, catalytic asymmetric synthesis, including both metal- and enzyme-catalyzed reactions, has been a highly active area of research [27]. Today, kinetic resolution of racemic substrates by enzyme catalysis has become a standard reaction in organic synthesis [74-80]. A kinetic resolution is generally defined as a process where the two enantiomers of a racemic mixture are transformed to products at different rates. Thus, in an efficient enzymatic resolution, one of the enantiomers of the racemate is selectively transformed to product, whereas the other is left behind [81,82].

This chapter reports on the application of the diamine-bis(ether–phosphine)-ruthenium(II) complexes $\mathbf{3L_1}$-$\mathbf{3L_3}$, $\mathbf{3L_7}$, and $\mathbf{3L_8}$ in the *selective* and *enantioselective* hydrogenation of *trans*-4-phenyl-3-butene-2-one. Particular interest is directed to complexes with the chiral diamines $\mathbf{L_7}$ and $\mathbf{L_8}$, which are able to perform the asymmetric hydrogenation of ketones affording enantiomerically enriched secondary alcohols. In a consecutive approach, the enantiomerically pure alcohol (> 99% ee) was obtained either by lipase-catalyzed transesterification of the enantiomerically enriched secondary alcohol or by lipase-catalyzed hydrolysis of the corresponding acetate.

The Lipase section has been carried out by A. Ghanem, in Professor V. Schurig group.

6.2 Enantioselectivity of the Ruthenium(II) Complexes $3L_1$-$3L_3$, $3L_7$, and $3L_8$

In the case of $\mathbf{3L_7}$ and $\mathbf{3L_8}$ containing chiral ligands the substrate *trans*-4-phenyl-3-butene-2-one was transformed to the enantiomerically enriched alcohol **A** which was detected as (*RS*)-**10** (Scheme 9 and Figure 13).

The product resulting from the hydrogenation of *trans*-4-phenyl-3-butene-2-one in the presence of $\mathbf{3L_7}$ and $\mathbf{3L_7}$ with (*R,R*)- and (*S,S*)-diamines $\mathbf{L_7}$ and $\mathbf{L_8}$ afforded the alcohols (*S)*-**A** and (*R)*-**A**, respectively, with ee values of 45% ($[\alpha]_D^{20}$ − 6.0 / +6.0) (Figures 13 and 14).

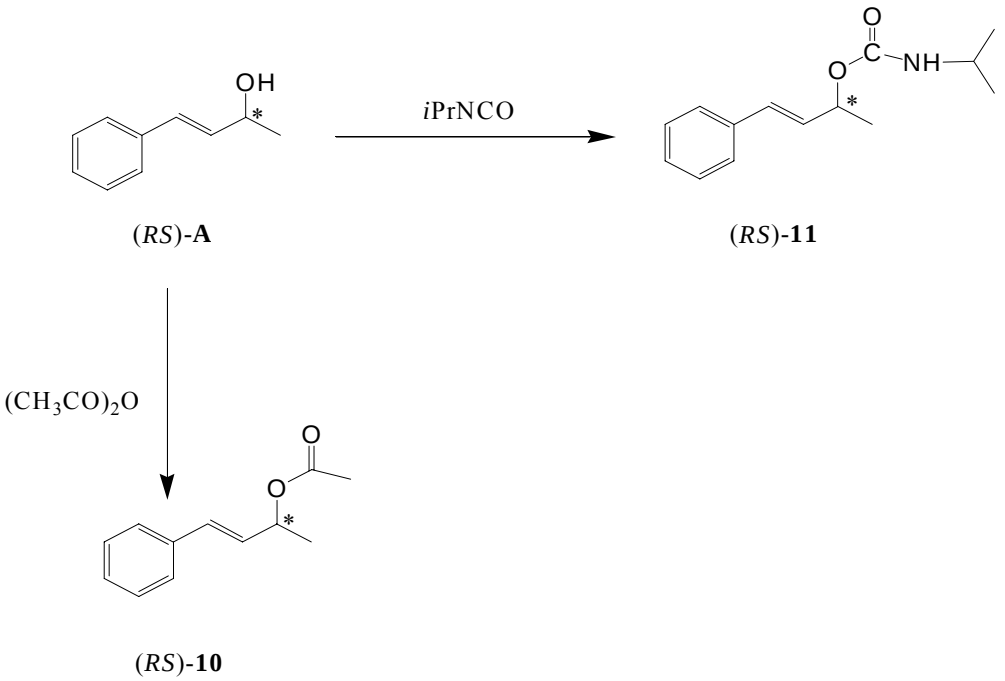

Scheme 9. Derivatization of (*RS*)-**A** with *i*PrNCO (carbamate) and $(CH_3CO)_2O$ (acetate) to achieve a base-line separation in GC

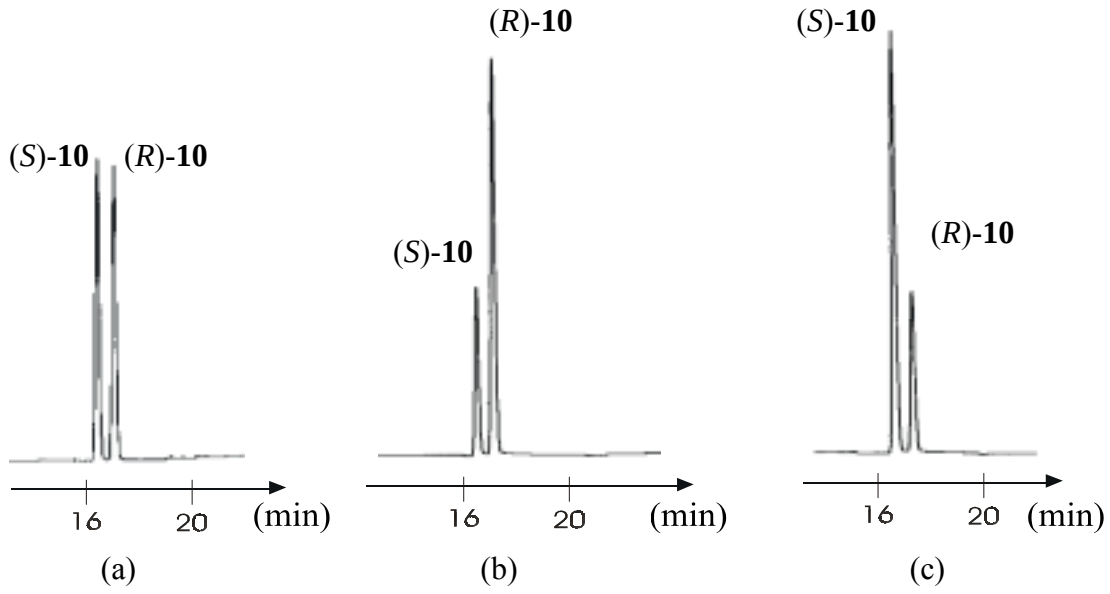

Figure 13. Gas-chromatographic separation of (*RS*)-**A** derivatized as acetate (*RS*)-**10** (a), enantiomerically enriched (*R*)-**A** (45% ee) resulting from catalyst **3L$_8$** and derivatized acetate (*R*)-**10** (b), enantiomerically enriched (*S*)-**A** (45% ee) resulting from catalyst **3L$_7$** and derivatized acetate (*S*)-**10** (c). Heptakis-(2,3-di-*O*-methyl-6-*O*-*tert*-butyldimethylsilyl)-β-cyclodextrin was used as chiral stationary phase. Oven temperature was 130 isothermal for 20 min

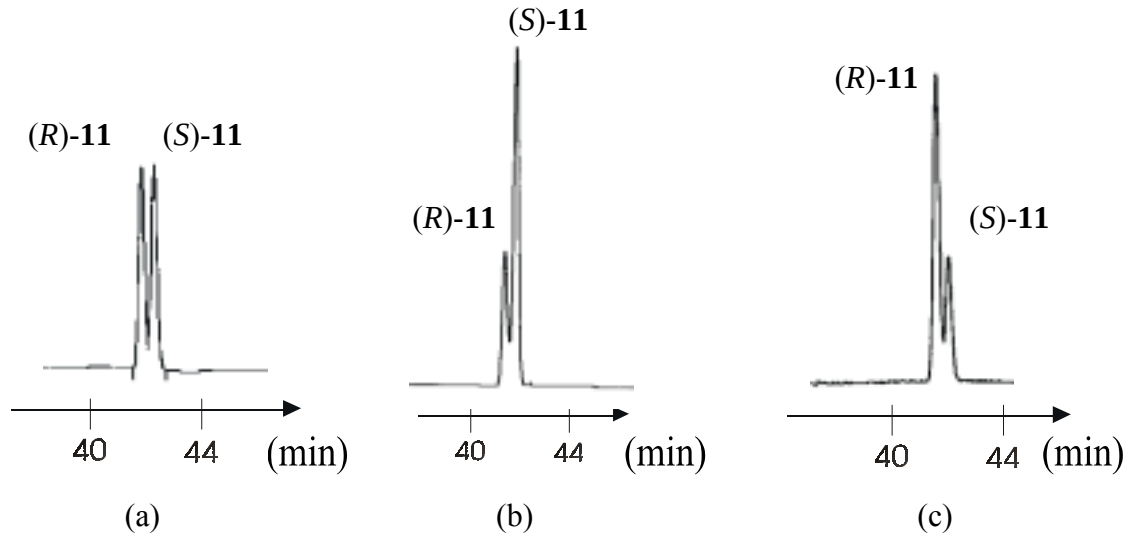

Figure 14. Gas-chromatographic separation of the racemic mixture (*RS*)-**A** derivatized as carbamate (*RS*)-**11** (a), enantiomerically enriched (S)-**A** (45% ee) resulting from catalyst **3L$_7$**, and derivatized carbamate (*S*)-**11** (b), enantiomerically enriched (*R*)-**A** (45% ee) resulting from catalyst **3L$_8$**, and derivatized carbamate (*R*)-**11** (c). Heptakis-(2,3-di-*O*-methyl-6-*O*-*tert*-butyldimethylsilyl)-β-cyclodextrin was used as chiral stationary phase. Oven temperature was 130 isothermal for 20 min, 30^{o}C/min until 160 ^{o}C for 25 min

6.3 Lipase-Catalyzed Kinetic Resolution of the Enantiomerically Enriched Alcohol A

The use of an enantiomerically enriched alcohol rather than a racemic one should reduce the time needed to effect complete resolution [80-84]. The kinetic resolution of **A** was performed starting from the enantiomerically enriched alcohol (*R*)- or (*S*)-**A** (45% ee) obtained by the ruthenium-catalyzed asymmetric hydrogenation of *trans*-4-phenyl-3-butene-2-one with the aim to reach ~100% ee in a consecutive approach. Four lipases from *Pseudomonas cepacia* (PSL), *Pseudomonas cepacia* immobilized on diatomaceous earth (PSL-D), Novozyme 435 (CAL-B) and Lipozyme RM IM (RML) were screened in resolving the enantiomerically enriched **A** either in the enantioselective transesterification of (*S*)-**A** (45% ee) using isopropenyl acetate as an acyl donor in toluene in non-aqueous medium or in the enantioselective hydrolysis of the corresponding acetate (*R*)-**10**, (45% ee) using a phosphate buffer (pH 6) in aqueous medium. The transesterification of **A** (45% ee *S*) was carried out at 40 °C in toluene at a molar ratio of isopropenyl acetate: **A** of 2:1 to ensure the reaction was irreversible (Scheme 10).

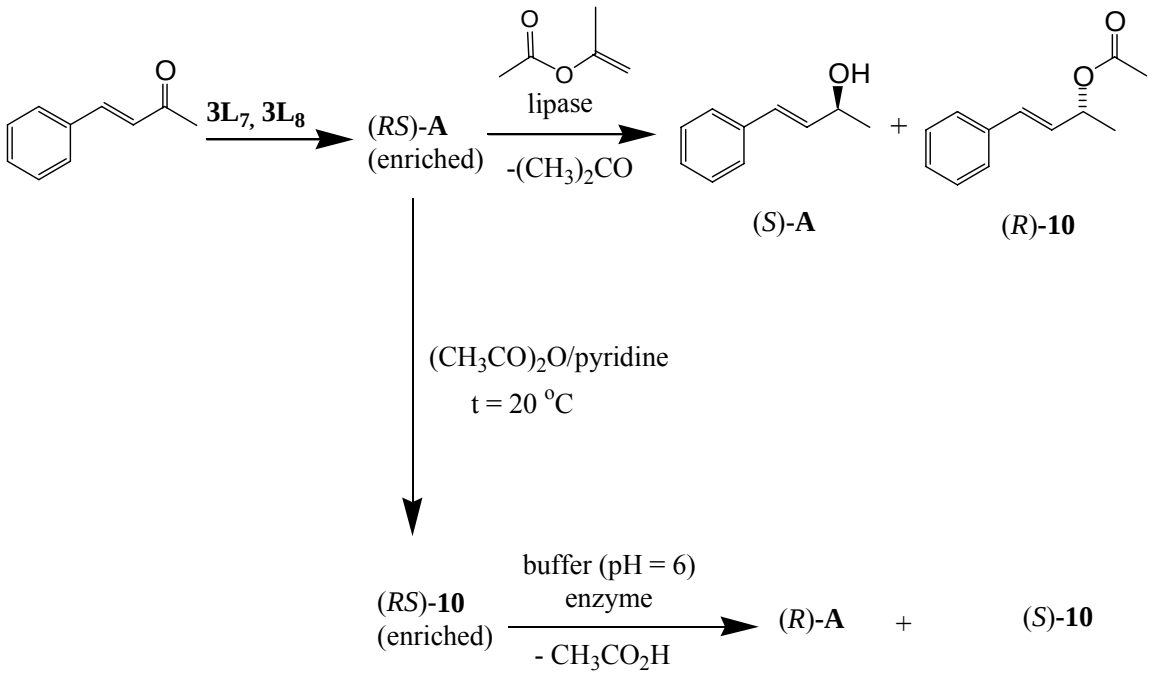

Scheme 10. 3L$_7$, **3L$_8$** / lipase-catalyzed separation of enriched (*RS*)-**A**

The results of the lipase-catalyzed transesterification of enriched (*RS*)-**A** are summarized in Table 11.

Table 11. Lipase-catalyzed transesterification of scalemic **A** using isopropenyl acetate in toluene (analytical scale)

Lipase	Time (h)	ee_s (%)[a] (*S*)-**A**	ee_p (%)[b] (*R*)-**10**	Conversion (%)	E[c]
PSL	2	97.2	86.9	52.8	60
PSL-D	2	>99	91.8	52.1	230
CAL-B	4	>99	80.3	55.4	95
RML	4	49.2	>99	33.0	3800

[a] ee_s: enantiomeric excess of substrate (*S*)-**A**.
[b] ee_p: enantiomeric excess of product (*R*)-**10**.
[c] E : ratio ee_s : ee_p.

In the transesterification reaction of scalemic **A,** (R)-**A** was the faster reacting enantiomer yielding (R)-**10** in high ee and leaving (*S*)-**A** unreacted in enantiomerically pure form. Both lipases from *Pseudomonas cepacia* immobilized on diatomaceous earth (PSL-D) and CAL-B displayed high enantioselectivity towards (*RS*)-**A** (Table 11). In regard to the ee-value of the remaining substrate (*S*)-**A** and that of the product (*R*)-**10** as well as the rate of conversion (52.1% in 2 h) and enantiomeric ratio E>200, PSL-D was the best lipase employed in the transesterification of (*RS*)-**A**. PSL-D was the enzyme of choice applied in the transesterification of (*RS*)-**A** using isopropenyl acetate in toluene on a preparative scale. An *E* value of 300 was observed and the reaction was terminated after 3 h yielding (*S*)-**A** with > 99% ee and the ester (*R*)-**10** (Scheme 10) was recovered with 86% ee determined by capillary GC after 50 % conversion. 4 Å molecular sieves were added in order to scavenge the liberated

acetone formed as a by-product from the lipase-catalyzed reaction using isopropenyl acetate as an acyl donor.

Compared to the transesterification experiments in nonaqueous medium described above, the enzymatic hydrolysis of *R*-enriched **10** proceeded slowly. Only moderate conversion (45 %) but enantioselectivity (up to 99 % for the alcohol (*R*)-**A** and 80.8 % for the remaining unreacted ester (*S*)-**10** (Table 12) was achieved after 24 hours using Novozyme IM (CAL-B). In all cases, the hydrolysis reaction still fast until reaching 9 h, afterwards, the reaction proceeded very slowly.

Table 12. Lipase-catalyzed enantioselective hydrolysis of enriched (*RS*)-**10** using a phosphate buffer of pH 6 (analytical scale)

Lipase	Time (d)	ee_s (%) [a] (*S*)-**10**	ee_p (%) [b] (*R*)-**A**	Conversion (%)	E [c]
PSL	2	57.5	>99	36.5	5000
PSL-D	4	30.2	>99	23.2	4000
CAL-B	1	80.8	>99	45.0	7500
RML	4	39.9	>99	28.6	1500

[a] ee_s: enantiomeric excess of substrate (*S*)-**10**.
[b] ee_p: enantiomeric excess of product (*R*)-**A**.
[c] E : ratio ee_s : ee_p.

This is probably due to product inhibition resulting from the accumulation of products when the conversion is increased in the enzymatic hydrolysis of *R*-enriched **10**, thus competing with the active site of the enzyme. Adding to that, the acid released from the enzymatic hydrolysis (Scheme 10) might be involved in the acylation of the resulting unreacted enantiomerically pure alcohol (*R*)-**A**, thus, increasing the amount of the racemic

ester **10** leading to a decrease in the conversion and enantiomeric excess.

CAL-B (Novozyme) not only showed the best performance in the analytical runs, but also gave an excellent result for the hydrolysis of (*RS*)-**10** enriched at a multi-gram scale (in 24 h, ee_s 74.5%, ee_p >99, conv. 43 and E >300).

6.4 Conclusion

The complexes $\mathbf{3L_7}$ and $\mathbf{3L_8}$ containing chiral diamine ligands afforded the enantiomerically enriched unsaturated alcohol **A** in 45%. The absolute configuration of the resulting alcohol depends on the configuration of the diamine ligands in the ruthenium complexes. Several co-catalysts e.g. KOH, *t*BuOK, AgOTf were tested in the hydrogenation process in the presence of $\mathbf{3L_7}$ and $\mathbf{3L_8}$ at different conditions. A consecutive approach using the ruthenium(II) complexes $\mathbf{3L_7}$, $\mathbf{3L_8}$ for the enantioselectivity reduction and lipase-catalyzed kinetic resolution of the *R* or *S* enriched *trans*-4-phenyl-3-butene-2-ol (**A**) (45% ee) was applied. Four lipases were screened through the transesterification/hydrolysis reactions in order to obtain both *R* and *S* enantiomers of the alcohol with > 99 % ee.

Experimental Section

1. General Remarks

All reactions and manipulation were carried out in an inert atmosphere (argon) by using standard high vacuum and Schlenk-line techniques unless otherwise noted. Prior to use CH_2Cl_2, *n*-hexane, and Et_2O were distilled from CaH_2, $LiAlH_4$, and from sodium/ benzophenone, respectively. All solvent and reagents were stored under argon.

1.1 Reagents

trans-4-Phenyl-3-butene-2-one, Ph_3P, BuLi, $CH_3OCH_2CH_2Cl$, AgOTf, $AgBF_4$, and $RuCl_3 \cdot 3\ H_2O$ were available from Merck and Chempur respectively, and were used without further purification. 1,3-Bis(diphenylphosphino)propane (dppp), $RuCl_2(dppp)_2$ [62], $RuCl_2(PPh_3)_3$ [85], the ether-phosphine ligand $Ph_2PCH_2CH_2OCH_3$ [86] and the (ether-phosphine)ruthenium(II) complex **2** [86], were synthesized a according to literature methods. The diamines were purchased from Acros, Fluka, and Merck and had to be purified by distillation and recrystallization, respectively. Lipases from *Pseudomonas cepacia* (PSL), *Pseudomonas cepacia* immobilized on diatomaceous earth (PSL-D) were gifts from Amano (Nagoya, Japan), Novozyme 435 (an immobilized non-specific lipase, Candida antarctica B, CAL-B, produced by submerged fermentation of a genetically modified *Aspergillus oryzae* microorganism and adsorbed on a macroporous resin) and Lipozyme RM IM (RML, an immobilized 1,3-specific lipase from *Rhizomucor miehei* produced by submerged fermentation of a genetically modified *Aspergillus oryzae* microorganism) were gifts from Novo Nordisck *A/S* Denmark.

1.2 Elemental Analyses, NMR Spectroscopy, IR, Mass Investigation, and GC Analyses

Elemental analyses were carried out on an Elementar Vario EL analyzer. High-resolution ^{1}H, $^{13}C\{^{1}H\}$, DEPT 135, and $^{31}P\{^{1}H\}$ NMR spectra were recorded on a Bruker DRX 250 spectrometer at 298 K. Frequencies are as follows: ^{1}H NMR 250.12 MHz, $^{13}C\{^{1}H\}$ NMR 62.9 MHz, and $^{31}P\{^{1}H\}$ NMR 101.25 MHz. Chemical shifts in the ^{1}H and $^{13}C\{^{1}H\}$ NMR spectra were measured relative to partially deuterated solvent peaks which are reported relative to TMS. ^{31}P chemical shifts were measured relative to 85% H_3PO_4 ($\delta = 0$). IR data were obtained on a Bruker IFS 48 FT-IR spectrometer. Mass spectra: EI-MS; Finnigan TSQ70 (200 ^{o}C). FAB-MS; Finnigan 711A (8 kV), modified by AMD and reported as mass/charge *(m/z).* The analyses of the hydrogenation experiments were performed on a GC 6000 Vega Gas 2 (Carlo Erba Instrument) with a FID and capillary column PS 255 [10 m, carrier gas, He (40 kPa), integrator 3390 A (Hewlett Packard)]. The enantiomers of the underivatized allylic alcohol (*RS*)-**A** could not be separated on heptakis-(2,3-di-*O*-methyl-6-*O*-*tert*-butyldimethylsilyl)-β-cyclodextrin used as chiral stationary phase in GC, however, upon derivatization with acetic anhydride (the acetate (*RS*)-**10**) or isopropyl isocyanate (the carbamate (*RS*)-**11**, see Scheme 9) a base-line separation has been achieved (Figures 13 and 14). Thus the enantioselective analysis of racemic (*RS*)-**A** as carbamate (*RS*)-**11** and acetate (*RS*)-**10** were performed simultaneously using gas chromatograph (Hewlett Packard 580, Waldbronn, Germany) equipped with a flame ionization detector (FID). The chiral stationary phase heptakis(2,3-di-*O*-methyl-6-*O*-tert-butyldimethylsilyl)-β-cyclodextrin, 20% (w/w) was dissolved in PS 86 (Gelest, ABCR GmbH & Co., Karlsruhe, Germany) and coated on a 25 m x 0.25 mm fused silica capillary column (0.25 μm film thickness) according to the literature [87]. The analytical conditions were: injector temperature, 200 ^{o}C; FID temperature, 250^{o}C;

oven temperature 130^{o}C for 18 min then 30 ^{o}C/min untill 160 for 25 min. Hydrogen was used as the carrier gas (40 KPa column head pressure). The retention time of (*S*)-**10**, (*R*)-**10**, (*R*)-**A**, (*S*)-**A**, were 16.4, 17.0, 40.8, 41.2 min, respectively. Upon derivatization of the racemic alcohol (*RS*)-**A** with acetic anhydride, the elution of the resulting acetate (*RS*)-**10** was in the order (S) < (R) with 16.4 and 17.0 min, respectively and a separation factor of α = 1.08 and resolution of R_s = 2.83. Upon derivatization of the racemic alcohol (*RS*)-**A** with isopropyl isocyanate, the elution of the resulting carbamate (*RS*)-**11** was in the reverse order (R) < (*S*) with 40.8 and 41.2 min, respectively and a separation factor of α = 1.01 and resolution of R_s = 1.07.

The substrate **A**, and the product **10** were identified by using a GC/MSD-system HP 6890/5973 (Hewlett Packard, Waldbronn, Germany) equipped with an HP 7683 autosampler.

The enantiomeric excess ee of both substrate (ee_s) and product (ee_p) as well as the conversion (conv.) and the enantiomeric ratio (E) were determined by a computer program available on the internet http://www.orgc.TUGraz.at/orgc/programs/selectiv/selectiv.htm.

1.3 EXAFS Spectroscopic Measurements

The EXAFS (Extended X-ray Absorption Fine Structure) spectroscopy measurements were carried out in collaboration with the research group of Prof. Dr. H. Bertagnolli, Institute of Physical Chemistry, University of Stuttgart, Germany.

The EXAFS spectroscopy using a synchrotron radiation source is a useful method for probing the neighborhood environment of a selected atom in amorphous materials irrespective of the physical state of the sample. The parameters extracted include the nature

of the surrounding atoms, coordination numbers, interatomic distances, and Debye-Waller factors which account for the degree of disorder (static and dynamic) [59].

The EXAFS measurements of all complexes were performed at the Ru K-edge at 22117 eV at the beam line X1.1 of the Hamburger Synchrotron Radiation Laboratory (HASYLAB) at DESY, Hamburg. The complexes were measured with a Si (311) double crystal monochromator under ambient conditions at a positron energy of 4.45 GeV and beam current 120 mA. Data were collected in transmission mode with ion chambers. Energy calibration was monitored using 20 μm thick ruthenium metal foil. The samples were prepared as a pellet of a mixture of the respective complex with polyethylene. The data were analyzed with a program package especially developed for the requirements of amorphous samples [60]. The program AUTOBK [88] of the University of Washington was used for the removal of the background and the program EXCURV92 [89] for the evaluation of the EXAFS function. The resulting EXAFS function was weighted with k^3 [90]. Curved wave theory of the program EXCURV92 was used for the data analysis in the k space. The mean free path of the scattered electrons were calculated from the imaginary part of the potential (VPI set to –4.00), the amplitude reduction factor AFAC was fixed at 0.8 and an overall energy shift ΔE_0 was introduced to give a best fit to the data. In the fitting procedure the coordination numbers were fixed to the known values for the ligands around the ruthenium atom in the complexes and other parameters (interatomic distances, Debye-Waller factor and energy zero value) were varied by iterations.

1.4 Catalysis

The catalytic hydrogenation experiments were carried out under exclusion of arial oxygen in 250 ml pressure Schlenk tubes. The solutions were degassed by three freeze-pump-

thaw cycles, and then magnetically stirred in a temperature-controlled oil bath. The pressure was kept constant over the entire reaction time by a special (RMT) valve.

2. Preparation of the Materials

2.1 General Procedure for the Preparation of the Diamine(ether-phosphine)-ruthenium(II) Complexes $3L_1$ [25], $3L_2$ [25], $3L_3$, $3L_4$, $3L_5$ [25], $3L_6$-$3L_8$, $3L_9$ [25], $3L_{10}$-$3L_{13}$, and $3L_{14}$ [25]

The corresponding diamine ligand (10 % excess of $\mathbf{L_3}$, $\mathbf{L_4}$, $\mathbf{L_6}$-$\mathbf{L_8}$, and $\mathbf{L_{10}}$-$\mathbf{L_{13}}$) was dissolved in 25 ml of dichloromethane and the solution was added dropwise to a stirred solution of **2** in 25 ml of dichloromethane. After the reaction mixture was stirred approximately for 45 min at room temperature the color changed from red to yellow. After removal of any turbidity by filtration (P4), the volume of the solution was concentrated to about 5 ml under reduced pressure. Addition of 40 ml of diethyl ether caused the precipitation of a solid which was filtered (P4), then dissolved again in 40 ml of dichloromethane and concentrated under vacuum to a volume of 5 ml. Addition of 80 ml of *n*-hexane caused the precipitation of a solid which was filtered (P4) and washed three times with 25 ml of *n*-hexane each and dried under vacuum.

2.1.1 $3L_3$

Complex **2** (300 mg, 0.454 mmol) was treated with $\mathbf{L_3}$ (0.05 ml, 0.50 mmol) to give $\mathbf{3L_3}$. Yield 299 mg (88 %) of a yellow powder, m.p 227 ^{o}C, dec. 250 ^{o}C. ^{1}H NMR ($CDCl_3$): δ (ppm) 1.1 (s, 6H, CH_3), 2.5 (m, 4H, PCH_2), 2.8 (m, 4H, CH_2O), 2.8 - 3.0 (m, 6H, NH_2CH_2), 2.94, 2.96 (s, 6H, OCH_3), 7.17 - 7.60 (m, 20H, C_6H_5). $^{31}P\{^{1}H\}$ NMR ($CDCl_3$): δ (ppm) 39.0,

38.3 (AB pattern, $^{2}J_{PP}$ = 36.29 Hz). $^{13}C\{^{1}H\}$ NMR ($CDCl_3$): δ (ppm) 25.5 (m, PCH_2), 29.1 (s, CH_3), 54.7 (s, NCH_2), 55.7 (s, $NC(CH_3)_2$), 58.2 (s, OCH_3), 69.22, 69.29 (2s, CH_2O), 128.3 (m [91a], N = 14.14 Hz, *m*-C_6H_5), 129.3 (s, *p*-C_6H_5), 133.1 (m [91b], N = 8.08 Hz, *o*-C_6H_5), 134.17, 134.67 (2m [91c], N = 8.08 Hz, *i*-C_6H_5). FAB - MS: *(m/z)* 748.2 (M^+). *Anal*. Calc. for $C_{34}H_{46}Cl_2N_2O_2P_2Ru$: C, 54.55; H, 6.19; Cl, 9.47; N, 3.74. Found: C, 54.38; H, 6.47; Cl, 9.35; N, 3.64%.

2.1.2 3L$_4$ (with *trans*–**L$_4$**)

Complex **2** (300 mg, 0.454 mmol) was treated with **L$_4$** (0.061 ml, 0.50 mmol) to give **3L$_4$**. Yield 337 mg (96 %) of a yellow-brown powder, m.p. 221 °C, dec. 224 °C. ^{1}H NMR ($CDCl_3$): δ (ppm) 1.0 - 3.4 (m, 22H, CH_2CH_2, PCH_2, NCH, NH_2, OCH_2), 2.9 (s, 6H, OCH_3), 7.2 - 7.7 (m, 20H, C_6H_5). $^{31}P\{^{1}H\}$ NMR ($CDCl_3$): δ (ppm) 38.8 (s). $^{13}C\{^{1}H\}$ NMR ($CDCl_3$): δ (ppm) 24.9 (s, CH_2), 25.4 (m, PCH_2), 36.2 (s, CH_2), 57.7 (s, NCH), 58.2 (s, OCH_3), 69.3 (s, CH_2O), 128.3 (m [91a], *N* = 8.08 Hz, *m*-C_6H_5), 129.2, 129.4 (2s, *p*-C_6H_5), 132.6, 133.4 (2 m [91b], N = 8.08, *o*-C_6H_5), 134.4, 134.7 (2 m [91c], N = 69.72, *i*-C_6H_5). FAB-MS: *(m/z)* 774.2 (M^+). *Anal.* Calc. for $C_{36}H_{48}Cl_2N_2O_2P_2Ru$: C, 55.55; H, 6.19; Cl, 9.47; N, 3.74. Found: C, 55.33 ; H, 6.43; Cl, 9.35; N, 3.42%.

2.1.3 3L$_4$ (mixture of *cis / trans*–**L$_4$**)

Complex **2** (300 mg, 0.454 mmol) was treated with **L$_4$** (0.060 ml, 0.50 mmol) to give **3L$_4$**. Yield 337 mg (96 %) of a yellow-brown powder, m.p. 218 °C, dec. 221 °C. ^{1}H NMR ($CDCl_3$): δ (ppm) 1.0 - 3.4 (m, 22H, CH_2CH_2, PCH_2, NCH, NH_2, OCH_2). 2.9 (s, 6H, OCH_3), 7.1 - 7.8 (m, 20H, C_6H_5). $^{31}P\{^{1}H\}$ NMR ($CDCl_3$): δ (ppm) 38.6, 38.9 (2s). $^{13}C\{^{1}H\}$ NMR

($CDCl_3$): δ (ppm) 22.2, 24.9 (2s, CH_2), 25.4 (m, PCH_2), 29.0, 36.2 (2s, CH_2), 54.1 (s, NCH), 57.7 (s, NCH), 58.2 (s, OCH_3), 69.3 (s, CH_2O), 128.3 (m [91a], *N* = 8.08 Hz, *m*-C_6H_5), 129.2, 129.3, 129.4 (3s, *p*-C_6H_5), 132.6, 132.9, 133.3 (3m [91b], N = 8.08, *o*-C_6H_5), 134.4, 134.7 (2m [91c], N = 69.72, *i*-C_6H_5). FAB-MS: *(m/z)* 774.2 (M^+). *Anal*. Calc. for $C_{36}H_{48}Cl_2N_2O_2P_2Ru$: C, 55.55; H, 6.19; Cl, 9.47; N, 3.74. Found: C, 55.45; H, 6.33; Cl, 9.28. N, 3.56%.

2.1.4 $3L_6$

Complex **2** (300 mg, 0.454 mmol) was treated with $\mathbf{L_6}$ (0.061 g, 0.50 mmol) to give $\mathbf{3L_6}$. Yield 337 mg (95 %) of a light orange powder, m.p. 220 ^oC, dec. 224 ^oC. ^1H NMR ($CDCl_3$): δ (ppm) 2.1 (s, 3H, CH_3), 2.4 (m, 4H, PCH_2), 2.9 (s, 6H, OCH_3,) 3.0 (m, 4H, OCH_2), 4.4 (br, 4H, NH_2), 6.5 - 7.8 (m, 23H, C_6H_5, C_6H_3). $^{31}P\{^1H\}$ NMR ($CDCl_3$): δ (ppm) 40.6 (s). $^{13}C\{^1H\}$ NMR ($CDCl_3$): δ (ppm) 21.0 (s, CH_3), 25.4 (m, PCH_2), 58.2 (s, OCH_3), 69.2 (s, CH_2O), 127.5, 128.2, 128.3 (3s, C_6H_3), 128.5 (m [91a], N = 8.76 Hz, *m*-C_6H_5), 129.6 (s, *p*-C_6H_5), 133.0 (m [27b], N = 8.76 Hz, *o*-C_6H_5), 134.4 (m [91c], N = 36.38 Hz, *i*-C_6H_5), 137.5, 139.9 (s, br, C_6H_3). FAB-MS: *(m/z)* 872.2 (M^+). ***Anal.*** Calc. for $C_{37}H_{44}Cl_2N_2O_2P_2Ru$: C, 56.78; H, 5.67; Cl, 9.06; N, 3.58. Found: C, 56.39; H, 6.00; Cl, 9.16; N, 3.79%.

2.1.5 $3L_7$

Complex **2** (300 mg, 0.454 mmol) was treated with $\mathbf{L_7}$ (0.105 g, 0.50 mmol) to give $\mathbf{3L_7}$. Yield 356 mg (90 %) of a yellow powder, m.p. 232 ^oC, dec. 239 ^oC. ^1H NMR ($CDCl_3$): δ (ppm) 2.2 - 4.2 (m, 14H, PCH_2, OCH_2, NH_2CH), 2.93 (s, 6H, OCH_3), 6.7 - 7.7 (m, 30H, C_6H_5). $^{31}P\{^1H\}$ NMR ($CDCl_3$): δ (ppm) 39.0 (s). $^{13}C\{^1H\}$ NMR ($CDCl_3$): δ (ppm) 25.8 (m,

PCH_2), 58.2 (s, OCH_3), 63.9 (s, NCH), 69.3 (s, OCH_2), 127.2 (s, *o*-C_6H_5), 128.2 (s, *p*-C_6H_5), 128.3 (m [91a], N = 8.08 Hz, *m*-C_6H_5), 128.9 (s, *m*- C_6H_5), 129.3, 129.5 (2s, *p*-C_6H_5), 132.6, 133.3 (2m [91b], N = 8.08 Hz, *o*-C_6H_5) 134.4 (2m, *i*-C_6H_5), 140.2 (s, *i*-C_6H_5). FAB-MS: *(m/z)* 872.2 (M^+). *Anal*. Calc. for $C_{44}H_{50}Cl_2N_2O_2P_2Ru$: C, 60.55; H, 5.77; Cl, 8.12; N, 3.21. Found: C, 60.28, H, 5.48; Cl, 7.98; N, 3.03%.

2.1.6 $3L_8$

Complex **2** (300 mg, 0.454 mmol) was treated with $\mathbf{L_8}$ (0.105 g, 0.50 mmol) to give $\mathbf{3L_8}$. Yield 348 mg (88 %) of a yellow powder, m.p. 220 °C, dec. 224 °C. ^{1}H NMR ($CDCl_3$): δ (ppm) 2.2 - 4.2 (m, 14H, PCH_2, OCH_2, NH_2CH), 2.93 (s, 6H, OCH_3), 6.7 - 7.7 (m, 30H, C_6H_5). $^{31}P\{^1H\}$ NMR ($CDCl_3$): δ (ppm) 39.0 (s). $^{13}C\{^1H\}$ NMR ($CDCl_3$): δ (ppm) 24.5 (m, PCH_2), 56.8 (s, OCH_3), 62.5 (s, NCH), 67.9 (s, CH_2O), 125.8 (s, *o*-C_6H_5), 126.8 (s, *p*- C_6H_5), 126.9 (m [91a], N = 8.79 Hz, *m*-C_6H_5), 127.6 (s, *m*- C_6H_5), 127.9, 128.1 (2s, *p*- C_6H_5), 131.1, 131.9 (2m [91b], N = 8.08 Hz, *o*-C_6H_5), 133.2 (2m, *i*-C_6H_5), 138.8 (s, *i*-C_6H_5). FAB-MS: *(m/z)* 872.2 (M^+). Anal. Calc. for $C_{44}H_{50}Cl_2N_2O_2P_2Ru$: C, 60.55; H, 5.77; Cl, 8.12; N, 3.21. Found: C, 60.31, H, 5.50; Cl, 7.97; N, 2.90%.

2.1.7 $3L_{10}$

Complex **2** (300 mg, 0.454 mmol) was treated with $\mathbf{L_{10}}$ (0.059 ml, 0.49 mmol) to give $\mathbf{3L_{10}}$. Yield 310 mg (90 %) of a yellow powder, m.p. 206 °C, dec. 213 °C. ^{1}H NMR (CD_2Cl_2): δ (ppm) 0.8 (s, 6H, $C(CH_3)_2$), 2.2 (m, 4H, NCH_2), 2.6 (m, 2H, PCH_2), 2.8 (br, s, 10H, NH_2, OCH_3), 2.9 (s, 4H, CH_2O), 7.2 - 7.7 (m, 20H, C_6H_5). $^{31}P\{^1H\}$ NMR (CD_2Cl_2): δ (ppm) 40.69 (s). $^{13}C\{^1H\}$ NMR (CD_2Cl_2): δ (ppm) 25.4 (s, $C(CH_3)_2$), 26.2 (m, PCH_2), 34.5 (s, $C(CH_3)_2$),

50.0 (s, CH_2N), 58.1 (s, OCH_3), 69.5 (s, CH_2O), 128.2 (m [91a], *N* = 8.77 Hz, *m*-C_6H_5), 129.2 (s, *p*-C_6H_5), 132.7 (m [91c], *N* = 33.68 Hz, *i*-C_6H_5) 133.2 (m [91b], *N* = 7.42 Hz, *o*-C_6H_5). FAB-MS: *(m/z)* 734.2 (M^+). *Anal*. Calc. for $C_{35}H_{48}Cl_2N_2O_2P_2Ru$: C, 55.12; H, 6.34; Cl, 9.30; N, 3.67. Found: C, 54.94; H, 5.92; Cl, 9.20; N, 3.59%.

2.1.8 $3L_{11}$

Complex **2** (300 mg, 0.454 mmol) was treated with $\mathbf{L_{11}}$ (0.059 ml, 0.49 mmol) to give $\mathbf{3L_{11}}$. Yield 308 mg (88 %) of a yellow powder, m.p. 197 ^oC, dec. 199 ^oC. ^1H NMR ($CDCl_3$): δ (ppm) 0.9 (t, $^3J_{HH}$ = 7.38 Hz, CH_3), 1.1 - 2.6 (m, 19H, $CH_2CHCH_2CH_2$, NH_2, PCH_2, CH_2O), 2.6 (s, 6H, OCH_3), 7.2 - 7.7 (m, 20H, C_6H_5). $^{31}P\{^1H\}$ NMR ($CDCl_3$): δ (ppm) 40.2, 40.7 (AB pattern, $^2J_{PP}$ = 35.35 Hz). $^{13}C\{^1H\}$ NMR ($CDCl_3$): δ (ppm) 9.2 (s, CH_3), 25.5 (m, PCH_2), 32.8 (s, CH_2CH_3), 34.3 (s, CH_2CH_2N), 39.6 (s, CH_2N), 51.3 (s, CHN), 57.6 (s, OCH_3), 68.9 (s, CH_2O), 127.8 - 128.2 (m, *m*-C_6H_5), 129.5 - 129.6 (m, *p*-C_6H_5), 132.5 (m, *i*-C_6H_5) 133.2-133.7 (m, *o*-C_6H_5). FAB-MS: *(m/z)* 762.2 (M^+). *Anal.* Calc. for $C_{35}H_{48}Cl_2N_2O_2P_2Ru$: C, 55.12; H, 6.34; Cl, 9.30; N, 3.67. Found: C, 54.89. H, 5.96; Cl, 9.29; N, 3.69%.

2.1.9 $3L_{12}$

Complex **2** (300 mg, 0.454 mmol) was treated with $\mathbf{L_{12}}$ (0.043 ml, 0.494 mmol) to give $\mathbf{3L_{12}}$. Yield 152.7 mg (45 %) of a yellow powder, m.p. 132 ^oC, dec. 141 ^oC. ^1H NMR ($CDCl_3$): δ (ppm) 1.6 (br, 8H, $2CH_2CH_2$), 2.3 (m, 4H, PCH_2), 2.62 - 3.1 (br, 8H, NH_2, CH_2O), 2.9 (s, 6H, OCH_3), 7.1 - 7.6 (m, 20H, C_6H_5). $^{31}P\{^1H\}$ NMR ($CDCl_3$): δ (ppm) 40.2 (s). $^{13}C\{^1H\}$ NMR ($CDCl_3$): δ (ppm) 27.7 (m, PCH_2), 40.3 (s, CH_2), 56.6 (s, NCH_2), 57.5 (s, OCH_3), 68.5 (s, CH_2O), 128.3 (m [91a], *N* = 8.78 Hz, *m*-C_6H_5), 129.4 (s, *p*-C_6H_5), 133.6 (m

[91c], *N* = 33.68 Hz, *i*-C_6H_5) 133.7 (m [91b], *N* = 7.42 Hz, *o*-C_6H_5). FAB-MS: *(m/z)* 747.87 (M^+). *Anal.* Calc. for $C_{34}H_{46}Cl_2N_2O_2P_2Ru$: C, 54.55; H, 6.19; Cl, 9.47; N, 3.74. Found: C, 54.28; H, 6.40; Cl, 9.34, N, 3.73%.

2.1.10 $3L_{13}$

Complex **2** (300 mg, 0.454 mmol) was treated with $\mathbf{L_{13}}$ (0.141 g, 0.50 mmol) to give $\mathbf{3L_{13}}$. Yield 368 mg (86 %) of a light brown powder, m.p. 210 ^oC, dec. 215.1 ^oC. ^1H NMR ($CDCl_3$): δ (ppm) 1.7 (m. 4H, PH_2), 2.9 (s, 6H, OCH_3), 3.0 (m, 4H, CH_2O), 4.3 (d, $^2J_{HH}$ = 8.55 Hz, 2H, NH_2), 5.0 (d, $^2J_{HH}$ = 8.55 Hz, 2H, NH_2), 64 - 7.9 (m, 32H, C_6H_5, $C_{20}H_{12}$). $^{31}P\{^1H\}$ NMR ($CDCl_3$): δ (ppm) 43.4 (s). $^{13}C\{^1H\}$ NMR ($CDCl_3$): δ (ppm) 24.6 (m, PCH_2), 58.2 (s, OCH_3), 69.4 (s, CH_2O), 128.3 – 129.2 (m, *m*-C_6H_5), 129.7, 130.1 (2s, *p*-C_6H_5), 132.4, 134.3 (2m, *o*-C_6H_5) 133.3 (m, *i*-C_6H_5), 119.9, 123.4, 124.8, 125.8, 126.7, 131.3, 133.8, 134.0, 134.1, 140.6 (10s, $C_{20}H_{12}$). FAB-MS: *(m/z)* 774.2 (M^+). *Anal*. Calc. for $C_{36}H_{48}Cl_2N_2O_2P_2Ru$: C, 63.56; H, 5.33; Cl, 7.50; N, 2.96. Found: C, 63.17; H, 5.6; Cl, 7.43; N, 2.82%.

2.2 General Procedure for the Preparation of the Cationic Diamine(ether-phosphine)-ruthenium(II) Complexes $4L_3$, $4L_4$, $4L_5$ [25], $4L_7$, $4L_8$, $4L_{10}$, and $4L_{14}$ [25]

a) Excess (2%) of AgOTf was added to the neutral complexes $\mathbf{3L_4}$, $\mathbf{3L_7}$, and $\mathbf{3L_8}$ in a 100 ml Schlenk tube. The solid mixture was stirred and warmed for 5 min, then 20 ml of dichloromethane was added and the solution was stirred for 5 min. After filtration through silica the solution was concentrated to about 2 ml under reduced pressure. The corresponding cationic complex was precipitated by addition of 30 ml of diethyl ether, filtered off (P3), washed three times with 25 ml portions of diethyl ether, and dried under vacuum.

b) A solution of $AgBF_4$ (5% excess) in 25 ml of dichloromethane was added to a solution of the neutral complexes **3L$_3$** and **3L$_{10}$** in 25 ml of dichloromethane and the solution was stirred for 4 h. After filtration through silica the solution was concentrated to a small volume (2 ml). The addition of 100 ml of diethyl ether caused the precipitation of a solid, which was filtered off (P3), washed three times with 25 ml portions of diethyl ether, and dried under vacuum.

2.2.1 4L$_3$

Complex **3L$_3$** (300 mg, 0.401 mmol) was treated with $AgBF_4$ (79 mg, 0.406 mmol) to give **4L$_3$**. Yield 244 mg (77%) of a yellow powder. ^{1}H NMR (CD_2Cl_2): 2.0-4.0 (m, 14H, CH_2P, $H_2NCH_2CNH_2$, CH_2O), 0.99, 1.10, 1.18, 1.24 (4s, 6H, $C(CH_3)_2$), 2.98, 3.06, 3.71, 3.79 (4s, 6H, OCH_3), 6.42-8.21 (m, 20H, C_6H_5). $^{31}P\{^1H\}$ NMR (CD_2Cl_2): isomer a (67%), δ (ppm) 56.6 (d, $^2J_{PP}$ = 38.14 Hz), 48.7 (d, $^2J_{PP}$ = 38.14 Hz), isomer b (33%), 55.6 (d, $^2J_{PP}$ = 37.23 Hz), 47.0 (d, $^2J_{PP}$ = 37.23 Hz). FAB-MS: (*m*/*z*) 713.2 (M^+-BF_4). *Anal. Calc*. for $C_{34}H_{46}BClF_4N_2O_2P_2Ru$: C, 51.05; H, 5.79; Cl, 4.43; N, 3.50. Found: C, 51.11; H, 5.71; Cl, 4.34; N, 3.50%.

2.2.2 4L$_4$

Complex **3L$_4$** (300 mg, 0.387 mmol) was treated with AgOTf (100 mg, 0.389 mmol) to give **4L$_4$**. Yield 313 mg (91%) of a yellow powder. ^{1}H NMR (CD_2Cl_2): 0.8-4.0 (m, 22H, CH_2P, $H_2NCHCH_2CH_2$, CH_2O), 2.89, 3.10, 3.64, 3.70 (4s, 6H, OCH_3), 6.4-8.1 (m, 20H, C_6H_5). $^{31}P\{^1H\}$ NMR (CD_2Cl_2): isomer a (80%), δ (ppm) 58.7 (d, $^2J_{PP}$ = 37.23 Hz), 48.3 (d, $^2J_{PP}$ = 37.23 Hz); isomer b (20%), 56.8 (d, $^2J_{PP}$ = 37.23 Hz), 49.4 (d, $^2J_{PP}$ = 37.23 Hz).

$^{13}C\{^1H\}$ NMR (CD_2Cl_2): 24.2-36.3 (8s, $NH_2CHCH_2CH_2$), 30.1-36.0 (m, PCH_2), 56.9-61.7 (8s, NCH, OCH_3), 68.29, 68.85, 73.79, 74.25 (4d, $^3J_{PC}$ = 4.88 Hz, CH_2O), 128.2-131.4 (C_6H_5). FAB-MS: (*m*/*z*) 739.2 (M^+ - OTf). *Anal. Calc*. for $C_{37}H_{48}ClF_3N_2O_5SP_2Ru$: C, 50.03; H, 5.45; Cl, 3.99; N, 3.15; S, 3.61. Found: C, 50.17; H, 5.35; Cl, 4.20; N, 3.07; S, 3.48%.

2.2.3 $4L_7$

Complex $\mathbf{3L_7}$ (300 mg, 0.344 mmol) was treated with AgOTf (89 mg, 0.346 mmol) to give $\mathbf{4L_7}$. Yield 319 mg (95%) of a yellow powder. ^1H NMR (CD_2Cl_2): 0.7-4.3 (m, 14H, CH_2P, OCH_2, H_2NCH), 2.86, 2.94, 4.1, 4.3 (4s, 6H, OCH_3), 6.3-7.7 (m, 30H, C_6H_5). $^{31}P\{^1H\}$ NMR (CD_2Cl_2): isomer a (80%), δ (ppm) 58.4 (d, $^2J_{PP}$ = 37.23 Hz), 47.5 (d, $^2J_{PP}$ = 37.23 Hz); isomer b (20%), 54.4 (d, $^2J_{PP}$ = 37.23 Hz) 47.4 (d, $^2J_{PP}$ = 37.23 Hz). $^{13}C\{^1H\}$ NMR (CD_2Cl_2): 23.1-32.4 (m, PCH_2), 58.3-69.3 (8s, H_2NCH, OCH_3), 68.61, 69.25, 74.21, 74.63 (4d, $^3J_{PC}$ = 4.52 Hz, CH_2O), 126.6-130.1 (C_6H_5). FAB-MS: (*m*/*z*) 837.2 (M^+-OTf). *Anal. Calc*. for $C_{45}H_{50}ClF_3N_2$-O_5SP_2Ru: C, 54.79; H, 5.11; Cl, 3.59; N, 2.84; S, 3.25. Found: C, 54.74; H, 5.37; Cl, 3.47; N, 2.97; S, 3.59%.

2.2.4 $4L_8$

Complex $\mathbf{3L_8}$ (300 mg, 0.344 mmol) was treated with AgOTf (89 mg, 0.346 mmol) to give $\mathbf{4L_8}$. Yield 320 mg (96%) of a yellow powder. ^1H NMR (CD_2Cl_2): 0.7-4.6 (m, 14H, CH_2P, OCH_2, H_2NCH), 2.88, 2.97, 4.2, 4.4 (4s, 6H, OCH_3), 6.5-7.8 (m, 30H, C_6H_5). $^{31}P\{^1H\}$ NMR (CD_2Cl_2): isomer a (80%), δ (ppm) 58.5 (d, $^2J_{PP}$ = 37.23 Hz), 47.7 (d, $^2J_{PP}$ = 37.23 Hz); isomer b (20%), 54.8 (d, $^2J_{PP}$ = 37.23 Hz) 47.6 (d, $^2J_{PP}$ = 37.23 Hz). $^{13}C\{^1H\}$ NMR (CD_2Cl_2):

24.2-32.8 (m, PCH_2), 58.7-69.2 (8s, H_2NCH, OCH_3), 68.62, 69.26, 74.30, 74.58 (4d, $^3J_{PC}$ = 4.52 Hz, CH_2O), 127.6-131.4 (C_6H_5). FAB-MS: (*m*/*z*) 837.2 (M^+ - OTf). *Anal. Calc*. for $C_{45}H_{50}Cl\text{-}F_3N_2O_5SP_2Ru$: C, 54.79; H, 5.11; Cl, 3.59; N, 2.84, S, 3.25. Found: C, 54.70; H, 5.30; Cl, 3.67; N, 2.98; S, 3.60%.

2.2.5 $4L_{10}$

Complex $\mathbf{3L_{10}}$ (300 mg, 0.394 mmol) was treated with $AgBF_4$ (78 mg, 0.401 mmol) to give $\mathbf{4L_{10}}$. Yield 224 mg (70%) of a yellow powder. ^1H NMR (CD_2Cl_2): δ (ppm) 0.42, 0.83 (2s, 6H, CH_3), 1.2–3.7 (m, 16H, CH_2P, H_2NCH_2, CH_2O), 3.00, 3.66 (2s, 6H, OCH_3), 6.4-8.1 (m, 20H, C_6H_5). $^{31}P\{^1H\}$ NMR (CD_2Cl_2): δ (ppm) 51.4 (d, $^2J_{PP}$ = 37.21 Hz), 43.0 (d, $^2J_{PP}$ = 37.21 Hz). $^{13}C\{^1H\}$ NMR (CD_2Cl_2): 18.41, 25.37 (2s, $2CH_3$), 23.88, 29.54 (2d, $^1J_{PC}$ = 4.4 Hz, PCH_2), 47.16, 50.75 (2s, NCH_2), 56.81, 58.75 (2s, OCH_3), 66.54, 71.55 (2d, $^3J_{PC}$ = 4.50 Hz, CH_2O), 126.4-135.4 (C_6H_5). FAB-MS: (*m*/*z*) 727.2 (M^+ - BF_4). *Anal. Calc*., for $C_{35}H_{48}BClF_4N_2O_2P_2Ru$: C, 51.64; H, 5.94; Cl, 4.36, N, 3.44. Found: C, 51.20; H, 5.60; Cl, 4.28; N, 3.05%.

2.3 General Procedure for the Preparation of the Diamine(dppp)ruthenium(II) Complexes $6L_1$-$6L_{12}$

The corresponding diamine (10 % excess of $\mathbf{L_1}$-$\mathbf{L_{12}}$) was dissolved in 10 ml of dichloromethane and the solution was added dropwise to a stirred solution of **5** in 10 ml of dichloromethane within 5 min. The mixture was stirred for ca. 10-30 min at room temperature while the color changed from brown to yellow. After removal of any turbidity by filtration

(P4), the volume of the solution was concentrated to about 5 ml under reduced pressure. Addition of 40 ml of diethyl ether caused precipitation of a solid, which was filtered (P4). After recrystallization from dichloromethane/*n*-hexane, the corresponding complexes were obtained in analytically pure form.

2.3.1 $6L_1$

Complex **5** (500 mg, 0.50 mmol) was treated with $\mathbf{L_1}$ (0.035 ml, 0.55 mmol) to give $\mathbf{6L_1}$. Yield 312 mg (97%) of a yellow powder, m.p. 310 ^{o}C (dec.). ^{1}H NMR ($CDCl_3$): δ (ppm) 1.82 (m, 2H, CH_2), 2.74 (br, 12H, PCH_2, NH_2, NCH_2), 7.17 - 7.60 (m, 20H, C_6H_5). $^{31}P\{^{1}H\}$ NMR ($CDCl_3$): δ (ppm) 41.30. $^{13}C\{^{1}H\}$ NMR ($CDCl_3$): δ (ppm) 19.23 (s, CH_2), 26.1 (m [91c], N = 35.02 Hz, PCH_2), 43.64 (s, NCH_2), 128.32 (m [91a], N = 8.08 Hz, *m*-C_6H_5), 129.20 (s, *p*-C_6H_5), 133.13 (br, *o*-C_6H_5). FAB-MS; *(m/z)*: 644.1 (M^+). *Anal.* Calc. for $C_{29}H_{34}Cl_2N_2P_2Ru$: C, 54.04; H, 5.32; Cl, 11.00; N, 4.35. Found: C, 54.07; H, 5.16; Cl, 10.84; N, 4.19%.

2.3.2 $6L_2$

Complex **5** (500 mg, 0.50 mmol) was treated with $\mathbf{L_2}$ (0.048 ml, 0.55 mmol) to give $\mathbf{6L_2}$. Yield 302 mg (91 %) of a yellow powder, m.p. 291 ^{o}C (dec.). ^{1}H NMR ($CDCl_3$): δ (ppm) 0.92 (d, $^{3}J_{HH}$ = 6.28 Hz, 3H, CH_3), 1.82 (m, 2H, CH_2), 2.30-2.90 (m, 10H, PCH_2, NH_2, NCH_2), 3.11 (m, 1H, NCH), 7.17 - 7.60 (m, 20H, C_6H_5). $^{31}P\{^{1}H\}$ NMR ($CDCl_3$): δ (ppm) 41.22, 42.13 (AB pattern, $^{2}J_{PP}$ = 52.20 Hz). $^{13}C\{^{1}H\}$ NMR ($CDCl_3$): δ (ppm) 19.22 (s, CH_2), 20.53 (s, CH_3), 25.71 (d, $^{1}J_{PC}$ = 4.40 Hz, PCH_2), 26.10 (d, $^{1}J_{PC}$ = 4.40 Hz, PCH_2), 49.73 (s, NCH_2), 51.00 (s, NCH), 128.93 (m, *m*-C_6H_5), 131.21 (m, *p*-C_6H_5), 133.94 (m, *o*-C_6H_5),

137.55, 138.05 (m, *i*-C_6H_5) FAB-MS; *(m/z)*: 658.1 (M^+). *Anal*. Calc. for $C_{30}H_{36}Cl_2N_2P_2Ru$: C, 54.71; H, 5.51; Cl, 10.77; N, 4.25. Found: C, 55.26; H, 5.17; Cl, 10.91; N, 4.06%.

2.3.3 $6L_3$

Complex **5** (500 mg, 0.50 mmol) was treated with $\mathbf{L_3}$ (0.057 ml, 0.55 mmol) to give $\mathbf{6L_3}$. Yield 288 mg (85%) of a yellow powder, m.p. 302 ^oC (dec.). ^1H NMR ($CDCl_3$): δ (ppm) 1.12 (s, 6H, CH_3), 1.80 (m, 2H, CH_2), 2.66-2.91 (br, 10H, PCH_2, NH_2, NCH_2), 7.14 - 7.63 (m, 20H, C_6H_5). $^{31}P\{^1H\}$ NMR ($CDCl_3$): δ (ppm) 41.59, 42.32 (AB pattern, $^2J_{PP}$ = 52.20 Hz). $^{13}C\{^1H\}$ NMR ($CDCl_3$): δ (ppm) 19.44 (s, CH_2), 25.43 (dd, $^1J_{PC}$ = 4.4, $^3J_{PC}$ = 4.4 Hz, PCH_2) 25.74 (dd, $^1J_{PC}$ = 4.4, $^3J_{PC}$ = 4.4 Hz, PCH_2), 29.36 (s, CH_3), 53.17 (s, NC), 54.58 (s, NCH_2), 126.69 (m, *m*-C_6H_5), 127.75 (m, *p*-C_6H_5), 131.79 (m, *o*-C_6H_5), 136.44 (m, *i*-C_6H_5). FAB-MS; *(m/z)*: 672.1 (M^+). *Anal*. Calc. for $C_{31}H_{38}Cl_2N_2P_2Ru$: C, 55.36; H, 5.69; Cl, 10.54; N, 4.17. Found: C, 54.90; H, 5.33; Cl, 10.42; N, 4.11%.

2.3.4 $6L_4$

Complex **5** (500 mg, 0.50 mmol) was treated with $\mathbf{L_4}$ (0.060 g, 0.55 mmol) to give $\mathbf{6L_4}$. Yield 348 mg (99 %) of a yellow–brown powder, m.p. 298 ^oC (dec.). ^1H NMR ($CDCl_3$): δ (ppm) 0.88-2.14 (m, 10H, C_6H_{10}), 1.81 (m, 2H, CH_2), 2.49-2.81 (m, 8H, PCH_2, NH_2), 7.12 - 7.66 (m, 20H, C_6H_5). $^{31}P\{^1H\}$ NMR ($CDCl_3$): δ (ppm) 41.63. $^{13}C\{^1H\}$ NMR ($CDCl_3$): δ (ppm) 19.31 (s, CH_2), 24.96 (s, CH_2CH_2CH), 26.15 (m [91c], N = 35.02 Hz, PCH_2), 36.39 (s, $NCHCH_2$), 57.62 (s, $NCHCH_2$), 128.16 (m, *m*-C_6H_5), 129.15 (m, *p*-C_6H_5), 133.11 (m, *o*-C_6H_5). FAB-MS; *(m/z)*: 698.1 (M^+). *Anal.* Calc. for $C_{33}H_{40}Cl_2N_2P_2Ru$: C, 56.73; H, 5.77; Cl, 10.15; N, 4.01. Found: C, 56.48; H, 5.76; Cl, 10.03; N, 4.07%.

2.3.5 $6L_5$

Complex **5** (500 mg, 0.50 mmol) was treated with $\mathbf{L_5}$ (0.06 g, 0.55 mmol) to give $\mathbf{6L_5}$. Yield 279 mg (81 %) of a light brown powder, m.p. 303 ^{o}C (dec.). ^{1}H NMR ($CDCl_3$): δ (ppm) 1.75 (m, 2H, CH_2), 2.67 (br, 4H, PCH_2), 4.13 (br, 4H, NH_2), 6.72 - 7.74 (m, 24H, C_6H_5, C_6H_3). ^{31}P{^{1}H} NMR ($CDCl_3$): δ (ppm) 43.00. ^{13}C{^{1}H} NMR ($CDCl_3$): δ (ppm) 19.22 (s, CH_2), 25.59 (m [91c], *N* = 35.02 Hz, PCH_2), 127.40, 129.08, 135.57 (s, C_6H_4), 128.28 (m, *m*-C_6H_5), 129.48 (s, *p*-C_6H_5), 133.10 (m, *o*-C_6H_5). FAB-MS; *(m/z)*: 692.1 (M^+). ***Anal.*** Calc. for $C_{33}H_{34}Cl_2N_2P_2Ru$: C, 57.23; H, 4.95; Cl, 10.24; N, 4.04%. Found: C, 57.33; H, 4.62; Cl, 9.93; N, 3.59%.

2.3.6 $6L_6$

Complex **5** (500 mg, 0.50 mmol) was treated with $\mathbf{L_6}$ (0.067 g, 0.55 mmol) to give $\mathbf{6L_6}$. Yield 312 mg (88 %) of a brown powder, m.p. 290 ^{o}C (dec.). ^{1}H NMR ($CDCl_3$): δ (ppm) 1.86 (m, 2H, CH_2), 2.12 (br, 3H, CH_3), 2.79 (br, 4H, PCH_2), 4.25 (br, 4H, NH_2), 6.5 - 7.8 (m, 23H, C_6H_5, C_6H_3). ^{31}P{^{1}H} NMR ($CDCl_3$): δ (ppm) 42.70. ^{13}C{^{1}H} NMR ($CDCl_3$): δ (ppm) 19.29 (s, CH_2), 20.98 (s, CH_3), 25.66 (m [91c], *N* = 35.02 Hz, PCH_2), 126.27, 127.92, 128.19, 128.81, 137.49, 139.91 (s, C_6H_3), 128.34 (m, *m*-C_6H_5), 129.43 (m, *p*-C_6H_5), 133.09 (m, *o*-C_6H_5). FAB-MS; *(m/z)*: 706.1 (M^+). ***Anal.*** Calc. for $C_{34}H_{36}Cl_2N_2P_2Ru$: C, 57.79; H, 5.14; Cl, 10.03; N, 3.96. Found: C, 57.73; H, 4.68; Cl, 9.87; N, 3.89%.

2.3.7 $6L_7$

Complex **5** (500 mg, 0.50 mmol) was treated with $\mathbf{L_7}$ (0.116 g, 0.55 mmol) to give $\mathbf{6L_7}$. Yield 374 mg (96 %) of a yellow powder, m.p. 318 ^{o}C (dec.). ^{1}H NMR ($CDCl_3$): δ (ppm) 1.87 (m, 2H, CH_2), 2.76 (br, 4H, PCH_2), 3.00 (d, $^{3}J_{HH}$ = 8.80 Hz, 2H, NH), 3.50 (m, 2H, CHN) 4.24 (d, $^{3}J_{HH}$ = 8.8 Hz, 2H, NH), 6.64 - 7.73 (m, 23H, C_6H_5, C_6H_3). $^{31}P\{^{1}H\}$ NMR ($CDCl_3$): δ (ppm) 41.53. $^{13}C\{^{1}H\}$ NMR ($CDCl_3$): δ (ppm) 21.40 (s, CH_2), 28.20 (m [91c], N = 35.02 Hz, PCH_2), 65.69 (s, HCN), 125.84, 128.24, 130.54, 131.23, 131.36, 131.95, 139.34, 148.62 (C_6H_5). FAB-MS; *(m/z)*: 796.2 (M^+). Anal Calc. for $C_{41}H_{42}Cl_2N_2P_2Ru$: C, 61.81; H, 5.31; Cl, 8.90; N, 3.52. Found: C, 61.66; H, 5.17; Cl, 8.80; N, 3.21%.

2.3.8 $6L_8$

Complex **5** (500 mg, 0.5 mmol) was treated with $\mathbf{L_8}$ (0.116 g, 0.55 mmol) to give $\mathbf{6L_8}$. Yield 367 mg (94 %) of a yellow powder, m.p. 318 ^{o}C (dec.). ^{1}H NMR ($CDCl_3$): δ (ppm) 1.87 (m, 2H, CH_2), 2.75 (br, 4H, PCH_2), 3.05 (d, $^{3}J_{HH}$ = 8.8 Hz, 2H, NH), 3.55 (m, 2H, CHN) 4.22 (d, $^{3}J_{HH}$ = 8.8 Hz, 2H, NH), 6.5 - 7.8 (m, 23H, C_6H_5, C_6H_3). $^{31}P\{^{1}H\}$ NMR ($CDCl_3$): δ (ppm) 41.54. $^{13}C\{^{1}H\}$ NMR ($CDCl_3$): δ (ppm) 19.98 (s, CH_2), 26.57 (m [91c], N = 35.02 Hz, PCH_2), 64.03 (s, HCN), 129.5, 130.2, 130.5, 131.0, 131.1, 131.5, 135.3, 142.7 (C_6H_5). FAB-MS; *(m/z)*: 796.1 (M^+). *Anal.* Calc. for $C_{41}H_{42}Cl_2N_2P_2Ru$: C, 61.81; H, 5.31; Cl, 8.90; N, 3.52. Found: C, 61.69; H, 5.10; Cl, 8.74; N, 3.76%.

2.3.9 $6L_9$

Complex **5** (500 mg, 0.50 mmol) was treated with $\mathbf{L_9}$ (0.046 ml, 0.55 mmol) to give $\mathbf{6L_9}$. Yield 317 mg (96%) of a yellow powder, m.p. 288 ^{o}C (dec.). ^{1}H NMR ($CDCl_3$): δ (ppm) 1.52 (br, 6H, $N(CH_2)_3$, 1.84 (m, 2H, CH_2), 2.74, 2.81 (br, 8H, NH_2, PCH_2), 7.10 - 7.60 (m, 20H, C_6H_5). $^{31}P\{^{1}H\}$ NMR ($CDCl_3$): δ (ppm) 42.53. $^{13}C\{^{1}H\}$ NMR ($CDCl_3$): δ (ppm) 19.52 (s, PCH_2CH_2), 26.56 (m [91c], *N* = 35.02 Hz, PCH_2), 29.47 (s, NCH_2CH_2), 40.29 (s, NCH_2), 128.06 (m [91a], *N* = 8.08 Hz, *m*-C_6H_5), 129.4 (s, *p*-C_6H_5), 133.6 (br, *o*-C_6H_5), 136.4 (m , *i*-C_6H_5). FAB-MS; *(m/z)*: 685.1 (M^+). Anal. Found: C, 54.78; H, 5.17; Cl, 10.51; N, 3.99. Calc. for $C_{30}H_{36}Cl_2N_2P_2Ru$: C, 54.71; H, 5.51; Cl, 10.77; N, 4.25%.

2.3.10 $6L_{10}$

Complex **5** (500 mg, 0.5 mmol) was treated with $\mathbf{L_{10}}$ (0.065 ml, 0.55 mmol) to give $\mathbf{6L_{10}}$. Yield 291 mg (90 %) of a yellow powder, m.p. 270 ^{o}C (dec.). ^{1}H NMR ($CDCl_3$): δ (ppm) 0.75 (s, 6H, CH_3), 1.79 (m, 2H, CH_2), 2.50 (br, 4H, NCH_2), 2.73 (br, 8H, NH_2, PCH_2), 7.10 - 7.50 (m, 20H, C_6H_5). $^{31}P\{^{1}H\}$ NMR ($CDCl_3$): δ (ppm) 42.88. $^{13}C\{^{1}H\}$ NMR ($CDCl_3$): δ (ppm) 19.54 (s, CH_2), 24.79 (s, CH_3), 26.48 (m [91c], N = 32.02 Hz, PCH_2), 34.45 (s, $C(CH_3)_2$), 49.97 (s, NCH_2), 128.13 (m [26a], N = 8.08 Hz, *m*-C_6H_5), 129.24 (s, *p*-C_6H_5), 133.61 (br, *o*-C_6H_5), 136.24 (m, *i*-C_6H_5). FAB-MS; *(m/z)*: 681.1 (M^+). *Anal.* Calc. for $C_{32}H_{40}Cl_2N_2P_2Ru$: C, 55.98; H, 5.87; Cl, 10.33; N, 4.08. Found: C, 55.98; H, 5.48; Cl, 10.35; N, 3.64%.

2.3.11 $6L_{11}$

Complex **5** (500 mg, 0.5 mmol) was treated with $\mathbf{L_{11}}$ (0.066 ml, 0.55 mmol) to give $\mathbf{6L_{11}}$. Yield 291 mg (84 %) of a yellow powder, m.p. 280 ^{o}C (dec.). ^{1}H NMR ($CDCl_3$): δ (ppm) 0.35 (t, 3H, $^{3}J_{HH}$ = 7.5 Hz, CH_3), 1.07 (m, 1H, NCH), 1.27 (m, 2H, C*H*$_2$CH$_3$), 1.48 (m, 2H, PCH$_2$C*H*$_2$), 1.54 (m, 2H, CHC*H*$_2$), 2.58 (s, 4H, NH_2), 2.95 (m, 6H, PCH_2, NCH_2), 7.10 - 7.50 (m, 20H, C_6H_5). ^{31}P{^{1}H} NMR ($CDCl_3$): δ (ppm) 42.24, 42.53 (AB pattern, $^{2}J_{PP}$ = 52.20 Hz). ^{13}C{^{1}H} NMR ($CDCl_3$): δ (ppm) 9.70 (s, CH_3), 19.49 (s, PCH$_2$*C*H$_2$), 26.46 (2m, PCH_2), 33.15 (s, *C*H$_2$CH$_3$), 34.85 (s, CH*C*H$_2$CH$_2$), 40.50 (s, NCH_2), 52.35 (s, NCH), 127.83, 128.32, 129.37, 133.06, 134.04 (C_6H_5). FAB–MS; *(m/z)*: 686.1 (M^+). *Anal.* Calc. for $C_{32}H_{40}Cl_2N_2P_2Ru$: C, 55.98; H, 5.87; Cl, 10.33; N, 4.08. Found: C, 55.78; H, 5.76; Cl, 10.45; N, 4.07%.

2.3.12 $6L_{12}$

Complex **5** (500 mg, 0.5 mmol) was treated with $\mathbf{L_{12}}$ (0.057 ml, 0.55 mmol) to give $\mathbf{6L_{12}}$. Yield 219 mg (65%) of a yellow powder, m.p. 180 ^{o}C (dec.). ^{1}H NMR ($CDCl_3$): δ (ppm) 0.78 (m, 4H, C*H*$_2$CH$_2$N), 1.18 (m, 4H, CH_2N), 1.59 (m, 4H, CH_2), 2.63, 2.74 (m, 8H, PCH_2, NH_2), 7.12 - 7.68 (m, 20H, C_6H_5). ^{31}P{^{1}H} NMR ($CDCl_3$): δ (ppm) 41.71. ^{13}C{^{1}H} NMR ($CDCl_3$): δ (ppm) 19.57 (s, CH_2), 26.87 (m [91c], *N* = 34.02 Hz, PCH_2), 28.91 (s, *C*H$_2$CH$_2$N), 41.91 (s, NCH_2), 128.24, 129.43, 132.52, 133.93 (C_6H_5). FAB-MS; *(m/z)*: 672.1 (M^+). Anal. Calc. for $C_{31}H_{38}Cl_2N_2P_2Ru$: C, 55.36; H, 5.69; Cl, 10.54; N, 4.17. Found: C, 55.38; H, 5.47; Cl, 10.35; N, 3.84%.

2.4 General Procedure for the Preparation of the T-Silyl Functionalized Diamine(ether-phosphine)ruthenium(II) Complexes $8L_1(T^3)(Me\text{-}T^3)$, $8L_2(T^3)(Me\text{-}T^3)$, and $8L_9(T^3)$-$(Me\text{-}T^3)$

To a solution of **$7L_1(T^0)$**, **$7L_2(T^0)$**, and **$7L_9(T^0)$** in 5 ml of MeOH and 15 ml of THF the corresponding amount of the co-condensation agent **Me-T°**, H_2O, and 100 µl of (*n*–$Bu)_2Sn(OAc)_2$ were added. After 3 d stirring at room temperature, the precipitated gel was washed with 10 ml of toluene and diethyl ether each, and 15 ml of petroleum ether (40 – 70). Finally the xerogels were grinded and dried under vacuum for 24 h.

2.4.1 $8L_1(T^3)(Me\text{-}T^3)$

$7L_1(T^0)$ (300 mg, 0.235 mmol) and **Me-T°** (320 mg, 2.35 mmol) were sol–gel processed with water (300 µl, 16.6 mmol). After working up 333 mg (82 %) of a pale yellow powder was obtained. ^{31}P CP/MAS NMR: δ = 37.2. ^{13}C CP/MAS NMR: δ = –3.8 ($SiCH_3$), 12.9 ($SiCH_2$, spacer), 26.2 (PCH_2, $SiCH_2CH_2$, spacer), 43.0 (C-amine, $PhCH_2$, $C(O)NHCH_2$), 57.1 (OCH_3), 68.7 (CH_2O), 128.4 (br, C-phenyl), 158.5 (C=O). ^{29}Si CP/MAS NMR: δ = –58.0 (T^2), –65.2 (T^3). IR (KBr, cm^{-1}): ν(C=O) 1567, 1650. Anal. Calc. for $C_{52}H_{90}Cl_2N_6O_{22}P_2RuSi_{12}$: C, 36.26; H, 5.27; N, 4.88. Found C, 34.67; H, 4.94; N 4.00%.

2.4.2 $8L_2(T^3)(Me\text{-}T^3)$

$7L_2(T^0)$ (300 mg, 0.233 mmol) and **Me-T°** (317 mg, 2.33 mmol) were sol–gel processed with water (300 µl, 16.6 mmol). After working up 353 mg (87 %) of a pale yellow powder was obtained. ^{31}P CP/MAS NMR: δ = 38.3. ^{13}C CP/MAS NMR: δ = –4.1 ($SiCH_3$),

12.9 ($SiCH_2$, spacer), 21.5 (CH-amine), 26.2 (PCH_2, $SiCH_2CH_2$, spacer), 42.8 (C-amine, $PhCH_2$, $C(O)NHCH_2$), 57.4 (OCH_3), 68.7 (CH_2O), 128.4 (br, C-phenyl), 159.4 (C=O). ^{29}Si CP/MAS NMR: δ = –58.0 (T^2), –65.2 (T^3). IR (KBr, cm^{-1}): ν(C=O) 1559, 1653. Anal. Calc. for $C_{53}H_{92}Cl_2N_6O_{22}P_2RuSi_{12}$: C, 36.66; H, 5.34; N, 4.84. Found C, 34.00; H, 4.99; N 3.78%.

2.4.3 $8L_9(T^3)$(Me-T^3)

$7L_9(T^o)$ (300 mg, 0.233 mmol) and **Me-T°** (317 mg, 2.33 mmol) were sol–gel processed with water (300 µl, 16.6 mmol). After working up 321 mg (79 %) of a pale yellow powder was obtained. ^{31}P CP/MAS NMR: δ = 42.2. ^{13}C CP/MAS NMR: δ = –4.1 ($SiCH_3$), 12.9 ($SiCH_2$, spacer), 26.4 (PCH_2, $SiCH_2CH_2$, spacer), 42.1 (C-amine, $PhCH_2$, $C(O)NHCH_2$), 56.9 (OCH_3), 68.6 (CH_2O), 128.4 (br, C-phenyl), 158.8 (C=O). ^{29}Si CP/MAS NMR: δ = –58.0 (T^2), –65.2 (T^3). IR (KBr, cm^{-1}): ν(C=O) 1567, 1651. N_2 surface area: 5.94 $m^2\ g^{-1}$. Anal. Calc. for $C_{53}H_{92}Cl_2N_6O_{22}P_2RuSi_{12}$: C, 36.66; H, 5.34; N 4.84. Found C, 35.49; H, 5.58; N, 4.16%.

2.5 General Procedure for the Hydrogenations Using the Neutral Diamine(ether-phosphine and diphosphine)ruthenium(II) Complexes as Catalysts

The respective ruthenium(II) complex (0.026 and 0.012 mmol, respectively) was placed in a 150 and 200 ml Schlenk tube, respectively, and solid KOH (0.26 and 0.12 mmol, respectively) was added as a co-catalyst. The solid mixture was stirred and warmed during the evacuation process to remove oxygen and water. Subsequently the Schlenk tube was filled with argon and 20 ml of 2-propanol was added. The mixture was vigorously stirred, degassed by two freeze-thaw cycles, and then sonicated for 20-40 min (this is important to complete the

dissolving of the catalyst and co-catalyst). A solution of *trans*-4-phenyl-3-butene-2-one (26.0 and 12.0 mmol, respectively) in 60 and 40 ml of 2-propanol, respectively, was subjected to a freeze-thaw cycle in different 150 and 200 ml Schlenk tubes, respectively, and was added to the catalyst solution. Finally the reaction mixture was transferred to a pressure Schlenk tube which was pressurized with dihydrogen of 1-4, and 3 bar, respectively, after flushing the reaction vessel three times with H_2. The reaction mixture was vigorously stirred at 35 ^oC for 2 and 1 h, respectively. During the hydrogenation process samples were taken from the reaction mixture to control the conversion and turnover frequency. In the case of the dppp complexes after this procedure the pressure Schlenk tube was pressurized again with hydrogen (P_{H_2} = 3 bar). The samples were inserted by a special glass syringe into a gas chromatograph and the kind of the reaction products was compared with authentic samples.

2.6 General Procedure for the Hydrogenations Using the Monocationic Diamine(ether-phosphine)ruthenium(II) Complexes as Catalysts

The amount (0.026 mmol) of the respective diamine(ether-phosphine)ruthenium(II) complex **4L$_3$**-**4L$_5$**, **4L$_7$**, **4L$_8$**, **4L$_{10}$**, and **4L$_{14}$** was placed in a 50 ml Schlenk tube and solid AgOTf or $AgBF_4$ (0.026 mmol) was added. The Schlenk tube was evacuated several times and filled with argon. After that 5 ml of CH_2Cl_2 was added and the mixture was stirred (2 min in case of AgOTf and 2 h in case of $AgBF_4$). Subsequently AgCl was filtered off (P3) and the solution was transferred to a 200 ml Schlenk tube. Then CH_2Cl_2 was completely removed in vacuum. Afterwards KOH or *t*BuOK (0.26 mmol) as a co-catalyst and *trans*-4-phenyl-3-butene-2-one (26 mmol) were mixed together. The solid mixture was stirred and warmed during the evacuation process to remove oxygen. Subsequently the Schlenk tube was filled with argon and 80 ml of 2-propanol. The mixture was vigorously stirred, degassed by two freeze-thaw cycles, and then sonicated for 30 min (this is important to complete the

dissolution of the catalyst and co-catalyst). Finally the reaction mixture was transferred to a pressure Schlenk tube (250 ml) which was pressurized with H_2 of 3 bar after flushing with H_2 three times. The reaction mixture was vigorously stirred at 35 ^oC for 1-3 h. During the hydrogenation process samples were taken from the reaction mixture to control the conversion and turnover frequency. The samples were inserted by a special glass syringe into a gas chromatograph and the kind of the reaction products was compared with authentic samples.

2.7 General Procedure for the Hydrogenations Using the Interphase Catalysts $8L_1(T^3)(Me\text{-}T^3)$, $8L_2(T^3)(Me\text{-}T^3)$, and $8L_9(T^3)(Me\text{-}T^3)$

The respective heterogeneous diaminediphosphineruthenium(II) complex **$8L_1(T^3)$-$(Me\text{-}T^3)$**, **$8L_2(T^3)$-$(Me\text{-}T^3)$**, and **$8L_9(T^3)(Me\text{-}T^3)$** (100 mg, ~ 6% Ru) was placed in a 250 ml pressure Schlenk tube. Subsequently 0.06 mmol of KOH and 60 mmol of the substrate *trans*-4-phenyl-3-butene-2-one were added. The solids were stirred and warmed to approximately 50 ^oC during the evacuation process to remove oxygen and traces of water. Then the Schlenk tube was filled with argon and 80 ml of 2-propanol. Under vigorously stirring the Schlenk tube was degassed by two freeze-thaw cycles and then the suspension was sonicated for 30 min (this is important to increase the homogeneity of the mixture). Finally the reaction mixture was pressurized with 2 bar of H_2 after flushing the reaction vessel three times with H_2. The suspension was vigorously stirred at 35 ^oC for 2 d. During the hydrogenation process samples were taken to probe the proceeding reaction. The samples were inserted into a gas chromatograph by a special glass syringe and the reaction products were compared with authentic samples.

2.8 General Procedure for the Lipase-Catalyzed Asymmetric Transesterification of *S*- enriched (*S*)-A

All reactants (alcohols, esters) were stored over activated molecular sieves (4 Å). The enantiomerically enriched alcohol ((*S*)-**A**; 45% ee-74 mg 0.5 mmol, analytical scale or 8.8 g 0.06 mol, gram-scale resulting from the **3L**$_7$-catalyzed asymmetric hydrogenation of trans-4-phenyl-3-buten-2-one) and isopropenyl acetate (108.8 mg 1.0 mmol, analytical scale or 24 g 0.24 mol, gram-scale) were dissolved in toluene (3 ml analytical scale or 500 ml gram-scale) in a 5 ml reaction vial (analytical scale) or 1 L round-bottomed flask (gram-scale). The reaction mixture was thermostated in an oil bath to 40^{o}C. A 100 µl sample of the reaction mixture was withdrawn and derivatized with isopropyl isocyanate (10 µl) at 100 ^{o}C for 30 min, diluted with toluene (100 µl) and analyzed by GC (t = 0 of sample). Afterwards, lipase (100 mg, analytical scale or 3.08 g gram-scale) was added, followed by the addition of molecular sieves 4 Å (100 mg analytical scale or 5 g gram-scale). 100 µl samples were taken after several time intervals. The samples were centrifuged to separate lipase. The organic layer was treated with isopropyl isocyanate heated to 100 ^{o}C for 30 min, then diluted with toluene (100 µl) and analyzed by GC. The reaction progress was monitored qualitatively by thin layer chromatography using *n*-hexane/ethyl acetate (9:1 v/v) as eluent. An aliquot of the supernatant was used for GC analysis. When maximum conversion was reached (50% after 2h), the reaction was terminated by filtration. The enzyme was washed with acetone and then dried in air for further use. Substrate (*S*)-**A** and product (*R*)-**10** were separated by flash chromatography over silica gel (*n*-hexane/ethyl acetate 9:1) affording 4.1 g ((*S*)-**A**) (>99% ee by GC) $[\alpha]_D^{20}$ -19.9 (c 1, CH_2Cl_2) [lit. $[\alpha]_D^{20}$ -24.5 (c 5.16, $CHCl_3$), 98% ee], yield: 47% and 4.3 g ((*R*)-**10**) (87% ee by GC) $[\alpha]_D^{20}$ +74.2 (c 1, CH_2Cl_2), yield: 49%.

2.9 General Procedure for the Lipase-Catalyzed Asymmetric Hydrolysis of *R*-enriched (*R*)-**10**

Enzyme (100 mg, analytical scale or 3.15 g of Novozyme 435 gram-scale) was dissolved in phosphate buffer (pH 6.0, 2.8 ml analytical scale, or 250 ml, gram-scale) and added to the enantiomerically enriched acetate (*R*)-**10** (45% ee *R* , 0.5 mmol, analytical scale or 7.8 g, 40 mmol, gram-scale resulting from **3L$_8$**-catalyzed asymmetric reduction of *trans*-4-phenyl-3-butene-2-one) dissolved in toluene (1 ml, analytical scale or 20 ml gram-scale) in a 5 ml reaction vial (analytical scale) or 1 L round-bottomed flask (gram-scale). The reaction mixture was thermostated in an oil bath at 40 ^{o}C. Then, 100 µl of the reaction mixture (organic layer) was withdrawn at several time intervals, derivatized with isopropyl isocyanate, heated to 100 ^{o}C for 30 min, then diluted with toluene (100 µl) and analyzed by GC. The reaction progress was monitored qualitatively by thin layer chromatography (*n*-hexane/ethyl acetate 9:1). When maximum conversion was reached (44% after 24h), the reaction was terminated by filtration. Substrate (*S*)-**10** and product (*R*)-**A** were separated by column chromatography (*n*-hexane/ethyl acetate 9:1) affording the 3.3 g (*R*)-**A** (>99% ee by GC) $[\alpha]_D^{20}$ + 19.9 (c 1, CH_2Cl_2), yield: 43% and 3.5 g (*S*)-**10** (74.5% ee by GC) $[\alpha]_D^{20}$ -71.2 (c 1, CH_2Cl_2), yield: 46%.

3. Crystallographic Analyses

3.1 X-ray Structural Analyses of Complexes $3L_4$, $3L_7$, and $3L_{10}$

Crystals of **$3L_4$** and **$3L_{10}$** were grown by slow diffusion of diethyl ether into a solution of the complex in dichloromethane. Data were collected at 173(2) K on a Siemens P4 diffractometer operating in the ω scan mode, using graphite monochromated Mo-K_α radiation (λ = 0.71073 Å). Details of crystal data, data collection, and structure refinement are given in Table 13. The structures were solved by direct methods using the Bruker SHELXS-97 program [92] and refined by full-matrix least-squares on F^2 using the Bruker SHELXL-97 program [93]. Non-hydrogen atoms were refined with anisotropic displacement parameters. Hydrogen atoms were constrained to idealized positions using a riding model (with free rotation for methyl groups). The difference electron density map and thermal ellipsoids of **$3L_4$** indicated a disorder of the cyclohexane ring of the diamine; this disorder was treated by introducing split positions corresponding to the opposite enantiomeric form of the ligand; the occupation number was allowed to refine, giving a ratio of 0.708 : 0.292. Crystallographic data for the structural analyses have been deposited with the Cambridge Crystallographic Data Centre, CCDC No. 179993 (**$3L_4$**), and 179994 (**$3L_{10}$**).

Crystals of **$3L_7$** were obtained by slow diffusion of diethyl ether into a dichloromethane solution of **$3L_7$**. A selected crystal was mounted on a Siemens P4 four-circle diffractometer by using a perfluorinated polyether (Riedel de Haen) as protecting agent. Details of crystal data, data collection, and structure refinement are given in Table 13. Graphite-monochromated Mo-Kα radiation (λ = 0.71073 Å) was used for the measurement of

Table 13. Crystal data and structure refinement for **3L$_4$**, **3L$_7$** and, **3L$_{10}$**

	3L$_4$	**3L$_{10}$**	**3L$_7$**
Crystal habit	block	plate	block
Crystal color	orange	orange	orange
Crystal size (mm)	0.6 × 0.6 × 0.6	0.5 × 0.3 × 0.08	0.5 × 0.3 × 0.08
Empirical formula	$C_{36}H_{48}Cl_2N_2O_2P_2Ru$	$C_{35}H_{48}Cl_2N_2O_2P_2Ru$	$C_{44}H_{50}Cl_2N_2O_2P_2Ru$
Formula weight	774.67	762.66	872.77
a (Å)	15.645(2)	11.4223(14)	12.136(4)
b (Å)	9.5424(15)	28.394(4)	29.307(3)
c (Å)	24.828(7)	12.2829(13)	12.898(3)
α (°)	90	90	90
β (°)	92.640(15)	117.654(11)	114.194(17)
γ (°)	90	90	90
Crystal system	monoclinic	monoclinic	Monoclinic
Space group	$P2_1/c$	$P2_1/c$	$P2_1$
Z	4	4	4
Reflections collected/unique	18307 / 8506	9684 / 8091	20134 / 18465
R_{int}	0.0319	0.0391	0.0391
Limiting indices	$-20 \le h \le 1, -12 \le k \le 12, -32 \le l \le 32$	$-1 \le h \le 14, -1 \le k \le 36, -15 \le l \le 14$	$-1 \le h \le 14, -1 \le k \le 36, -15 \le l \le 14$
θ range for data collection (°)	2.29 to 27.50	2.00 to 27.51	2.20 to 27.91
Completeness to θ (%)	99.8	99.9	99.9
Absorption coefficient (mm^{-1})	0.688	0.720	0.617
Absorption correction	none	none	none
Data/restraints/parameters	8506 / 0 / 464	8091 / 0 / 402	18465 /1/ 959
Goodness-of-fit on F^2	1.060	1.033	1.009
Final *R* indices [$I>2\sigma(I)$], R_1/wR_2	0.0240 / 0.0605	0.0568 / 0.1885	0.0443 / 0.0861
R indices (all data), R_1/wR_2	0.0271 / 0.0619	0.0812 / 0.2261	0.0704 / 0.0958
Extinction coefficient	0.00301(16)	0.00010(5)	0.00301(6)
Largest diff. peak / hole (e $Å^{-3}$)	0.353 / –0.641	1.770 / –1.708	0334/ -0.596

intensity data in the ω-scan mode at a temperature of 173(2) K. Cell parameters were determined from 50 automatically centered reflections. The intensity data were corrected for polarization and Lorentz effects. The structure was solved by direct methods with SHELXS-86 [94]. Refinement was carried out by full-matrix least-squares methods based on F^2 in SHELXL-97 [93], with anisotropic thermal parameters for all non-hydrogen atoms. Hydrogen atoms were included at calculated positions using a riding model with isotropic temperature factors equal to 1.2 times the U_{eq} value of the corresponding parent atom. Crystallographic data (excluding structure factors) for the structure in this paper have been deposited with the Cambridge Crystallographic Data Centre as supplementary publication number CCDC 190369.

3.2 X-ray Structural Analysis of Complex $3L_3$

Crystal structure analysis of **$4L_3$** $(C_{34}H_{46}ClN_2O_2P_2Ru)(BF_4) \cdot H_2O$ M = 818.01, monoclinic, *C*2/c, a = 38.284(7), b = 9.6965(17), c = 20.547(13) Å, β = 102.32(3)°, V = 7452(5) Å^3, Z = 8, D_c = 1.458 g cm^{-3}, μ(Mo-Kα) = 0.634 mm^{-1}. Crystal size 0.6 × 0.3 × 0.2 mm^3. Siemens P4 four-circle diffractometer, Mo-Kα radiation (λ = 0.71073 Å), T = 173(2) K. θ range for data collection 2.03 to 27.51°, limiting indices $-1 \le h \le 49$, $-12 \le k \le 1$, $-26 \le l \le 26$. 10020 reflections collected, with 8573 unique reflections [R(int) = 0.0294]. Direct methods, full-matrix least-squares on F^2 [19], heavy atoms refined anisotropically, hydrogen atoms in calculated positions (riding model), except for the protons of water (located in difference map, refined isotropically). The tetrafluoroborate anion is rotationally disordered about the B(1)-F(2) bond and was treated by introducing split positions. GooF = 1.025, $R1$ [$I > 2\sigma(I)$] = 0.0408, $wR2$ (all data) = 0.0925. Crystallographic data for the structure have been

deposited with the Cambridge Crystallographic Data Center as supplementary publication number CCDC **209190**.

3.3 X-ray Structural Analyses of Complexes $6L_1$, $6L_2$, and $6L_8$

Crystallographic details of the structure determination of **$6L_1$**, **$6L_2$**, and **$6L_8$** are summarized in Table 14. Crystals of **$6L_1$**, **$6L_2$**, and **$6L_8$** were obtained by slow diffusion of diethyl ether into a dichloromethane solution of the complexes. A selected crystal was mounted on a Siemens P4 four-circle diffractometer by using a perfluorinated polyether (Riedel de Haen) as protecting agent. Graphite-monochromated Mo-K_α radiation (λ = 0.71073 Å) was used for the measurement of intensity data in the ω-scan mode at a temperature of 173(2) K. Cell parameters were determined from 35-50 automatically centered reflections. The intensity data was corrected for polarization and Lorentz effects. Structure solution and refinement were carried out using the Bruker SHELXTL package [95]. The structures were solved by Patterson synthesis, followed by identification of non-hydrogen atoms in successive Fourier maps. Refinement was carried out with full-matrix least-squares methods based on F^2, with anisotropic thermal parameters for all non-hydrogen atoms. Hydrogen atoms were included at calculated positions using a riding model with isotropic temperature factors equal to 1.2 times the U_{eq} value of the corresponding parent atom. Crystallographic data (excluding structure factors) for the structures in this paper have been deposited with the Cambridge Crystallographic Data Centre as supplementary publication number CCDC **190294**, **190295**, **190296**. These data can be obtained free of charge via www.ccdc.cam.ac.uk/conts/retrieving.html (or from the CCDC, 12 Union Road, Cambridge CB2 1EZ, UK; fax: +44-1223-336033; e-mail: deposit@ccdc.cam.ac.uk).

Table 14. Crystal data and structure refinement parameters for **6L$_1$**, **6L$_2$**, and **6L$_8$**

	6L$_1$	**6L$_2$** •CH_2Cl_2	**6L$_8$**
Empirical formula	$C_{29}H_{34}Cl_2N_2P_2Ru$	$C_{31}H_{38}Cl_4N_2P_2Ru$	$C_{41}H_{42}Cl_2N_2P_2Ru$
Formula weight	644.49	743.44	796.68
Crystal color	yellow	yellow	orange
Crystal size (mm)	0.6 × 0.3 × 0.1	0.4 × 0.4 × 0.2	0.1 × 0.7 × 0.3
Crystal system, space group	triclinic, $P\bar{1}$	triclinic, $P\bar{1}$	triclinic, $P1$
a (Å)	9.984(4)	10.0194(15)	10.2172(12)
b (Å)	12.519(7)	12.397(2)	13.4835(17)
c (Å)	13.476(8)	14.500(5)	14.3403(14)
α (°)	109.38(8)	82.51(3)	107.817(9)
β (°)	105.78(5)	74.387(18)	93.685(11)
γ (°)	105.15(4)	68.441(15)	102.019(12)
Z	2	2	2
μ (mm^{-1})	0.881	0.942	0.697
F(000)	660	760	820
θ range (°)	2.27 to 27.52	2.25 to 27.50	2.06 to 27.50
Limiting indices, *hkl*	-12-12; -14-14; -17-17	-12-12; -16-15; -18-18	-12-13; -16-16; -18-18
Reflections collected/unique	12434 / 6234 [R_{int} = 0.0352]	14759 / 7384 [R_{int} = 0.0225]	16453 / 16453 [R_{int} = 0.0000]
Absorption correction	empirical	none	empirical
Max. and min. transmission	0.9169 and 0.7419	-	0.8335 and 0.5580
Data/restraints/parameters	6234 / 0 / 326	7384 / 0 / 363	16453 / 3 / 866
Goodness-of-fit on F^2	1.083	1.042	1.047
Final R indices [$I>2\sigma(I)$], R_1 / wR_2	0.0318 / 0.0755	0.0290 / 0.0728	0.0276 / 0.0687
R indices (all data), R_1 / wR_2	0.0366 / 0.0800	0.0326 / 0.0747	0.0315 / 0.0706
Absolute structure parameter	-	-	-0.021(18)
Extinction coefficient	0.0057(5)	0.0027(4)	0.0086(3)
Largest diff. peak and hole (e.$Å^{-3}$)	0.652 and -1.447	1.196 and -0.815	0.533 and -0.513

References

[1] S. Bhaduri, D. Mukesh, *Homogenous Catalysts Mechanisms and Industrial Applications*, Wiley, New York (2000).

[2] P. V. Ramachandran, H. C. Brown, *Reduction in Organic Synthesis: Recent Advances and Practical Applications*": ACS Symp. Ser. 169 (1996) 641.

[3] J. Seyden-Penne, *Reductions by the Alumino and Borohydrides in Organic Synthesis*; VCH: New York, (1991).

[4] A. Aramini, L. Brinchi, R. Germani, G. Savelli, *Eur. J. Org. Chem*. (2000) 1793.

[5] R. Noyori, *Asymmetric Catalysis in Organic Synthesis*, Wiley, New York (1994).

[6] J. G. Handique, A. Purkayashtha, J. B. Baruah, *J. Organomet. Chem*. 620 (2001) 90.

[7] E. J. Corey, C. J. Helal, *Tetrahedron Lett*. 36 (1995) 9153.

[8] T. Ohkuma, H. Ooka, T. Ikariya, R. Noyori, *J. Am. Chem. Soc*. 117 (1995) 10417.

[9] T. Ohkuma, H. Ooka, S. Hashiguchi, T. Ikariya, R. Noyori, *J. Am. Chem. Soc*. 117 (1995) 2675.

[10] R. Noyori, T. Ohkuma, *Angew. Chem., Int. Ed*. 40 (2001) 40.

[11] H. Doucet, T. Ohkuma, K. Murata, T. Yokozawa, M. Kozawa, E. Katayama, A. F. England, T. Ikariya, R. Noyori, *Angew. Chem., Int. Ed*. 37 (1998) 1703.

[12] T. Ohkuma, M. Koizumi, H. Doucet, T. Pham, M. Kozawa, K. Murata, E. Katayama, T. Yokozawa, T. Ikariya, R. Noyori, *J. Am. Chem. Soc*. 120 (1998) 13529.

[13] T. Ohkuma, H. Takeno, Y. Honda, R. Noyori, *Adv. Synth. Catal*. 343 (2001) 369.

[14] M. Yamakawa, H. Ito, R. Noyori, *J. Am. Chem. Soc*. 122 (2000) 1466.

[15] R. Noyori, M. Yamakawa, S. Hashiguchi, *J. Org. Chem.* 66 (2001) 7931.

[16] O. Pämies, J. E. Bäckvall, *Chem. Eur. J*. 7 (2001) 5052.

[17] M. J. Burk, W. Hems, D. Herzberg, C. Malan, A. Zanotti-Gerosa, *Org. Lett*. 2 (2000) 4173.

[18] O. M. Akotsi, K. Metera, R. D. Reid, R. McDonald, S. H. Bergens, *Chirality* 12 (2000) 522.

[19] R. Noyori, *Angew. Chem., Int. Ed*. 41 (2002) 2008.

[20] T. Ohkuma, M. Koizumi, K. Muniz, G. Hilt, C. Kabuta, R. Noyori, *J. Am. Chem. Soc*. 124 (2002) 6508.

[21] R. Hartmann, P. Chen, *Angew. Chem*., Int. Ed. 40 (2001) 3508.

[22] K. Abdur-Rashid, A. J. Lough, R. H. Morris, *Organometallics* 20 (2001) 1047.

[23] K. Abdur-Rashid, M. Faatz, A. J. Lough, R. H. Morris, *J. Am. Chem. Soc*. 123 (2001) 7473.

[24] K. Abdur-Rashid, M. Faatz, A. J. Lough, R. H. Morris, *J. Am. Chem. Soc*. 124 (2002) 15104.

[25] C. Nachtigal, S. Al-Gharabli, K. Eichele, E. Lindner, H. A. Mayer, *Organometallics* 21 (2002) 105.

[26] E. Lindner, I. Warad, K Eichele, H. A. Mayer, *Inorg. Chim. Acta*, 350 (2003) 49.

[27] E. Lindner, A. Ghanem, I. Warad, K. Eichele, H. A. Mayer, V. Schurig, *Tetrahedron: Asymmetry* 14 (2003) 1045.

[28] E. Lindner, I. Warad, K. Eichele, H. A. Mayer, *J. Organomet. Chem*. 665 (2003) 176.

[29] E. Lindner , I. Warad, Z. Lu, S. Al-Gharabli, K. Eichele, H. A. Mayer, *Inorg. Chim. Acta* 2003, in preparation.

[30] Bader, A.; Lindner, E. *Coord. Chem. Rev*. 108 (1991) 27.

[31] Lindner, E.; Jaeger, A.; Wegner, P.; Mayer, H. A.; Benez, A.; Adam, D.; Plies, E. *J. Non-Cryst. Solids* 255 (1999) 208.

[32] Lindner, E.; Wielandt, W.; Baumann, A.; Mayer, H. A.; Reinoehl, U.; Weber, A.; Ertel, T. S.; Bertagnolli, H. *Chem. Mater*. 11 (1999) 1833.

[33] Lindner, E.; Kemmler, M.; Mayer, H. A.; Wegner, P. *J. Am. Chem. Soc*. 116 (1994) 348.

[34] Lindner, E.; Kemmler, M.; Mayer, H. A. *Z. Anorg. Allg. Chem*. 620 (1994) 1142.

[35] Lindner, E.; Kemmler, M.; Mayer, H. A. *Chem. Ber*. 125 (1992) 2385.

[36] E. Lindner, S. Al-Gharabli, I. Warad, H. A. Mayer S. Steinbrecher, E. Plies, M. Seiler, H. Bertagnolli, *Z. Anorg. Allg. Chem*. 629 (2003) 161.

[37] E. Lindner, Th. Schneller, F. Auer, H. A. Mayer, *Angew. Chem*., Int. Ed. 38 (1999) 2154.

[38] E. Lindner, A. Enderle, A. Baumann, *J. Organomet. Chem*. 558 (1998) 235.

[39] E. Lindner, S. Al-Gharabli, H. A. Mayer, *Inorg. Chim. Acta* 334 (2002) 113.

[40] E. Reddington, A. Sapienza, B. Gurau, R. Viswanathan, S. Sarangapani, E. S. Smotkin, T. E. Mallouk, *Science* 280 (1998) 1735.

[41] R. H. Crabtree, *Chem. Commun*. (1999) 1611.

[42] E. Lindner, Th. Salesch, S. Brugger, S. Steinbrecher, E. Plies, H. Bertagnolli, H. A.

Mayer, *Eur. J. Inorg. Chem*. (2002) 1998.

[43] Th. Bein, *Angew. Chem*., Int. Ed. 38 (1999) 323.

[44] E. Lindner, R. Schreiber, Th. Schneller, P. Wegner, H. A. Mayer, W. Göpel, Ch. Ziegler, *Inorg. Chem*. 35 (1996) 514.

[45] E. Lindner, A. Jäger, F. Auer, W. Wielandt, P. Wegner, *J. Mol. Catal. A* 129 (1998) 91.

[46] E. Lindner, Th. Schneller, F. Auer, P. Wegner, H. A. Mayer, *Chem. Eur. J*. 3 (1997) 1833.

[47] E. Lindner, Th. Schneller, F. Auer, H. A. Mayer, *Angew. Chem*., Int. Ed. 38 (1999) 2154.

[48] E. Lindner, A. Baumann, P. Wegner, H. A. Mayer, U. Reinöhl, A. Weber, T. S. Ertel, H. Bertagnolli, *J. Mater. Chem*. 10 (2000) 1655.

[49] E. Lindner, Th. Salesch, S. Brugger, F. Hoehn, P. Wegner, H. A. Mayer, *J. Organomet. Chem*. 641 (2002) 165.

[50] E. Lindner, A. Möckel, H. A. Mayer, H. Kühbauch, R. Fawzi, M. Steimann, *Inorg. Chem*. 32 (1993) 1266.

[51] E. Lindner, St. Pautz, M. Haustein, *Coord. Chem. Rev*. 155 (1996) 145.

[52] E. Lindner, Q. Wang, H. A. Mayer, R. Fawzi, M. Steimann, *Organometallics* 12 (1993) 1865.

[53] E. Lindner, K. Gierling, M. Geprägs, R. Fawzi, M. Steimann, *Inorg. Chem*. 34 (1995) 6106.

[54] A. Maj, K. Pietrusiewicz, I. Suisse, F. Agbossou, A. Mortreux, *J. Organomet. Chem*. 626

(2001) 157.

[55] E. Lindner, I. Warad, K. Eichele, H. A. Mayer, unpublished results.

[56] M. F. DaCruz, M. Zimmer, *Inorg. Chem*. 35 (1996) 2872.

[57] E. A. Stern, *Phys. Rev. B* 10 (1974) 3027.

[58] F. W. Lytle, D. E. Sayers, E. A. Stern, *Phys. Rev.* B 11 (1975) 4825.

[59] H. Bertagnolli, T. S. Ertel, *Angew. Chem. Int. Ed. Engl.* 33 (1994) 45.

[60] T. S. Ertel, H. Bertagnolli, S. Hückmann, U. Kolb, D. Peter, *Appl. Spectrosc*. 46 (1992) 690.

[61] Z. Lu, K. Eichele, I. Warad, H. A. Mayer, E. Lindner, Z. Jiang, V. Schurig, *Z. Anorg. Allg. Chem*. 629 (2003) 1308.

[62] M. M. Fontes, G. Oliva, L. C. Cordeiro, A. Batista, *J. Coord. Chem*. 30 (1993) 125.

[63] Z.-L Lu, E. Lindner, H. A. Mayer, *Chem. Rev*. 102 (2002), 3543.

[64] O. Lavastre, J. P. Morken, *Angew. Chem., Int. Ed.* 38 (1999) 3163.

[65] E. Lindner, F. Auer, A. Baumann, P. Wegner, H. A. Mayer, H. Bertagnolli, U. Reinöhl, T. S. Ertel, A. Weber, *J. Mol. Cat. A* 97 (2000) 157.

[66] D. E. Rolison, *Science* 299 (2003) 1698.

[67] M. E. Davis, *Nature* 812 (2002) 813.

[68] H. Egelhaaf, E. Holder, P. Herman, H. A. Mayer, D. Oelkrug, E. Lindner, *J. Mater. Chem.* 11 (2001) 2445.

[69] J. C. Brinker, W. G. Scherer, *Sol Gel Science*, Academic Press, London (1990).

[70] G. E. Maciel, D. W. Sindorf, *J. Am. Chem. Soc*. 102 (1980) 7607.

[71] C. A. Fyfe, *Solid State NMR for Chemists*, CRC Press, Gulph, ON, 1984.

[72] J. Gao, H. Zhang, X. Yl, P. Xu C. Tang, H. Wan, K. Tsai, T. Ikariya, *Chirality* 12 (2000) 383.

[73] A. Koskinen, *Asymmetric Synthesis of Natural Products*; Wiley, New York (1993).

[74] M. Ohno, M. Otsaka, *Org. React*. 37(1990) 1.

[75] E. Santaniello, P. Ferraboschi, P. Grisenti, A. Manzocchi, *Chem. Rev*. 92 (1992) 1071.

[76] E.; Schoffers, A. Golebiowski,; R. C. Johnson, *Tetrahedron* 52 (1996) 3769.

[77] Wong, C. H.; Whitesides, G. M. *Enzymes in Synthetic OrganicChemistry*; Elsevier Science Ltd.: Amsterdam (1994).

[78] K. Faber, *Biotransformations in Organic Chemistry*, Springer-Verlag: Heidelberg, (1992).

[79] F. Theil, *Chem. Rev*. 95 (1995) 2203.

[80] R. D. Schmid, R. Verger, *Angew. Chem*., Int. Ed. 37 (1998) 1608.

[81] A. Persson, A. Larsson, M. Le Ray, J. E. Baeckvall, *J. Am. Chem. Soc*. 121 (1999) 1645.

[82] O. Pamies, J. E. Baeckvall, *J. Org. Chem*. 2002, 67(4), 1261.

[83] M. J. Palmer, M. Wills, *Tetrahedron: Asymmetry* 10 (1999) 2045.

[84] U.T. Bornscheuer, R. J. Kazlauskas, *Hydrolases in Organic Synthesis*. Wiley-VCH: Weinheim, Germany, (1999).

[85] T. A. Stephenson, G. Wilkinson, *J. Inorg. Nucl. Chem.* 28 (1966) 945.

[86] E. Lindner, S. Meyer, P. Wegner, B. Karle, A. Sickinger, B. Steger, *J. Organomet. Chem.* 335 (1987) 59.

[87] A. Dietrich, B. Maas, W. Messer, G. Bruche, V. Karl, A. Kaunzinger, A. Mosandl, *High Resolut. Chromatogr*. 15 (1992) 590.

[88] M. Newville, P. Livins, Y. Yakobi, J. J. Rehr, E. A. Stern, *Phys. Rev. B* 47 (1993) 14126.

[89] S. J. Gurman, N. Binsted, I. Ross, *J. Phys. C* 19 (1986) 1845.

[90] V. D. Scott, G. Love, *X-Ray Spectrom.* 21 (1992) 27.

[91] A part of an AXX pattern: a) N = \$^3J_{PC} + {}^5J_{PC}$\; b) N = \$^2J_{PC} + {}^4J_{PC}$\; c) N = \$^1J_{PC} + {}^3J_{PC}$\.

[92] G. M. Sheldrick, SHELXS-90; University of Göttingen, Göttingen, Germany 1990.

[93] G. M. Sheldrick, SHELXS-97; University of Göttingen, Göttingen, Germany 1997.

[94] G. M. Sheldrick, SHELXS-86; University of Göttingen, 1986.

[95] SHELXTL NT 5.10, Bruker AXS, Madison, WI, USA, 1998.

Summary

Catalysis plays a vital role in chemical synthesis. In particular, efficient molecular organometallic catalysis, provides a logical basis for molecular science and related technologies. Although selectivity, particularly in the control of absolute stereochemistry, is a major concern in modern organic synthesis, reactivity and productivity are also important in making reactions efficient and practical. A useful catalysis must show a high turnover number (TON), and a high turnover frequency (TOF) under mild conditions. In addition, reactions should be operationally simple, safe, and environmentally friendly. These important attributes can be obtained only by designing suitable molecular catalysts and reaction conditions through a deep understanding of, or an unique insight into, the catalytic cycle. In fact, to a large extent the discovery of efficient catalytic reactions still relies on serendipity but originates from sound, comprehensive chemical knowledge. Combinatorial approaches coupled with high-throughput screening techniques obviously facilitate the discovery process but their powers are still not that evident in the field of molecular catalysis. Most excellent new catalysts are optimized forms of existing catalysts rather than being truly novel.

The objective of this thesis was the preparation and characterization of ruthenium(II) complexes with different types of diamine and phosphine ligands. Such species are active in the selective hydrogenation of α,ß-unsaturated ketones under mild conditions in homogeneous and heterogeneous phase.

In the first part of this work the synthesis of a set of novel neutral and cationic diamine-bis(ether-phosphine)ruthenium(II) complexes was carried out by treatment of the precursor complex $RuCl_2(\eta^2\text{-}Ph_2PCH_2CH_2OCH_3)_2$ with various chelating 1,2-, 1,3- 1,4-diamines, or chiral, achiral, aliphatic, cycloaliphatic, and aromatic diamines. Due to the hemilabile character the (ether)oxygen function can easily be replaced by incoming substrates like diamines. Compounds of this type are potential candidates for the application of parallel methods. Thus, diamines which are easily accessible in various forms were introduced as co-ligands to modify the (ether-phosphine)ruthenium(II) complexes in order to create a large array of structurally different compounds. The structures of the complexes have been investigated by elemental analyses, infrared spectroscopy, mass spectroscopy, ^1H, $^{13}C\{^1H\}$, H,H COSY NMR experiments, and where appropriate also by $^{31}P\{^1H\}$ NMR spectroscopy and X-ray crystallography. X-ray structural investigations reveal three possible isomers of the octahedrally coordinated ruthenium complexes $RuCl_2$(ether-phosphine)-(diamine). In solution, however, only the *trans*-chloro-*cis*-phosphine-*cis*-diamine ruthenium(II) configuration was found. A comparative study between EXAFS and X-ray diffraction methods of the neutral diamine(ether-phosphine)ruthenium(II) complexes was carried out. Structural data which were obtained from X-ray diffraction and EXAFS are in very good agreement with each other.

In the second part of this work, some of the neutral diamine(ether-phosphine)-ruthenium(II) complexes were transformed to their cationic relatives. Treatment of $RuCl_2(\eta^1\text{-}Ph_2PCH_2CH_2OCH_3)_2$(diamine) with one equivalent of AgOTf or $AgBF_4$ in CH_2Cl_2 results in the formation of the monocationic ruthenium(II) complexes $[RuCl(\eta^1\text{-}Ph_2PCH_2CH_2OCH_3)(\eta^2\text{-}Ph_2PCH_2CH_2OCH_3)(diamine)]^+X^-$ (X = OTf, BF_4). The ether-oxygen atom which may be

regarded as an intermolecular solvent is able to stabilize a metal center after substrate dissociation and therefore a decomposition may be suppressed. These complexes were characterized by NMR, IR, and mass spectroscopy as well as by elemental analyses, and X-ray structural analysis.

In a third chapter novel diamine(dppp)ruthenium(II) complexes are described, which have been made accessible by a very fast reaction of equimolar amounts of $RuCl_2(dppp)_2$ with different types of diamines in excellent yields. As their ether-phosphine congeners in solution all these complexes prefer a *trans*-$RuCl_2$ configuration, whereas in the solid state *cis*- and *trans*-isomers are observed.

In an other section of this work, a several diamine(ether-phosphine)ruthenium(II) complexes have been successfully supported onto a polysiloxane matrix by the sol-gel process after modifying the ether-phosphine ligand with T-silyl function. The sol-gel process was carried out in the presence of the co-condensation agent **Me-T^0**. $(n\text{-Bu})_2Sn(OAc)_2$ was used as catalyst. The amorphous polymeric materials were characterized by multinuclear CP/MAS solid-state NMR spectroscopy as well as by EXAFS, EDX, SEM, and BET methods.

In a fifth chapter the catalytic activity of the homogeneous and interphase ruthenium(II) catalysts in the selective hydrogenation of α,ß-unsaturated ketones as model substrates has been probed under mild conditions (1-4 bar hydrogen pressure, T = 35 C^o, using several co-catalysts like KOH, *t*BuOK, and AgOTf) in a special low-pressure Schlenk. In solution, the neutral as well as the cationic diamine(ether-phosphine)ruthenium(II) and diamine-(diphosphine)ruthenium(II) complexes proved to be suitable precursors for the

hydrogenations. With the exception of materials with aromatic, aprotic and 1,4-diamines, all other complexes are highly catalytically active in the hydrogenation of the α,ß-unsaturated ketone *trans*-4-phenyl-3-butene-2-one. In most cases the conversions and selectivities toward the formation of the unsaturated alcohol *trans*-4-phenyl-3-butene-2-ol are 100% with high turnover frequencies, which are influenced by the hydrogen pressure. Complexes with 1,3-diamines as co-ligands show a decrease in the selectivity, in favor of the hydrogenation of the C=C bond. In some cases when a large excess of the co-catalyst (KOH) was used the regioselectivity toward the full hydrogenation has been detected in a small amount. However, the cationic species showed only half of the catalytic activity compared to their neutral counterparts. Further experiments were devoted to the role of the co-catalysts. It was evidenced that co-catalysts like OH^- or tBuO$^-$ are able to occupy the *pseudo*-vacant coordination site to give neutral species, which are still active as catalysts. Because of their instability no further experiments could be carried out.

Also the supported diamine(ether-phosphine)ruthenium(II) complexes showed a satisfying activity and selectivity in the hydrogenation of *trans*-4-phenyl-3-butene-2-one, but with typical decreased in both the activity and the selectivity compared by the corresponding complexes in homogeneous phase.

In the last part of this thesis the neutral diamine(ether-phosphine)ruthenium(II) complexes were probed as catalysts in the asymmetric hydrogenation of *trans*-4-phenyl-3-butene-2-one. Complexes with achiral diamines afforded the racemic *trans*-4-phenyl-3-butene-2-ol alcohol, those with chiral (*RR* and *SS*) diamines allowed the formation of the corresponding enantiomerically enriched secondary alcohols with (*S* and *R*, respectively) with ee values of 45%. To improve the enantioselectivity of the secondary alcohol, the kinetic

resolution of enantiomerically enriched *trans*-4-phenyl-3-butene-2-ol was performed in a consecutive approach using lipase-catalyzed enantioselective transesterification of the alcohol in toluene. Several lipases were screened through an transesterification or hydrolysis reactions until more than 99% *R* and *S* single enantiomeric alcohol was obtained. The hydrogen pressure and the co-catalyst (KOH, *t*BuOK, AgOTf), do not effect the enantioselectivity.

Meine akademische Ausbildung verdanke ich:

H. Hillal, K. Albert, S. Khalaf, H. Bertagnolli, T. Al-Tel, M. M. El-Abadelah, Z. L. Lu, G. Jung, E. Lindner, R. Abu-Halawa, H. A. Mayer, R. Al-Qauasmy, B. Speiser, J. Strähle, W. Voelter, K. P. Zeller, U. Nagel, H. Egelhaaf, D. Krug, V. Schurig, M. Abu-Eid, W. Al-Jondi, A. Abu-Ebid, M. Mosmar, V. Hoffman, L. Majad, S. Zakarya, B. Shraydeh, K. Eichele.

Lebenslauf

Persönliche Daten	
Name:	Ismail Khalil Warad
Geburtstag/-ort:	19. Sept. 1972 in Plästina
Eltern:	Khalil Ibnya Warad
	Fayza Fawaz Saleh
Staatsangehörigkeit:	Palästinenser
Schulbildung:	
1978–1984	Grundschule in Boreen
1985–1988	Gymnasium in Nablus
07.1990	Abitur in Nablus-Palästina
Hochschulbildung	
09.1990 - 06.1994	B.Sc. Studium an der An-Najah National Universität in Nablus- Palästina
07.1994	B.Sc. Titel
09.1995 – 03.1998	M.Sc. Studium an der "An-Najah National University" in Nablus- Palästina
03.1998	M.Sc. Examen mit dem Thema "Kinetics and Mechanism of Oxidation of Cysteine by Complexation Process Using Iron(III) and Nitrogen Chelate Organic Ligands DPKTH and Ferrozine am Institut für Chemie der "An-Najah National University

03.03.1998	Zeugnis der M.Sc. Prüfung in Chemie
	Dissertation unter Leitung von Herrn Prof. Dr. E. Lindner am Institut für Anorganische Chemie mit dem Thema:
02.2001–07.2003	Diamin(phosphin)ruthenium(II) Komplexe und ihre Anwendung in der katalytischen Hydrierung von α,ß-ungesättigten Ketonen in homogener und heterogener Phase

Beschäftigung

05.1995 – 06.2000	Lehrer für Chemie in Akraba and Madma
06.2000 – 02.2001	Ausbildungsleiter für Chemie und Technologie im Bildungs-Ministerium in Palästina
02.2001–05.2001	Wissenschaftliche Hilfskraft, Institut für Anorganische Chemie, Universität Tübingen
seit 01.07.2001	Doktorandenstipendium und Mitglied im Graduiertenkolleg "Chemie in Interphasen"
02.2001–07.2003	Assistent im Anorganisch-chemischen Praktikum für Fortgeschrittene, Teil II